5-2019

Investigating the Masking Effects of Blood on Organic Gunshot Residue Using GC/MS, Raman, and ATR-FTIR

Tyler Willits
University of New Haven

THE UNIVERSITY OF NEW HAVEN

INVESTIGATING THE MASKING EFFECTS OF BLOOD ON ORGANIC GUNSHOT RESIDUE USING GC/MS, RAMAN, AND ATR-FTIR

A THESIS

submitted in partial fulfillment

of the requirements for the degree of

MASTERS SCIENCE IN FORENSIC SCIENCE

BY

Tyler Willits

ADVISER

Dr. Virginia Maxwell, D.Phil.

University of New Haven

West Haven, Connecticut

May, 2019

ACKNOWLEDGMENTS

Sincerest thanks to Doctor Virginia Maxwell, Doctor Robert Powers, Doctor Brooke Kammrath, and to all the staff of the forensic science department for their patience and support.

Special thanks also to Robert Willits and Joyce Willits; and appreciation to UNH.

ABSTRACT

Gunshot residue (GSR) can be an indicator for determining the distance of a firearm discharge and linking potential suspects and witnesses to a shooting event. However, the evidentiary value of inorganic gunshot residue (IGSR), commonly used to detect GSR, has been called into question due to the potential for false negatives and false positives. Organic gunshot residue (OGSR) acts as supporting evidence; this increases the overall confidence of the examiner, as well as the value of gunshot residue evidence as a whole.

Current research has focused on three main areas for OGSR. The first is what compounds we should identify as relevant and in enough quantity to reliably find at the scene. Next, is how to collect OGSR. Standard swabs and different styles of aluminum stubs have been tested and validated. Lastly, is the type of instrumentation to be used. Currently, research is focusing on the use of high-performance liquid chromatography paired with mass spectrometry (HPLCMS), gas chromatography paired with mass spectrometry (GCMS), and multiple spectroscopy techniques.

This study aims to validate the identification of six common OGSR compounds contaminated with blood using gas chromatography paired with mass spectrometry (GCMS), Raman spectroscopy, and Attenuated Total Reflectance Fourier Transform Infrared Spectroscopy (ATR-FTIR). For each instrumentation, samples were analyzed separate of blood contamination or substrate. Then, they were analyzed in relation to 100% cotton substrate. Lastly, they were analyzed with blood contamination. GCMS showed masking for 2-4 Dinitrotoluene, Raman interpretation was not possible, and a majority of ATR-FTIR results were masked.

TABLE OF CONTENTS

Introduction

The discipline of gunshot residue is in a state of transition. In the world of forensic science, gunshot residue provides physical evidence in determination of distance to the victim, location of the shooter, and linking a suspect to a shooting. In recent years, there has been a growing interest in the applications of organic gunshot residue. GSR research has escalated from better inorganic gunshot residue detection methods for lead, antimony, and barium to detection of relevant OGSR compounds. The individual elements found in IGSR particles have been found environmentally in substances unrelated to gunpowder, have a tendency to be washed off, and are not present in many of the non-toxic ammunitions available on the market today. These can cause problems with false positives and false negatives for an examiner.

Currently, research into OGSR seems to be aligned with the best methods for identification and collection, as well as classification of compounds. What is problematic for OGSR research currently is the effects of environmental constituents on the relevance or quality of OGSR at the scene. Blood is a common body fluid associated with crime scenes on the victim, perpetrator, and the scene. However, research has not been performed to test the potential for blood to act as a masking agent on the presence of OGSR.

The intent of this thesis is to extend environmental OGSR research to the effects of blood on crime scene OGSR, found on different common fabrics, using GC/MS. Will blood have a masking impact on crime scene available OGSR? Can we create a validated, consistent method using GCMS, Raman, and ATR-FTIR to determine the availability of OGSR compounds? Will the methods we create using known standards be transferrable to samples collected from the field? How would the presence of different common fabrics correlate with this interaction?

Blood should have a masking impact on OGSR. For the purposes of this study, we will only be using compound standards provided from an outside vendor. The purpose of this is to validate both our instrumental analysis as well as determine which collection method will be suitable for the greatest sample uptake. This also allows for consistency in what we are testing. Gunshot residue tends to have burnt and unburnt particulates with varying concentrations of OGSR present. Samples will be taken without blood stains or substrates as well as a means of control and verification of spectra identification. Blank samples will also be performed to create confidence in the consistency of our analysis. For analysis, we will be using GCMS as it provides the sensitivity required to identify the minute samples provided by OGSR deposition at a crime scene. Raman and ATR-FTIR will also be utilized as environmental contaminants have not been identified within the literature.

The impact of trace evidence on crime scene work cannot be understated and because of the sheer number of gun crimes, this extends to all fields of firearms examinations as well. IGSR has many faults as evidence that make OGSR much more beneficial to find and quantify. Without GSR, we would have difficulty using physical evidence to determine the location of the shooter after a crime as well as identify suspects. To this end, methods for improvement of both detection and compositional identification of gunpowder compounds are imperative. Because blood will usually be present when a victim is involved, it is important that it be considered as an environmental factor when looking for GSR at a crime scene. Determining how great of an effect bloody fabric have in determining the presence and quantities of OGSR analytes will have a direct impact on not only crime scene investigation, but research into GSR going forward as well. This study is significant as a stepping stone to this end.

Literature Review

1.1 Composition

The purpose of this study is to determine the effects of blood on organic gunshot residue under GCMS analysis. Blood is a unique environmental aspect that has not been explored in relation to OGSR. The composition of a projectile as well as the firing event leading up to expulsion of GSR will be examined as well as the historical perspective and instrumentation of IGSR analysis. Previous research into multiple aspects of OGSR includes compositional identification of powders, proper sampling techniques, and necessary instrumentation in the analysis of OGSR.

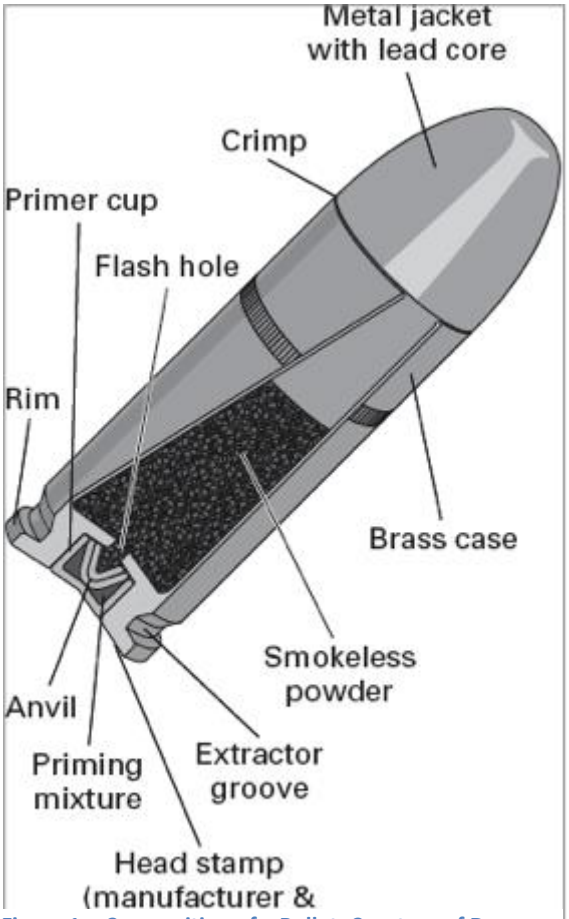

Figure 1a: Composition of a Bullet. Courtesy of Dr. Howard Harris

First, it is important to highlight the composition of a bullet and the events that take place during the discharge of a firearm. Ammunition, in any form, is a synthesis of a projectile (pellets, slug, or bullet), propellant powder, and primer powder. All of these elements are placed into a cartridge case which fits into the firing chamber of a specified firearm. The projectile itself will be at the tip of the ammunition; bullets are external and crimped to the cartridge case, while a slug or pellets in a shotgun shell will be internal near the head of the shell. Primer powder is what begins the chain of events leading to the expulsion of the projectile. It is made of shock sensitive explosive, oxidizer, fuel, and sensitizer compounds. It will

detonate when struck with the firing pin of a firearm. The primer, in turn, ignites the propellant powder. The propellant consists of chemicals that create a rapid production of gases, create pressure behind the projectile, propelling it forward through the barrel. This creates a plume of GSR, which will be expelled through any openings in the firearm [3]. This plume was found to settle anywhere between 5 to 23 seconds using first order approximations and Stokes Law [9].

Most propellants ignited by the primer, as described above, are smokeless powders. Nitrocellulose, a compound in smokeless gunpowder, is commonly used to produce energy quickly. When used alone, it is known as a single base powder. Single base propellants are used in small caliber ammunition. When nitrocellulose is combined with nitroglycerine, it is instead a double base powder. Double base powder is used in higher caliber small arms ammunition. The last category of smokeless gunpowder is a triple base powder. when nitrocellulose and nitroglycerin are used in combination with nitroguanidine, it is a triple base powder. Triple base powder tends to be more stable and is used in the creation of larger, artillery-based gun-powders [19]. Other compounds that can be found in smokeless propellant powder include stabilizers, plasticizers, flash inhibitors, coolants, moderants, surface lubricants, and anti-wear additives. These other compounds occur in differing concentrations depending on the ammunition manufacturer [3]. This study will focus on OGSR compounds originating from this smokeless propellant powder, in contrast to the primer powder.

Primer mainly consists of inorganic elements and while OGSR is the focus of this study, it is important to clarify what inorganic gunshot residue is and what elements it is composed of. IGSR is the condensation and deposition of the metallic components of GSR and originate in the primer powder. There are three main components to IGSR. The initiator of the primer powder, lead styphnate, which is the initial explosion set off by the firing pin. The oxidizer, barium

nitrate, which supplies the oxygen needed for the fuel. Lastly, the fuel, antimony sulfide, burns and ignites the propellant powder [9].

When the primer elements cool and fall after firing, they can combine into particles of three classifications. They can become round particles, irregular particles, and lead layered particles. Round particles are spheres that can get up to 10 micro meters in size. Sometimes, the shape is not round. Irregular particles are fusions of small and large particles that form amorphous shapes. Lastly, lead layered particles are those with a sheet of lead surrounding a core of barium and antimony. The combination of lead, barium, and antimony into one singular particle is unique to IGSR. Other particles can form that may have one individual element or two of the elements combined. In this case, we would say the particle is characteristic of IGSR [9].

The aforementioned GSR particulates are found at many crime scenes. According to the National Institute of Justice, in 2011, over 414,562 cases involved the use of a firearm [7]. For decades, tests have been evaluated and expanded to identify gunshot residue. Chang et al. describes the history of gunshot residue's evidentiary value as dating back to 1959, beginning with spot tests and advancing to paraffin and dermal nitrate tests, combined with triphenylmethylarsonium iodide to determine the presence of IGSR on the hands of suspects [3]. This method was valid through the 1970s, but it was quickly identified as a non-specific test for GSR [3].

1.2 Instrumentation

Historically, instrumental techniques soon became available to bulk analyze barium, lead, and antimony on samples. Neutron activation analysis (NAA) and atomic absorption spectrometry (AAS) were two of the initial instrumentations used in the detection of inorganic

gunshot residue. NAA could detect antimony and barium, while AAS could detect antimony, barium, and lead. These were historically used in combination to detect the metallic elements of IGSR [3] These are no longer used for IGSR analysis and have been replaced.

The modern instrumentation for GSR detection currently is scanning electron microscope-energy dispersive X-ray analysis (SEM-EDS). SEM-EDS uses three-dimensional analysis of particles that are collided with electrons. This creates a 3-D image of particles the examiner is interested in and eliminates any other particles as a background value. When done properly, it can detect combined particles of lead, barium, and antimony used to confirm the presence of GSR through a combination of morphology and composition [3].

1.3 Evidence Value and Limitations

After SEM-EDS analysis, investigators can use GSR evidence multiple ways. GSR can be used in the reconstruction of an event, generally through estimation of the shooting distance and indication of the trajectory via the determination of the entry and exit point of a bullet hole [1]. Shooting distance can be determined due to drop off values at varying distances for GSR. Grabmuller et al. describes four relevant distances GSR is useful as evidence. A contact shot, in which the firearm's muzzle is in contact with the victim, a shot in which the muzzle is only a few centimeters away, an intermediate shot in which there are traces of GSR, but they are much lesser than that of the first two, and lastly a shot in which firearm traces can no longer be observed [6]. Interestingly, the entry and exit point for a bullet can be determined with GSR; the entry point can have a varying amount of GSR, while the exit point should have little to no GSR. The ring of powder that forms around an entry wound is known as bullet wipe and can create an abrasion ring that discolors the tissues surrounding the wound [3].

While GSR is useful for scene reconstruction, false positives from environmental sources have been studied to establish limitations. Hofstetter et al. stated that of the relevant transfer studies done in the past for OGSR, transfer is a low possibility. One study found that of 255 police station specimens taken, 24, or 9%, were positive for some form of OGSR. In a later study, of 70 specimens taken from officers in Pittsburgh, only 4, or 6%, were positive for OGSR. Population data outside of police personnel was negative most of the time, as they had under a 5% positive rate [1]. Though the possibility of secondary transfer exists with OGSR, these results indicate transfer possibility to both officers and the general population is low. This would give support to the idea of OGSR having a low chance of transfer from the environment, further strengthening its evidentiary value in contrast to IGSR. IGSR elements are commonly found in the environment.

While OGSR is the focus of this research, it is important to highlight why we are interested in it instead of IGSR. IGSR, while useful, has disadvantages. Sometimes it is simply missing from a shooter due to actions they have taken after the event [1]. Hand washing or movement in general tends to knock GSR particles off skin and clothing. In contrast, OGSR tends to be absorbed and adhere to skin due to their lipophilic properties [1]. Heavy metal particles in the environment can cause false positives when high enough levels of barium, antimony, or lead are present such as the case in some industry processes [1, 2]. Lastly, non-toxic and heavy metal free ammunition can cause false negatives [1, 2] due to the absence of those particles in the IGSR when they would normally be present. When using SEM-EDS, environmental sources of lead, barium, and antimony cannot be eliminated, another limitation examiners must acknowledge.

Table 1. Experimental compositions of lead-free ammunition in previously published studies

Cartridge	Experimental composition	Reference
Sintox	Titanium, Zinc	25
CCI Clean Fire	Strontium	33
Winchester WinClean	Potassium, traces of aluminium, silicone, calcium, sulfur, zinc, copper, nickel, chromium, magnesium, iron	34
Remington/UMC Leadless	Aluminium, silicone, potassium, sodium, calcium, traces of magnesium	34
Federal BallistiClean	Barium, silicone, aluminium	34
Speer Lawman CleanFire	Strontium, oxygen, aluminium, chlorine	34
CleanRange	Strontium (first generation) Potassium, aluminium, silicone, calcium (second generation)	35

Figure 2: Composition of current lead-free ammunitions. Original source Chang et al. [3]

Because of these limitations, OGSR is becoming a much more accepted research focus as valuable supporting evidence to IGSR analysis. Goudsmits et al. claims OGSR compounds are not generally found in the natural environment. This makes the presence of many of these OGSR compounds unique [5]. IGSR particles tend to be evaluated through SEM-EDS when the GSR particles are 1-10 um in size. However, Bueno et al. claims that OGSR particles are considered more likely to be collected at crime scenes as they vary in size from visible to fine particles [24].

1.4 Organic Gunshot Residue

The literature for OGSR has focused on multiple topics. One focus has been on what environmental constituents can create false positives. Goudsmits et al. claims that of the 136 compounds classified as OGSR, only four specifically are very rarely found in the environment itself and only 20 would they consider for OGSR testing. The four priority compounds of interest rarely found in the environment are ethyl centralite (EC1), methyl centralite (MC1), nitroglycerin, and nitroguanidine. Other potential useful and environmentally rare compounds include 2-4 dinitrotoluene (2-4 DNT), akardite II, 2-Nitrodiphenylamine, 4-nitrodiphenylamine,

and a combination of diphenylamine (DPA) plus nitrated-derivatives. Anything outside of these has a higher risk of environmental contamination [5]. Blood has not been considered as a contributor to false negatives. This is the potential niche this study will investigate and fulfill within the literature.

Another focus is how OGSR distributes and is retained on the body and clothing of a shooter. Before Hofstetter et al., there was no true study on how OGSR is distributed on the skin or clothing of the shooter. Interestingly, a previous study indicated that clothes could retain GSR particles up to five days after the shooting event [36]. Hofstetter et al. identified that the right side of the body of the shooter generally had the vast majority of OGSR particulates as well due to the ejection port being on this side. Common fabrics associated with general wear included 100% cotton cloth, polyester, nylon, denim, and leather [1].

The greatest method for sample collection has also been an area of research. Hofstetter et al. used aluminum stubs with carbon adhesion for their OGSR collection [1]. Gassner et al. specifically compared two different swabs and four different stubs. They found tape stubs to be the most efficient collection method in their tests, swabs had problems with human error due to the different methods of those who swabbed the hands [4]. Though these methods worked for their studies, this is a limitation on their part. The problem with using aluminum stubs on fabrics or skin is that you can remove fibers or skin cells unrelated to the OGSR with it [1]. Human error in swabbing and excess matrix compounds added through stub uptake make reproducibility for sampling an issue [4]. It also must be considered that blood spattered on top of OGSR could completely block its uptake onto a stub or swab. For this study solvent extraction, a common GC sample preparation method, was considered and used for samples. For this solvent extraction, solvent choice is also something to consider. Previous studies had access to many possibilities

including 0.1 percent dilution of formic acid, methanol, acetonitrile [1], and acetone [8]. Previous studies have used many types of solvents; methanol was used for this study and was successful as a solvent for the OGSR compounds used.

Instrumentational analysis for OGSR is also a focus for research. Gassner et al. briefly highlights why certain instrumentations cannot be used for OGSR analysis, why some instruments are not ideal for OGSR analysis, and why GCMS and LCMS are ideal instrumental candidates for this type of study. Adding mass spectrometry (MS) to these is an option, but matrix effects become detrimental to the sensitivity. Pairing MS with a separation instrument all but eliminates matrix effects. Capillary electrophoresis is not sensitive enough for OGSR compounds. GCMS has excellent sensitivity and result speed, however, it suffers a unique drawback. Because of the high temperatures required for GCMS, thermally unstable compounds common in OGSR such as nitroglycerin and nitrosodiphenylamines will not survive analysis without being denatured. Liquid chromatography paired with mass spectrometry (LCMS) has shown a high sensitivity and rapid results without the drawback of making thermally unstable compounds denature during analysis [4]. There will be limitations in instrumentation available for this study, as such; we will be using GC/MS. This will limit the potential compounds to those that are thermally stable. In contrast to this, a review of current capabilities released by Goudsmits et al. in 2015 determined spectroscopy has many capabilities and conveniences that chromatography would not be capable of. It also highlighted articles in which Ion Mobility Spectrometry (IMS), Raman, and FTIR could identify OGSR compounds [22].

Table 5
Advantages and disadvantages of recent analytical developments in OGSR analysis

Technique	Advantages	Disadvantages
SPME-GC-MS	Simultaneous extraction and preconcentration	Laboratory based technique
	Simple method	Relatively slow (around 30 min)
	No solvents required	Unsuitable for non-volatiles
	Applicable to solid, liquid and gaseous samples	
	Over 70 OGSR compounds already detected	
	Confirmatory technique	
UPLC-MS/MS	Relatively fast (8 min)	Laboratory based technique
	Better resolution than HPLC-MS	Not applicable to airborne samples
	Positive and negative ions in single run	Laborious sample preparation
	Around 20 OGSR compounds already detected	Solvents needed
	Confirmatory technique	
IMS	Rapid (seconds)	May be unsuitable for complex mixtures
	Real time analysis	More false positives than GC-MS
	Portable/field deployable	
	Structural information	
	Compatible with SPME & swipe method	
	Low detection limits	
	Simple method	
DESI-MS	Rapid (seconds)	May be unsuitable for complex mixtures
	Real time analysis	Only four OGSR compounds tested
	Portable/field deployable	Not applicable to airborne samples
	Structural information	
	No separate sample prep or collection method required	
	Subsequent SEM-EDX on same sample possible	
	Simple method	
Raman/FTIR	Non-destructive	Laboratory based technique
	OGSR and IGSR	Further development needed
EC	IGSR and OGSR in a single run	Not yet tested on GSR
	Potentially field deployable	Only four OGSR compounds included
	Rapid	Potential peak overlap when adding compounds
	Sensitive	
	Simple method	

Figure 3: Advantages and disadvantages of instrumentation for OGSR Analysis. Original source Goudsmits et al. [22]

One such article in 2012 indicated that Raman had been used to successfully determine methyl centralite, ethyl centralite, dinitrotoluene, and diphenylamine. The authors of the article indicated the OGSR spectra showed great similarity to that of the unfired portion of the ammunition used. Moreover, they indicated it was easy to distinguish between OGSR and materials that could be confused with OGSR like sand, black ballpoint ink, and dried blood [22].

The article in question released in 2012 by Lopez-Lopez et al. set out to determine if ammunition could be distinguished between one another and identified based on peaks of stabilizers present between the fired propellants and the unburned propellants. They had also taken samples of sand, ink, and dried blood. Results indicated presumptive capabilities to distinguish between different ammunitions based on the peaks present for the stabilizers ethyl

centralite and diphenylamine. Spectra for the three contaminants were taken and shown to not overlap based on the spectra of the burnt and unburnt propellants [23].

However, their methodology is vastly different from that proposed in this study. In the Lopez-Lopez et al. study, samples consisted of gunshot residue retained on cotton cloth and unfired propellent powder. While useful when comparing distinctions between two different propellants, it does not distinguish between the spectra for the OGSR of interest in this study. They did use standards of OGSR compounds, however, the standards of EC1, MC1, 2-4 DNT, and DPA they used were solid standards at a concentration too high to be applicable to OGSR we would likely find at a scene. However, a unique advantage of using a high concentration of OGSR standard and burnt or unburnt particulates for Raman lies in the ability to quickly focus samples in the 50 μm pinhole commonly used for the scope, something this study had difficulty in accomplishing. Because samples of the sand, ink, and dried blood were separated from samples containing GSR, the interaction between the two samples cannot be seen. Masking effects cannot apply if the contaminant in question is not introduced to the OGSR sample itself. This stark discrepancy in the literature led to the inclusion of Raman instrumentation for this study.

Bueno et al. created data supporting the proposed hypothesis that statistical wavenumber data of Attenuated Total Reflectance Fourier Transformed Infrared Spectroscopy (ATR-FTIR) will be similar for the same GSR and different for other GSR profiles. Specific OGSR compounds were shown to have characteristic wavenumbers. For example, nitrocellulose was shown to have characteristic bands during ATR-FTIR analysis at 1629 cm, 1270 cm, and 816 cm. Bueno et al. does acknowledge differentiation will be difficult between residues from similar types of ammunition [24]. However, the data would suggest ATR-FTIR has potential as a

presumptive test for the identification of GSR using OGSR compounds. As such, ATR-FTIR instrumentation was included for the analysis of blood effects in this study due to the lack of literature relating the masking effects of blood to the identification of GSR on a substrate for ATR-FTIR.

To expand on ATR-FTIR research, fabric substrates may pose additional challenges to peak interpretation. Zhenyu et al. demonstrated the effects of fabrics on the peak interpretation of blood proteins. Results indicated the spectral regions of cotton can interfere with the detection limit of blood [39]. Based on these results, it can be interpreted the strong spectral regions for cotton can interfere with the results produced by ATR-FTIR in this study, creating a potential limitation.

In contrast to spectroscopy, studies have been done with GC/MS to determine standard protocols as well as reliability in consistently detecting specific compounds of OGSR. In Joshi et al., solid phase microextraction sampling paired with GC/MS was performed on ethyl centralite, methyl centralite, diethyl phthalate, dibutyl phthalate, 2, 4-dinitrotoluene, nitroglycerin, and nitrosodiphenylamine. Of those, everything but nitroglycerin and nitrosodiphenylamine, two known thermo labile compounds, were able to be detected through analytical GC/MS [17]. In another study performed by Tarifa et al., they used capillary extraction of microvolatiles sampling paired with GC/MS. When looking at samples obtained from swabs collected after firing range field exercises, they determined that when looking for ethyl centralite, diphenylamine, 2,4-dinitroluene, and nitroglycerin, they were only able to detect nitroglycerin and diphenylamine [18]. These tests seem to indicate a gap in analytical replication from standards of OGSR samples to field test OGSR samples. However, this does reinforce the applicability of using GC/MS. GC/MS will also be utilized as instrumentation for this study.

1.5 Gas Chromatography Mass Spectrometry

The underlying principles of each instrumentation utilized will be described in detail, beginning with GC and MS. *The Principles of Instrumental Analysis* by Skoog et al. describes GC as a separation technique capable of component separation and differentiation of a complex mixture. A sample is placed in an inlet, vaporized, and carried by a carrier gas through a column with a solid phase wall. Interactions with this wall cause analytes to elute at varying times through a detector [29]. The mobile phase, or carrier gas, must be a gas that is chemically inert; though Helium is usually used. In some cases, argon, nitrogen, and hydrogen may also be used. These gases do not interact with the analyte at all, merely transport it through the column to the detector. For columns, two different types exist. Packed chromatographic columns, which have been largely replaced by the second type, capillary columns. The capillary columns can vary in length up to 100 meters and are generally constructed of fused silica or stainless steel. The column is generally wrapped around a holder and placed in an oven held at a specific temperature. Depending on the boiling point of the analytes of interest, this temperature will vary. It also can be programmed to ramp up in temperature throughout the elution process to decrease elution time [29]. Multiple detection systems are available, including MS.

Taudte et al. states mass spectrometry is ideal instrumentation in the analysis of organic gunshot residue. It is much more sensitive to smaller quantities of particulates than other instrumentations [2]. This is important because OGSR is in microgram (ug) to nanogram (ng) levels of concentration [2]. As an example, methyl centralite has been detected on the hands of shooters from 3 nanograms to 19 nanograms [2]. There are four phases to an MS system. The first involves an ion source that ionizes the compounds. This works by knocking electrons off a vaporized source to form a positive ion. The second step accelerates the ions to the same speed,

creating a homogenous control for the deflection that will occur next. The third step involves a mass analyzer, a large electromagnet that will separate the compounds according to a mass to charge ratio (*m/z*). The lighter ions will be deflected more while heavier ions will be deflected less. Finally, the detector will generally be a charged anode that when an ion hits it, it will produce many electrons that will be analyzed. This is detected as an electrical current created when a metal ion in the detector shifts to the flowing ions. The electrical current is interpreted by software and given as a mass to charge ratio for each ion [2, 11]. Afterwards, the results are shown as a spectra.

The results of a mass spectrometer are known as a mass spectrum and is shown as a stick diagram. The vertical axis relates to the abundance of the ion called "relative abundance", while the horizontal axis is the measured mass to charge ratio. When looking at organic compounds, these ions are known as "fragments". These will either be the positive fragment ions we see on the diagram, or uncharged free radicals that will be excised by the vacuum pump and not show up on the mass spectrum diagram. Generally, compounds will have many positive ions, though

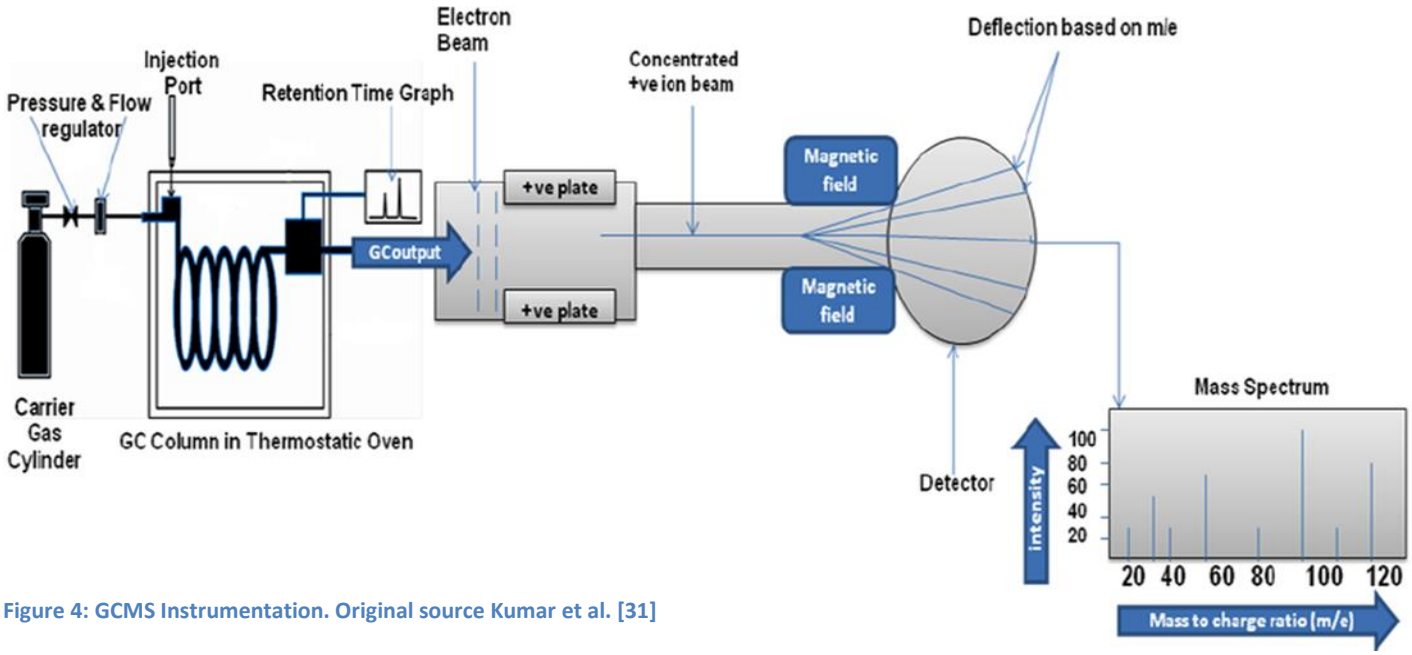

Figure 4: GCMS Instrumentation. Original source Kumar et al. [31]

only those in relatively high abundance will be of importance [10]. The high abundance ions produced by the above MS process can be used for quantitative interpretation. The ratios of the highest three ions called for a vaporized substance can be compared to one another as ratios and compared to the ratios of those same ions in a known standard of the vaporized substance. If this data is combined with the retention time of the substance on the GC column, an analyst may interpret the identity of the substance as the same or different from the standard.

1.6 Raman Spectroscopy

Raman spectroscopy is described as a spectroscopy technique that provides complementary data to that of IR techniques. Raman scattering, the energy being measured, are caused by a laser source hitting a sample, the energy that is scattered from this interaction is measured at an angle. This causes absorption bands that elute as measurable wavenumbers. Because the scattered radiation is close or in the visible region, more sensitive detectors can be used. This helps prevent issues caused by fluorescence during analysis [29]. Generally, the instrumentation necessary for Raman analysis include a laser source, an illumination system for the sample, a wavelength selector, a radiation transducer, and computer software for interpretation. Lasers are necessary as a radiation source due to the low signal to noise ratio they produce. An illumination system is generally the substrate that a sample is placed on. Because the read radiation is close to near visible light, glass or quartz slides are used. A wavelength selector separates the Raman scattering into Raman lines that are measured, and background Rayleigh scattered radiation that would interfere with analysis. Recently notch filters have been utilized for this purpose. These, combined with high quality grating monochromators, are in most commercial Raman instruments. The radiation transducer turns the radiation signal into an

electrical signal that can be read by software. Lastly, the software allows for the interpretation of wavenumbers associated with the scattered properties of the samples [29].

When using Raman, a substrate must be used for the analyte to be placed on. Normally, glass or quartz slides are used as a substrate for materials that would be analyzed for Raman. However, because of the low concentrations of the compounds used in this study, the application of Surface enhanced Raman Scattering (SERS) was necessary. The use of a reflective material can increase Raman signals up to 10^{10} the initial signal. Materials such as gold, silver, copper, or aluminum are commonly used for SERS [37].

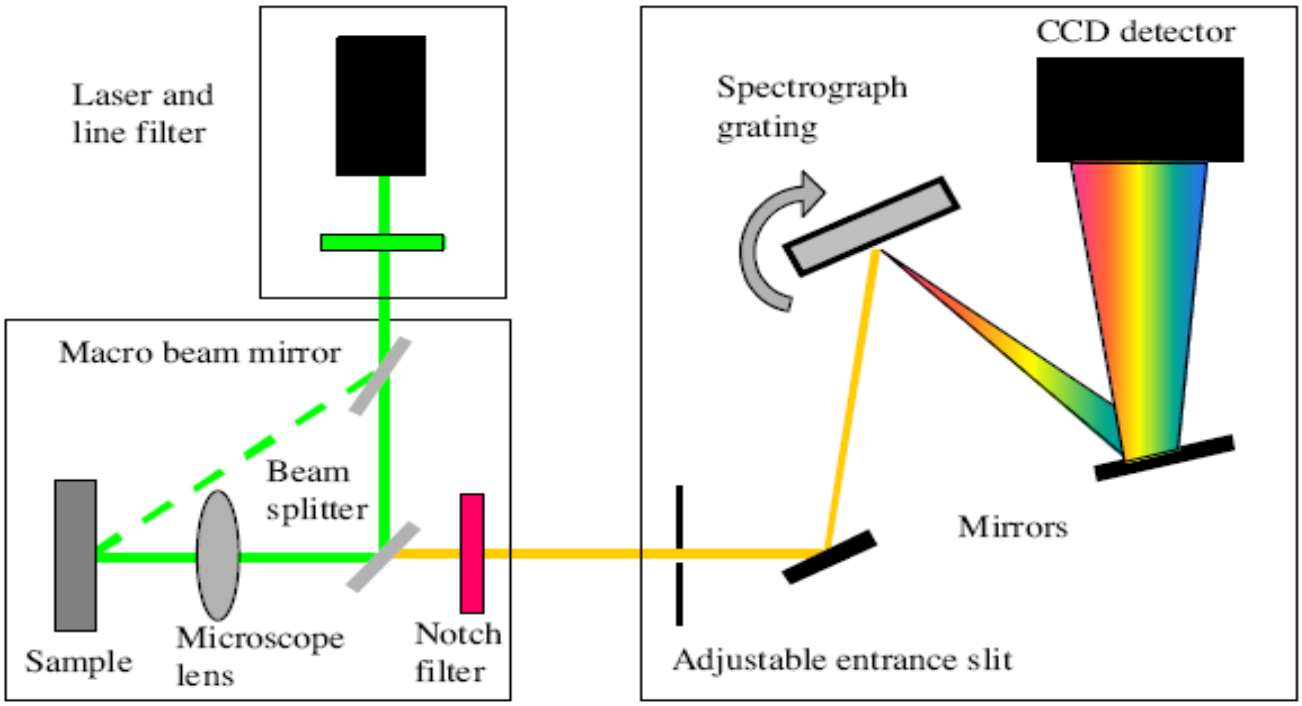

Figure 5: Raman instrument. Original source sas.upenn.edu

1.7 Attenuated Total Reflectance Fourier Transformed Infrared Spectroscopy

Another spectroscopy method utilized for this will be ATR-FTIR. In IR spectroscopy, the wavenumbers range from 12,800 cm^{-1} all the way to 10 cm^{-1}. This is divided into the near, mid, and far IR regions. For our purposes, we will be discussing and employing methods used for the

mid IR region. When mid IR instrumentation began, it was generally based on diffraction instrumentation. Over time, Fourier transform instrumentation became available, increasing distance in signal to noise ratio and improving detection limits as a result. Further on, Attenuated Total Reflectance allowed for a crystal apparatus to be used to penetrate a sample with IR with little to no preparation beforehand [29].

Unlike Raman, mid IR spectra occur from energy taking molecules from one energy state to another. This change in energy is what account for the wavenumbers seen. Molecular vibrations occur causing this energy change. They are categorized as either stretching or bending motions. Much like Raman, IR relies on a source, wavelength selector, detector, and computer system. There are multiple different types of sources, and the premise is they are heated to a point they release radiation. [29] From here, dispersive and Fourier transform differ. Dispersive involves the use of grating to separate wavelengths through individual slits and are measured one at a time at a detector. FTIR, in comparison, uses a beam splitter, two mirrors, a laser, and a detector to recombine two different beams at a beam splitter. One beam travels faster than the other creating an interference pattern, creating an interferogram. This travels to the sample and creates transmitted energy. This travels to the detector to be read [30]. FTIR offers many advantages over dispersive IR. Dispersive tends to have mechanical issues due to more moving parts, is sensitive to interfering light and heat, is slow. The FTIR negates all these disadvantages.

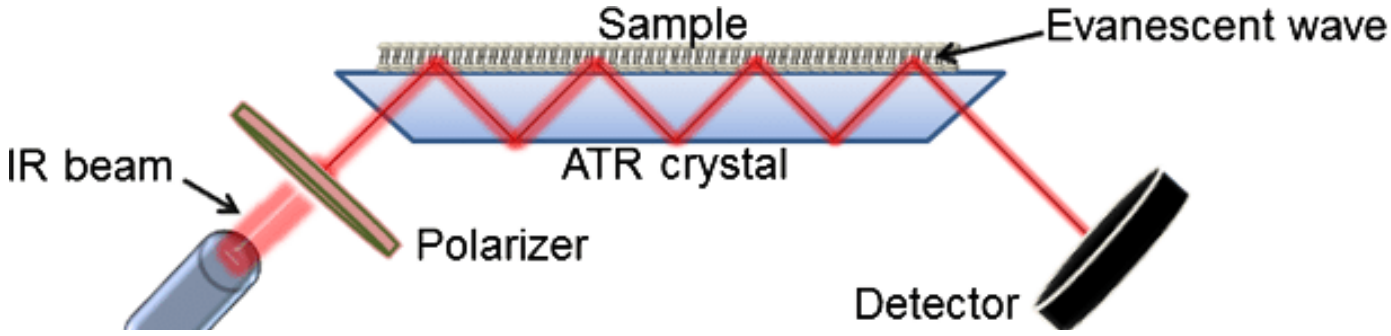

Figure 6: ATR-FTIR schematic. Original source Ausili et al. [32]

However, the double beam optics of dispersive IR collects backgrounds in real time, whereas with FTIR a background must be collected frequently to subtract from the sample [29].

Organic compound characteristic fragmentation patterns are known for compounds of interest in this study. These will be listed in descending order of most relevant ions to least relevant ions. Ethyl centralite has relevant ions at 120 *m/z*, 148 *m/z*, and 77 *m/z* [12], methyl centralite at 134 *m/z*, 106 *m/z*, and 77*m/z* [13], 2-4 dinitrotoluene at 165 *m/z*, 89 *m/z*, and 63 *m/z* [20], diphenylamine at 169 *m/z*, 168 *m/z*, and 167 *m/z* [21], nitroglycerin at 46 m/z, and 76 *m/z* [14], and nitroguanidine at 58 *m/z*, and 104 *m/z* [15].

Spectroscopy has also been successful in the identification of OGSR compounds. Specifically, Raman Spectroscopy and ATR-FTIR. Theoretical and practical wavenumbers have been identified for both instrumentation for the compounds of interest for this study. These values are listed in table 1.

Spectral Wavenumbers									
EC1 Raman	EC1 ATR-FTIR	MC1 Raman	MC1 ATR_FTIR	DPA Raman	DPA ATR-FTIR	2-4 DNT Raman	2-4 DNT ATR-FTIR	100% Cotton	Blood
342 cm-1	616 cm-1	327 cm-1	608 cm-1	130 cm-1	406 cm-1	219 cm-1	705 cm-1	3333 cm-1	699 cm-1
400 cm-1	642 cm-1	398 cm-1	643 cm-1	221 cm-1	436 cm-1	400 cm-1	732 cm-1	3286 cm-1	1078 cm-1
416 cm-1	696 cm-1	454 cm-1	694 cm-1	241 cm-1	489 cm-1	439 cm-1	791 cm-1	2897 cm-1	1160 cm-1
433 cm-1	753 cm-1	488 cm-1	752 cm-1	306 cm-1	501 cm-1	473 cm-1	835 cm-1	1637 cm-1	1245 cm-1
459 cm-1	776 cm-1	543 cm-1	781 cm-1	331 cm-1	567 cm-1	600 cm-1	917 cm-1	1428 cm-1	1390 cm-1
482 cm-1	830 cm-1	592 cm-1	830 cm-1	350 cm-1	612 cm-1	715 cm-1	1067 cm-1	1363 cm-1	1530 cm-1
498 cm-1	915 cm-1	621 cm-1	924 cm-1	407 cm-1	644 cm-1	750 cm-1	1151 cm-1	1334 cm-1	1600-1700 cm-1
552 cm-1	948 cm-1	651 cm-1	974 cm-1	415 cm-1	688 cm-1	793 cm-1	1205 cm-1	1314 cm-1	2800-3100 cm-1
608 cm-1	970 cm-1	698 cm-1	1023 cm-1	441 cm-1	698 cm-1	823 cm-1	1345 cm-1	1278 cm-1	2870 cm-1
618 cm-1	1024 cm-1	715 cm-1	1043 cm-1	491 cm-1	745 cm-1	836 cm-1	1529 cm-1	1205 cm-1	2960 cm-1
643 cm-1	1043 cm-1	757 cm-1	1073 cm-1	507 cm-1	791 cm-1	984 cm-1	1604 cm-1	1160 cm-1	3200-3500 cm-1
695 cm-1	1073 cm-1	776 cm-1	1089 cm-1	569 cm-1	840 cm-1	1043 cm-1		1104 cm-1	
710 cm-1	1088 cm-1	840 cm-1	1119 cm-1	586 cm-1	873 cm-1	1100 cm-1		1054 cm-1	
786 cm-1	1122 cm-1	949 cm-1	1132 cm-1	610 cm-1	904 cm-1	1134 cm-1		1029 cm-1	
839 cm-1	1132 cm-1	976 cm-1	1169 cm-1	617 cm-1	970 cm-1	1154 cm-1		1000 cm-1	
909 cm-1	1177 cm-1	1006 cm-1	1218 cm-1	641 cm-1	988 cm-1	1205 cm-1		983 cm-1	
941 cm-1	1258 cm-1	1030 cm-1	1283 cm-1	703 cm-1	1022 cm-1	1212 cm-1		897 cm-1	
976 cm-1	1280 cm-1	1077 cm-1	1295 cm-1	751 cm-1	1050 cm-1	1240 cm-1		701 cm-1	
1006 cm-1	1295 cm-1	1112 cm-1	1311 cm-1	801 cm-1	1079 cm-1	1347 cm-1		662 cm-1	
1026 cm-1	1311 cm-1	1127 cm-1	1361 cm-1	818 cm-1	1152 cm-1	1356 cm-1		608 cm-1	
1078 cm-1	1355 cm-1	1155 cm-1	1430 cm-1	833 cm-1	1172 cm-1	1415 cm-1		557 cm-1	
1121 cm-1	1376 cm-1	1178 cm-1	1454 cm-1	840 cm-1	1180 cm-1	1448 cm-1		519 cm-1	
1155 cm-1	1392 cm-1	1219 cm-1	1469 cm-1	875 cm-1	1219 cm-1	1541 cm-1		436 cm-1	
1172 cm-1	1443 cm-1	1287 cm-1	1496 cm-1	879 cm-1	1242 cm-1	1543 cm-1		398 cm-1	
1259 cm-1	1454 cm-1	1295 cm-1	1585 cm-1	906 cm-1	1246 cm-1	1580 cm-1		343 cm-1	
1287 cm-1	1493 cm-1	1322 cm-1	1590 cm-1	992 cm-1	1314 cm-1	1611 cm-1			
1310 cm-1	1581 cm-1	1362 cm-1	1649 cm-1	998 cm-1	1390 cm-1	1618 cm-1			
1349 cm-1	1598 cm-1	1433 cm-1	2910 cm-1	1029 cm-1	1417 cm-1	1900 cm-1			
1360 cm-1	1640 cm-1	1457 cm-1	2970 cm-1	1073 cm-1	1458 cm-1	2020 cm-1			
1381 cm-1	2865 cm-1	1470 cm-1	3004 cm-1	1086 cm-1	1494 cm-1				
1397 cm-1	2942 cm-1	1500 cm-1	3038 cm-1	1150 cm-1	1517 cm-1				
1442 cm-1	2978 cm-1	1597 cm-1	3055 cm-1	1160 cm-1	1595 cm-1				
1462 cm-1	2990 cm-1	1653 cm-1	3064 cm-1	1174 cm-1	2972 cm-1				
1497 cm-1	3054 cm-1	2912 cm-1		1178 cm-1	3002 cm-1				
1587 cm-1	3063 cm-1	2976 cm-1		1220 cm-1	3032 cm-1				
1594 cm-1		3009 cm-1		1241 cm-1	3088 cm-1				
1643 cm-1		3047 cm-1		1249 cm-1	3186 cm-1				
2876 cm-1		3060 cm-1		1281 cm-1	3381 cm-1				
2908 cm-1		3069 cm-1		1297 cm-1	3404 cm-1				
2948 cm-1				1305 cm-1					
2976 cm-1				1318 cm-1					
2996 cm-1				1336 cm-1					
3014 cm-1				1416 cm-1					
3048 cm-1				1457 cm-1					
3061 cm-1				1496 cm-1					
3071 cm-1				1511 cm-1					
				1580 cm-1					
				1593 cm-1					
				1603 cm-1					
				3051 cm-1					
				3063 cm-1					
				3081 cm-1					
				3162 cm-1					

Table 1: Raman and ATR-FTIR Wavenumbers

1.8 Blood

Though human blood would have been preferred for this study for field representation purposes, pigs' blood, which this study will use, has merit as being structurally like that of human blood. Mistek et al. denoted past research has been done in identifying variations between species of blood. Research indicates that between human, feline, and canine blood, major visual distinctions could not be made between the spectra of each. In order to determine differences, selective chemometrics must be applied [34]. Because of this, when looking at the masking effects of blood from a visual standpoint using spectroscopic methods, pigs' blood should be able to substitute for human blood.

1.9 Summary

In summary, Evidence value of GSR can assist in reconstructing an event through various means. OGSR supports GSR evidence overall, that alone makes it unique and worth approaching as a forensic subject. Environmental effects will always be present at a scene, including blood in the case of a shooting event. It is important to consider this relationship and how blood will affect OGSR evidence value when combined as a mixture.

Because of the unique nature of adding blood into the analysis of OGSR particulates, it became necessary to discard reliable and tested methods of OGSR collection and instead gravitate towards a new method of extraction. Though the technique will take some adjustment, it is worth exploring due to the potential it proposes in studying blood mixed with OGSR. This has future potential as well in that dirt, mud, or other environmental studies may benefit from this extraction method as well.

Finally, advances in instrumentation have made this study possible. GCMS and LCMS have become powerful, combined instrumentation for the analysis of OGSR. Because of limiting factors due to size of OGSR particulates and sensitivity. Previous successful of Raman and ATR-FTIR in OGSR give them merit in their analysis to determine their blood masking effects as well

Materials & Methods

Materials

For this study, pigs' blood was purchased from a local slaughterhouse. IACUC approval was not necessary to seek out for this study. The pigs' blood was left untreated by EDTA to avoid the potential of interference and used immediately upon acquisition for Raman and ATR-FTIR analysis. 2% EDTA pigs' blood was used in GCMS analysis. The interfering potential of EDTA had not been considered for GCMS before data analysis had begun. This blood was used to saturate 100% cotton at 11mm by 11mm squares from a Gildan® large t-shirt. The no EDTA additive blood was used for ATR-FTIR and Raman substrates while the 2% EDTA treated blood was used for GCMS substrates. This substrate preparation was used for all three instrumentations.

Solvents were used to dilute samples from standards. Solvents of interest included acetonitrile (ACN), methyl tert-butyl ether (MTBE), acetone, methanol, and dichloromethane (DCM). Generally, these are known and accepted solvents for use during OGSR analysis known for their relatively high extraction efficiencies over a wide range of explosive compounds [16]. Two liters of methanol (Sigma-Aldrich) were used for sample preparation for all samples.

Stock solutions of Ethyl Centralite, Methyl Centralite, 2-4 Dinitrotoluene, Diphenylamine, Nitroglycerin, and Nitroguanidine were purchased from Accustandard in 1 mL ampules at a concentration of 100 ug/mL. The stock solution solvents consisted of diphenylamine in dichloromethane, 2-4 dinitrotoluene in 50:50 methanol (MeOH) and acetonitrile (AcCN), ethyl centralite in 50:50 MeOH and AcCN, methyl centralite in 50:50 MeOH and AcCN, nitroglycerin in 50:50 MeOH and AcCN, and nitroguanidine in MeOH. These

were utilized for the entirety of GCMS instrumentation and initial trials during Raman and ATR-FTIR analysis. Later analysis using Raman and ATR-FTIR required higher concentration stock solutions. 100 grams of solid Ethyl Centralite, 2-4 Dinitrotoluene, and DPA were purchased from Sigma-Aldrich. Autosampler vials at 9mm and 2mL volume with screw cap threads were purchased from Fisher Scientific for GCMS sample analysis.

Instrumentation used included a BTLab System MINI Dry Bath for sample drying. This system consisted of a hot water bath paired with nitrogen drying to quickly evaporate samples to be reconstituted. For GCMS, an Agilent 6890N Gas Chromatograph with a DB-5ms column paired with an Agilent 5975 Mass Selective Detector using Chemstation software was utilized. These were paired with an Agilent 7683B Series Injector autosampler for automated sample injection.

Raman spectroscopy analysis was conducted using a Thermo Scientific DXR Raman Microscope utilizing OMNIC software. A Thermo Scientific Nicolet iS10 instrument utilizing OMNIC software was used for ATR-FTIR analysis.

Methods

Samples were first prepared for GCMS analysis. Stock solutions were opened and using glass pipettes, transferred to autosampler vials. These stock solutions were used to create samples at 10 ug/mL, 5 ug/mL, 3 ug/mL, 2 ug/mL, 1 ug/mL, and 0.5 ug/mL. Method development began to determine a standard method useable for GCMS analysis of each compound, as well as the limit of detection of each sample. Different inlet temperatures, oven temperatures, and oven ramp temperatures were utilized to determine greatest peak separation with reasonable elution times. Blanks were run at the beginning of every day and voltage checks were performed at the end of each day.

The method designated "UNI1" was utilized for general scan analysis. The parameters for this consist of an inlet temperature of 280℃, utilizing pulsed/splitless injection. The oven had an initial temperature of 60℃ and had three ramping temperature changes. Ramp 1 increased the temperature by 20℃ per minute for 5 minutes, up to 250℃. Ramp 2 brought the temperature to 240℃, followed by an increase at ramp 3 to the final temperature of 270℃. The run consisted of a 2-minute solvent delay with a total run time of 16 minutes with a helium carrier gas. An autotune file was utilized to keep consistency with the voltage for the instrument. Lastly, the column, a DB-5ms, was 30 meters in length, had a 250 μm internal diameter, and a .25 um film thickness.

When utilizing scan mode for individual compounds, four separate methods designated "EC1 SIM", "MC1 SIM", "2-4 DNT SIM", and "DPA SIM" were utilized. Scan mode allows for the visualization of all ions present in a mixture analyzed through GCMS, whereas SIM mode

targets specific ions the examiner designates. For EC1, MC1, 2-4 DNT, and DPA, each SIM mode was set to *m/z* ions as designated in the literature review.

Using method UNI1, standards were run at 100 ug/mL to confirm the presence of ions of interest at repeatable elution times for each compound. These were used as retention time and ion ratio targets for further compound analysis at lower concentrations under varying conditions. These samples were manually injected at 1 µL, leading to 100 ng/µL on column. All samples were injected at 1 µL, leading to 100 ng/µL, 10 ng/µL, 5 ng/µL, 3 ng/µL, 2 ng/µL, 1 ng/µL, and .5 ng/µL concentrations on column, respectively. Nitroglycerin and Nitroguanidine did not elute through GCMS at 100 µg/mL. This is most likely due to their thermolabile properties causing degradation in the inlet. Multiple degradations lead to Nitroglycerin and Nitroguanidine being discarded as compounds of interest from the study.

After retention times and target ions were established for EC1, MC1, 2-4 DNT, and DPA, limit of detection analysis began. All samples at 10 ug/mL or lower were run with their respective SIM mode methods. 10 ug/mL and 5 ug/mL samples were run as 6 replicates, while 3 ug/mL, 2 ug/mL, 1 ug/mL, and .5 ug/mL samples were run in triplicate. Manual injections were performed at 1 µL volumes for the first three 10 ug/mL and 5 ug/mL samples. Once automated injection became available, it was utilized for all further samples.

Samples were created with the compound of interest saturating pieces of cotton. To do this, 10 ug/mL and 5 ug/mL samples were created for each of the four compounds. These were placed on a 50 cm^2 piece of 100% cotton cloth separately. These cloths were hung to dry using a wire stand and alligator clips. After drying, each cloth was placed in an Eppendorf tube with 6 mL of methanol and vortexed for approximately five minutes. The cloth was then removed from

the solvent and originally were placed in a beaker to air dry in a fume hood. However, because this process could take up to 48 hours, alternative means of drying were sought. A BTLab System MINI Dry Bath was purchased and utilized to dry samples. Once dry, the samples were reconstituted in 1 mL of methanol, and placed into individual micro vials. These samples were run using their respective SIM methods in triplicate.

Samples were then created with the compound of interest saturating pieces of cotton which were then masked with 2% EDTA pigs' blood. To do this, three samples of 10 ug/mL were created for each of the four compounds. These were placed on a 50 cm^2 piece of 100% cotton cloth separately. These cloths were hung to dry using a wire stand and alligator clips. After drying, each cloth was placed in an Eppendorf tube with 6 mL of methanol and vortexed for approximately five minutes. The cloth was then extracted from the solvent and dried using a BTLab System MINI Dry Bath. Once dry, the samples were reconstituted in 1 mL of methanol, and placed into individual micro vials. Using their respective SIM methods, samples were run in four replicates each, creating a total of 12 blood replicates for each compound.

Samples created for Raman examination were run at concentrations of 100 ug/mL. Volumes of 10 µL were placed on glass slides covered with foil. Foil, for SERS, was chosen as a substrate to enhance the intensity of the Raman signal given off by the OGSR compounds. The first samples created were 50 ul in total and a second set of samples were 100 ul in total. Afterwards, quartz slides were utilized using the same volumes. The sample area was encircled by an 11mm diameter circle of china marker. This ensured samples would not spread out and rather layer on top of each other. 50 ul volumes were run in 15 replicates, while 100 ul volumes were run in five replicates. The method utilized was designated "TW Default". Samples were run with a 780 nm laser at 20 mW power. Samples were taken in 10 scans with a 5 second exposure

each, with an additional 10 background exposures. The aperture used was a 50 μm pinhole. Additional samples were planned to be prepared at 40 μL, 30 μL, 20 μL, and 10 μL volumes to determine a limit of detection. However, issues with repeatability of results for the 50 μL and 100 μL volumes did not make it necessary to reduce the volume.

ATR-FTIR analysis consisted of multiple samples created using solid compounds of EC1, 2-4 DNT, and DPA. The goal of this study was for both to determine the limit of detection of these straight OGSR compounds separate of one another and the effect blood has on masking wavenumbers presented in their spectra. Multiple methods utilizing different resolutions and number of scans were tested for efficacy. The final method utilized, designated "128 scans res 2 TW", consisted of 128 scans with a resolution of two per sample. Backgrounds were taken every hour. Solid samples were run in triplicate to establish standards that all lower concentrations would utilize to identify wavenumbers and concentrations in which wavenumbers were not detected.

Dilutions at 10,000 ug/mL, 1,000 ug/mL, 800 ug/mL, 600 ug/mL, 400 ug/mL, and 200 ug/mL were created and used for limit of detection analysis. Samples for this purpose wulere placed directly on the ATR diamond using 1 μL volumes. Each 1 μL volume was allowed to dry and another 1 μL volume was placed over the next, up to a total volume of 5 μL. Along with this, samples were created on 100% cotton cloth substrate at 50cm^2. This consisted of compounds diluted in methanol at 10,000 ug/mL and 1,000 ug/mL concentrations applied to the cotton at a volume of 500 μL. Further samples had these volumes placed on the cotton substrate and then covered with 1 mL of pigs' blood untreated with EDTA. In all cases, the compounds were allowed to dry completely onto the cloth substrate. For blood samples, the blood was allowed to dry completely over the top of the substrate and compounds of interest. All these samples were

run in triplicate with the designated methodology. All cloth samples were analyzed face down, with the side the compounds were applied to facing down towards the ATR diamond.

After sample analysis was complete, subtractions were performed to determine the remaining wavenumbers and abundances of compounds on the cloth substrate as well as samples in which blood was applied over the compounds of interest. Samples of 100% cotton without compounds of interest applied to them and straight blood samples were taken as reference spectra to subtract out contamination from that of the spectra of the compounds of interest applied to cloth and cloth masked with pigs' blood.

Method Development

This study was intended to be a field study in which range fired gunshot residue samples would be utilized. However, many alterations occurred to this study, transitioning it more towards a method development study. First, range samples in which ammunition was purchased to create gunshot residue samples were not performed. This change occurred due in part to GCMS analysis requiring lengthy development of a proper method as well as confirmation of its consistency and reliability with samples of interest. Though former studies utilized standards of the OGSR compounds of interest, they did not perform limit of detection studies for individual compounds. Instead, the standards were compared against peaks found in whole burnt or unburnt GSR particles. Other studies utilized injections from the headspace of the sample, instead of directly injecting the prepared sample. Our goal was to create a method that utilized a limit of detection study with a sample injected directly into the inlet.

As the study continued, complications with the GCMS instrumentation caused further delays. This included issues with hardware malfunction, increased machine upkeep to keep the column clean, and troubleshooting a sequence run. Due to these issues, different sample extraction methods initially planned to test for efficacy were not tested. Initially, samples were going to be extracted using dampened swabs, aluminum stubs, and extracting a small portion of the cloth where the sample was deposited to be directly extracted in solvent. The solvent extraction method was instead utilized for the whole sample, while the swabs and aluminum stubs were not utilized in this study. Other substrates were also considered for this study including, polyester and nylon. These were also not utilized in this study, due to time constraints.

The next major development occurred due to problems finding a reliable GCMS internal standard. For all four major components, no one internal standard had been designated in the literature. Multiple compounds were analyzed alongside all four compounds including 4-Nitrophenol, Naphthalene, 1-Napthol, and Trinitrotoluene at 10 ug/mL and 100 ug/mL alongside 100 ug/mL of each four compounds, separately, as a mixture. None of these internal standards eluted with the compound of interest remaining intact. A dissertation by Dennis indicated the use of Undecane for OGSR analysis using GCMS [35]. However, the GCMS instrumentation was no longer available to test Undecanes applicability. The solvents we had available would also not work as methanol is too polar to dissolve Undecane.

Another development occurred when attempting to acquire samples of a higher concentration for Raman and ATR-FTIR. This purchase was necessary to alleviate difficulties in identifying the compounds at the concentration of 10 ug/ml. Bottles of 100 grams of EC1, DPA, and 2-4 DNT (Sigma-Aldrich) were acquired. However, a source for compound MC1 could not be located. Because of this, MC1 was not analyzed during spectroscopic trials.

The final development occurred when attempting to analyze samples using Raman spectroscopy. Previous studies had used partial burnt and unburnt GSR particles in the analysis of OGSR samples. Because the aim of the study is to determine the masking effects of blood on the four individual OGSR compounds of interest, neat samples of low concentration were utilized for this study. Issues occurred with visualizing samples using the 50um pinhole. Results became difficult to replicate due to this inconsistency. Though visualization techniques such as fluorescent hyperspectral imaging may allow for this necessary visualization, it was not available for this study. Because of this issue, Raman spectroscopy was not utilized further in this study.

Results

Data for GCMS analysis as indicated by tables 1 to 4 compare the retention times and the ion ratios of samples to that of the standard runs indicated at the top of the tables. Ion ratios that fall within + or – 20% to the standard with retention times falling within + or – 5% indicate the compound of interest is present in the sample. These percentages provide a reasonable range in which the sample can be shown to qualitatively represent the standard identity. These percentages are commonly accepted standards as applied to GCMS [38]. Samples with ratios and retention times falling within those standards were accepted, while those that did not fall within those standards were rejected. If one or more rejections occurred within a sample, the target compound was indicated as not present. Peak resolutions of the compounds were also taken and are generally accepted at + or – 10%. Peak resolutions were not used to determine the presence of a compound but are an indicator of peak quality.

These results indicate that based on these parameters, EC1, MC1, and DPA eluted effectively down to a limit of 0.5 ng/ul on column and were not masked by the presence of 100% cotton cloth or 2% EDTA pigs' blood. Below 10 ng/ul on column, 2-4 DNT did not consistently elute properly. 100% cotton, as well as the 2% EDTA pigs' blood also caused elution problems with 2-4 DNT. Additional peaks present during 100% cotton and 2% EDTA pigs' blood samples were not identified due to the analysis being performed in SIM mode. When using SIM mode, the NIST database is unable to identify the composition of peaks.

GCMS

Ethyl Centralite

Standards:	Rt (min)	Ion 120 (1) abund	Ion 148 (2) abund	Ion 77 (3) abund	Ratio 1:2	Ratio 1:3	Ratio 2:3
1	11.223	999	704	481	999:704	999:481	704:481
2	11.235	999	715	536	999:715	999:536	715:536
Average:	11.229	999	709.5	512	999:709.5	999:512	709.5:512
SD:	0.008485	0	7.778	38.891	0.015	0.151	0.092
CV:	0.000756	0	0.011	0.076	0.011	0.076	0.066

	RT Acceptable Range:	10.668 : 11.790	+/- 5%
	Ratio 1:2 Acceptable Range:	1.126 : 1.690	+/- 20%
	Ratio 1:3 Acceptable Range:	1.561 : 2.341	+/- 20%
	Ratio 2:3 Acceptable Range:	1.109 : 1.663	+/- 20%

Samples:	Rt (min)	Ion 120 abund	Ion 148 abund	Ion 77 abund	Ratio 1:2	Ratio 1:3	Ratio 2:3	Rt OK?	Ratio 1 OK?	Ratio 2 OK?	Ratio 3 OK?	Target Compound Present?	Peak Resolution
100ng/ul	11.222	999	732	628	1.365	1.591	1.166	yes	yes	yes	yes	yes	100/100
100ng/ul	11.224	999	709	554	1.409	1.803	1.280	yes	yes	yes	yes	yes	100/100
100ng/ul	11.222	999	702	512	1.423	1.951	1.371	yes	yes	yes	yes	yes	100/99
10ng/ul	11.228	999	677	548	1.476	1.823	1.235	yes	yes	yes	yes	yes	100/100
10ng/ul	11.228	999	739	503	1.352	1.986	1.469	yes	yes	yes	yes	yes	100/100
10ng/ul	11.228	999	720	497	1.388	2.010	1.449	yes	yes	yes	yes	yes	100/99
5ng/ul	11.228	999	702	531	1.423	1.881	1.322	yes	yes	yes	yes	yes	100/100
5ng/ul	11.215	999	705	482	1.417	2.073	1.463	yes	yes	yes	yes	yes	100/100
5ng/ul	11.237	999	750	494	1.332	2.022	1.518	yes	yes	yes	yes	yes	100/100
5ng/ul	11.228	999	765	491	1.306	2.035	1.558	yes	yes	yes	yes	yes	100/97.2
3ng/ul	11.237	999	820	612	1.218	1.632	1.340	yes	yes	yes	yes	yes	100/99
3ng/ul	11.215	999	680	444	1.469	2.250	1.532	yes	yes	yes	yes	yes	99/100
3ng/ul	11.232	999	723	591	1.382	1.690	1.223	yes	yes	yes	yes	yes	100/100
2ng/ul	11.21	999	627	505	1.593	1.978	1.242	yes	yes	yes	yes	yes	100/100
2ng/ul	11.215	999	685	440	1.458	2.270	1.557	yes	yes	yes	yes	yes	98.5/100
2ng/ul	11.215	999	673	438	1.484	2.281	1.537	yes	yes	yes	yes	yes	100/98.1
1ng/ul	11.215	999	689	488	1.450	2.047	1.412	yes	yes	yes	yes	yes	100/100
1ng/ul	11.215	999	700	445	1.427	2.245	1.573	yes	yes	yes	yes	yes	96.9/100
1ng/ul	11.215	999	678	448	1.473	2.230	1.513	yes	yes	yes	yes	yes	100/100
.5ng/ul	11.215	999	727	487	1.374	2.051	1.493	yes	yes	yes	yes	yes	100/100
.5ng/ul	11.215	999	719	462	1.389	2.162	1.556	yes	yes	yes	yes	yes	95.3/100
.5ng/ul	11.215	999	680	482	1.469	2.073	1.411	yes	yes	yes	yes	yes	100/91.3
10ng/ul Cotton	11.228	999	715	539	1.397	1.853	1.327	yes	yes	yes	yes	yes	96.3/100
10ng/ul Cotton	11.228	999	719	554	1.389	1.803	1.298	yes	yes	yes	yes	yes	96.5/100
10ng/ul Cotton	11.228	999	742	536	1.346	1.864	1.384	yes	yes	yes	yes	yes	96.4/100
5ng/ul Cotton	11.224	999	699	535	1.429	1.867	1.307	yes	yes	yes	yes	yes	97.6/100
5ng/ul Cotton	11.224	999	690	556	1.448	1.797	1.241	yes	yes	yes	yes	yes	97.4/100
5ng/ul Cotton	11.228	999	781	490	1.279	2.039	1.594	yes	yes	yes	yes	yes	97.5/100
10ng/ul Blood	11.224	999	709	561	1.409	1.781	1.264	yes	yes	yes	yes	yes	97.5/100
10ng/ul Blood	11.228	999	806	501	1.239	1.994	1.609	yes	yes	yes	yes	yes	97.6/100
10ng/ul Blood	**13.803**	999	741	440	1.348	2.270	1.684	**no**	yes	yes	yes	**no**	100/100
10ng/ul Blood	11.215	999	724	469	1.380	2.130	1.544	yes	yes	yes	yes	yes	96.8/100
10ng/ul Blood	11.215	999	729	471	1.370	2.121	1.548	yes	yes	yes	yes	yes	97.8/100
10ng/ul Blood	11.215	999	730	473	1.368	2.112	1.543	yes	yes	yes	yes	yes	96.4/100
10ng/ul Blood	11.215	999	701	468	1.425	2.135	1.498	yes	yes	yes	yes	yes	92.5/100
10ng/ul Blood	11.215	999	678	469	1.473	2.130	1.446	yes	yes	yes	yes	yes	96.3/100
10ng/ul Blood	11.215	999	681	440	1.467	2.270	1.548	yes	yes	yes	yes	yes	95.5/100
10ng/ul Blood	11.215	999	704	449	1.419	2.225	1.568	yes	yes	yes	yes	yes	92/100
10ng/ul Blood	11.215	999	631	495	1.583	2.018	1.275	yes	yes	yes	yes	yes	95.9/100
10ng/ul Blood	11.215	999	627	499	1.593	2.002	1.257	yes	yes	yes	yes	yes	94.1/100

Table 2: GCMS results for EC1

GCMS

Methyl Centralite

Standards:	Rt (min)	Ion 134 (1) abund	Ion 77 (2) abund	Ion 106 (3) abund	Ion 240 (4) abun	Ratio 1:2	Ratio 1:3	Ratio 1:4	Ratio 2:3	Ratio 3:4
1.000	10.971	999	801	656	474	999:801	999:656	999:474	801:656	656:474
2.000	10.947	999	640	595	386	999:640	999:595	999:386	640:595	595:386
3.000	10.962	999	789	635	464	999:789	999:635	999:464	789:635	635:464
Average:	10.960	999	743.333	628.667	441.333	999:743.333	999:628.667	999:441.333	743.333:628.667	628.667:441.333
SD:	0.012	0	89.690	30.989	48.180	0.176	0.080	0.265	0.091	0.096
CV:	0.001	0	0.121	0.049	0.109	0.130	0.050	0.116	0.077	0.067
	RT Acceptable Range:						10.412 : 11.508		+/- 5%	
	Ratio 1:2 Acceptable Range:						1.075 : 1.613		+/- 20%	
	Ratio 1:3 Acceptable Range:						1.271 : 1.907		+/- 20%	
	Ratio 1:4 Acceptable Range:						1.811 : 2.716		+/- 20%	
	Ratio 2:3 Acceptable Range:						0.946 : 1.419		+/- 20%	
	Ratio 3:4 Acceptable Range:						1.140 : 1.709		+/- 20%	

Samples:	Rt (min)	Ion 134 (1) abund	Ion 77 (2) abund	Ion 106 (3) abund	Ion 240 (4) abun	Ratio 1:2	Ratio 1:3	Ratio 1:4	Ratio 2:3	Ratio 3:4	Rt OK?	Ratio 1:2 OK?	Ratio 1:3 OK?	Ratio 1:4 OK?	Ratio 2:3 OK?	Ratio 3:4 OK?	Target Compound Present?	Peak Resolution
100ng/ul	10.954	999	*	627	410	*	1.593	2.437	*	1.529	yes	*	yes	yes	*	yes	yes	100/100
100ng/ul	11.020	999	*	571	374	*	1.750	2.671	*	1.527	yes	*	yes	yes	*	yes	yes	100/100
100ng/ul	10.963	999	*	544	350	*	1.836	2.854	*	1.554	yes	*	yes	yes	*	yes	yes	100/100
10ng/ul	10.961	999	891	715	*	1.121	1.397	*	1.246	*	yes	yes	yes	*	yes	*	yes	100/100
10ng/ul	10.968	999	842	673	*	1.186	1.484	*	1.251	*	yes	yes	yes	*	yes	*	yes	100/100
10ng/ul	10.961	999	761	652	*	1.313	1.532	*	1.167	*	yes	yes	yes	*	yes	*	yes	100/100
10ng/ul	10.961	999	807	666	*	1.238	1.500	*	1.212	*	yes	yes	yes	*	yes	*	yes	100/100
5ng/ul	10.961	999	752	647	*	1.328	1.544	*	1.162	*	yes	yes	yes	*	yes	*	yes	100/100
5ng/ul	10.961	999	845	682	*	1.182	1.465	*	1.239	*	yes	yes	yes	*	yes	*	yes	100/100
5ng/ul	10.961	999	794	651	*	1.258	1.535	*	1.220	*	yes	yes	yes	*	yes	*	yes	100/100
5ng/ul	10.950	999	*	595	404	*	1.679	2.473	*	1.473	yes	*	yes	yes	*	yes	yes	100/100
5ng/ul	10.976	999	*	576	392	*	1.734	2.548	*	1.469	yes	*	yes	yes	*	yes	yes	100/100
5ng/ul	10.963	999	*	560	365	*	1.784	**2.737**	*	1.534	yes	*	yes	**no**	*	yes	**no**	100/100
3ng/ul	10.950	999	*	619	390	*	1.614	2.562	*	1.587	yes	*	yes	yes	*	yes	yes	100/100
3ng/ul	10.967	999	*	524	403	*	1.906	2.479	*	1.300	yes	*	yes	yes	*	yes	yes	100/98.3
3ng/ul	10.954	999	*	599	376	*	1.668	2.657	*	1.593	yes	*	yes	yes	*	yes	yes	100/100
2ng/ul	10.950	999	*	594	392	*	1.682	2.548	*	1.515	yes	*	yes	yes	*	yes	yes	100/100
2ng/ul	19.950	999	*	532	373	*	1.878	2.678	*	1.426	yes	*	yes	yes	*	yes	yes	100/98
2ng/ul	10.954	999	*	540	381	*	1.850	2.622	*	1.417	yes	*	yes	yes	*	yes	yes	100/100
1ng/ul	10.950	999	*	657	411	*	1.521	2.431	*	1.599	yes	*	yes	yes	*	yes	yes	100/96.7
1ng/ul	10.950	999	*	562	378	*	1.778	2.643	*	1.487	yes	*	yes	yes	*	yes	yes	100/93.3
1ng/ul	10.954	999	*	563	392	*	1.774	2.548	*	1.436	yes	*	yes	yes	*	yes	yes	100/96.5
.5ng/ul	10.950	999	*	604	392	*	1.654	2.548	*	1.541	yes	*	yes	yes	*	yes	yes	100/100
.5ng/ul	10.980	999	*	606	406	*	1.649	2.461	*	1.493	yes	*	yes	yes	*	yes	yes	100/100
.5ng/ul	10.963	999	*	652	424	*	1.532	2.356	*	1.538	yes	*	yes	yes	*	yes	yes	100/100
10ng/ul Cotton	10.961	999	905	693	*	1.104	1.442	*	1.306	*	yes	yes	yes	*	yes	*	yes	100/100
10ng/ul Cotton	10.970	999	879	576	*	1.137	1.734	*	**1.526**	*	yes	yes	yes	*	**no**	*	**no**	100/100
10ng/ul Cotton	10.961	999	887	706	*	1.126	1.415	*	1.256	*	yes	yes	yes	*	yes	*	yes	100/91.3
5ng/ul Cotton	10.962	999	718	624	*	1.391	1.601	*	1.151	*	yes	yes	yes	*	yes	*	yes	100/100
5ng/ul Cotton	10.961	999	988	661	*	**1.011**	1.511	*	**1.495**	*	yes	**no**	yes	*	**no**	*	**no**	**100/77**
5ng/ul Cotton	10.961	999	904	690	*	1.105	1.448	*	1.310	*	yes	yes	yes	*	yes	*	yes	100/100
10ng/ul Blood	10.961	999	752	578	*	1.328	1.728	*	1.301	*	yes	yes	yes	*	yes	*	yes	100/100
10ng/ul Blood	10.961	999	665	555	*	1.502	1.800	*	1.198	*	yes	yes	yes	*	yes	*	yes	100/100
10ng/ul Blood	10.962	999	681	572	*	1.467	1.747	*	1.191	*	yes	yes	yes	*	yes	*	yes	100/100
10ng/ul Blood	10.950	999	*	574	390	*	1.740	2.562	*	1.472	yes	*	yes	yes	*	yes	yes	100/100
10ng/ul Blood	10.950	999	*	565	388	*	1.768	2.575	*	1.456	yes	*	yes	yes	*	yes	yes	100/100
10ng/ul Blood	10.950	999	*	551	404	*	1.813	2.473	*	1.364	yes	*	yes	yes	*	yes	yes	100/100
10ng/ul Blood	10.945	999	*	597	391	*	1.673	2.555	*	1.527	yes	*	yes	yes	*	yes	yes	100/100
10ng/ul Blood	10.950	999	*	534	401	*	1.871	2.491	*	1.332	yes	*	yes	yes	*	yes	yes	100/100
10ng/ul Blood	10.950	999	*	584	387	*	1.711	2.581	*	1.509	yes	*	yes	yes	*	yes	yes	100/100
10ng/ul Blood	10.954	999	*	593	374	*	1.685	2.671	*	1.586	yes	*	yes	yes	*	yes	yes	100/96.2
10ng/ul Blood	10.958	999	*	603	392	*	1.657	2.548	*	1.538	yes	*	yes	yes	*	yes	yes	100/100
10ng/ul Blood	10.954	999	*	600	363	*	1.665	**2.752**	*	1.653	yes	*	yes	**no**	*	yes	**no**	100/100

Table 3: GCMS results for MC1

GCMS														
Diphenylamine														
Standards:	Rt (min)	Ion 169 (1) abund	Ion 168 (2) abund	Ion 167 (3) abund	Ratio 1:2	Ratio 1:3	Ratio 2:3							
1	9.72	999	628	346	999:628	999:346	628:346							
2	9.717	999	647	340	999:647	999:340	647:340							
3	9.717	999	656	337	999:656	999:337	656:337							
Average:	9.718	999	643.667	341	999:643.67	999:341	643.67:341							
SD:	0.002	0.000	14.295	4.583	0.035	0.039	0.067							
CV:	0.000	0.000	0.022	0.013	0.022	0.013	0.035							
	RT Acceptable Range:					9.232 : 10.204		+/- 5%						
	Ratio 1:2 Acceptable Range:					1.242 : 1.862		+/- 20%						
	Ratio 1:3 Acceptable Range:					2.344 : 3.516		+/- 20%						
	Ratio 2:3 Acceptable Range:					1.510 : 2.265		+/- 20%						
Samples:	Rt (min)	Ion 169 (1) abund	Ion 168 (2) abund	Ion 167 (3) abund	Ratio 1:2	Ratio 1:3	Ratio 2:3	Rt OK?	Ratio 1:2 OK?	Ratio 1:3 OK?	Ratio 2:3 OK?	Target Compound Present?	Peak Resolution	
100ng/ul	9.706	999	764	496	1.308	**2.014**	1.540	yes	yes	**no**	yes	**no**	100/100	
100ng/ul	9.71	999	663	360	1.507	2.775	1.842	yes	yes	yes	yes	yes	100/100	
100ng/ul	9.71	999	666	381	1.500	2.622	1.748	yes	yes	yes	yes	yes	100/100	
10ng/ul	9.719	999	627	324	1.593	3.083	1.935	yes	yes	yes	yes	yes	100/100	
10ng/ul	9.719	999	626	325	1.596	3.074	1.926	yes	yes	yes	yes	yes	100/100	
10ng/ul	9.719	999	594	292	1.682	3.421	2.034	yes	yes	yes	yes	yes	100/100	
5ng/ul	9.719	999	595	296	1.679	3.375	2.010	yes	yes	yes	yes	yes	100/100	
5ng/ul	9.719	999	601	296	1.662	3.375	2.030	yes	yes	yes	yes	yes	100/100	
5ng/ul	9.719	999	652	362	1.532	2.760	1.801	yes	yes	yes	yes	yes	100/100	
5ng/ul	9.706	999	647	343	1.544	2.913	1.886	yes	yes	yes	yes	yes	100/100	
5ng/ul	9.706	999	634	340	1.576	2.938	1.865	yes	yes	yes	yes	yes	100/100	
5ng/ul	9.706	999	646	377	1.546	2.650	1.714	yes	yes	yes	yes	yes	100/100	
3ng/ul	9.706	999	644	341	1.551	2.930	1.889	yes	yes	yes	yes	yes	100/100	
3ng/ul	9.706	999	666	369	1.500	2.707	1.805	yes	yes	yes	yes	yes	100/100	
3ng/ul	9.706	999	651	357	1.535	2.798	1.824	yes	yes	yes	yes	yes	100/100	
2ng/ul	9.706	999	649	352	1.539	2.838	1.844	yes	yes	yes	yes	yes	100/98	
2ng/ul	9.706	999	645	347	1.549	2.879	1.859	yes	yes	yes	yes	yes	100/100	
2ng/ul	9.706	999	678	383	1.473	2.608	1.770	yes	yes	yes	yes	yes	100/100	
1ng/ul	9.706	999	663	368	1.507	2.715	1.802	yes	yes	yes	yes	yes	100/100	
1ng/ul	9.706	999	656	367	1.523	2.722	1.787	yes	yes	yes	yes	yes	100/100	
1ng/ul	9.71	999	622	343	1.606	2.913	1.813	yes	yes	yes	yes	yes	100/96	
.5ng/ul	9.706	999	646	378	1.546	2.643	1.709	yes	yes	yes	yes	yes	100/94.3	
.5ng/ul	9.71	999	613	327	1.630	3.055	1.875	yes	yes	yes	yes	yes	100/100	
.5ng/ul	9.71	999	641	360	1.559	2.775	1.781	yes	yes	yes	yes	yes	100/93.4	
10ng/ul Cotton	9.715	999	632	331	1.581	3.018	1.909	yes	yes	yes	yes	yes	100/100	
10ng/ul Cotton	9.719	999	612	314	1.632	3.182	1.949	yes	yes	yes	yes	yes	100/100	
5ng/ul Cotton	9.715	999	627	350	1.593	2.854	1.791	yes	yes	yes	yes	yes	100/100	
5ng/ul Cotton	9.715	999	673	385	1.484	2.595	1.748	yes	yes	yes	yes	yes	100/100	
5ng/ul Cotton	9.715	999	656	354	1.523	2.822	1.853	yes	yes	yes	yes	yes	100/100	
10ng/ul Blood	9.715	999	642	343	1.556	2.913	1.872	yes	yes	yes	yes	yes	100/100	
10ng/ul Blood	9.715	999	649	361	1.539	2.767	1.798	yes	yes	yes	yes	yes	100/100	
10ng/ul Blood	9.706	999	608	301	1.643	3.319	2.020	yes	yes	yes	yes	yes	100/100	
10ng/ul Blood	9.706	999	580	288	1.722	3.469	2.014	yes	yes	yes	yes	yes	100/100	
10ng/ul Blood	9.706	999	590	294	1.693	3.398	2.007	yes	yes	yes	yes	yes	100/100	
10ng/ul Blood	9.706	999	629	363	1.588	2.752	1.733	yes	yes	yes	yes	yes	100/100	
10ng/ul Blood	9.706	999	626	347	1.596	2.879	1.804	yes	yes	yes	yes	yes	100/100	
10ng/ul Blood	9.706	999	617	331	1.619	3.018	1.864	yes	yes	yes	yes	yes	100/100	
10ng/ul Blood	9.706	999	598	327	1.671	3.055	1.829	yes	yes	yes	yes	yes	100/100	
10ng/ul Blood	9.706	999	613	340	1.630	2.938	1.803	yes	yes	yes	yes	yes	100/100	
10ng/ul Blood	9.706	999	598	326	1.671	3.064	1.834	yes	yes	yes	yes	yes	100/100	

Table 4: GCMS results for DPA

GCMS

2-4 Dinitrotoluene

Standards:	Rt (min)	Ion 165 (1) abund	Ion 88 (2) abund	Ion 63 (3) abund	Ratio 1:2	Ratio 1:3	Ratio 2:3	
1	9.204	999	793	463	999:793	999:463	793:463	
2	9.188	999	751	502.5	999:751	999:502.5	751:502.5	
Average:	9.196	999	772	482.75	999:772	999:482.75	772:482.75	
SD:	0.011	0.000	29.698	27.931	0.050	0.120	0.154	
CV:	0.001	0.000	0.038	0.058	0.038	0.058	0.096	
	RT Acceptable Range:					8.736 : 9.656		+/- 5%
	Ratio 1:2 Acceptable Range:					1.035 : 1.553		+/- 20%
	Ratio 1:3 Acceptable Range:					1.655 : 2.483		+/- 20%
	Ratio 2:3 Acceptable Range:					1.279 : 1.919		+/- 20%

Samples:	Rt (min)	Ion 165 (1) abund	Ion 88 (2) abund	Ion 63 (3) abund	Ratio 1:2	Ratio 1:3	Ratio 2:3	Rt OK?	Ratio 1:2 ok?	Ratio 1:3 ok?	Ratio 2:3 ok?	Target Compound Present?	Peak Resolution
100ng/ul	9.189	999	779	517	1.282	1.932	1.507	yes	yes	yes	yes	yes	100/100
100ng/ul	9.194	999	791	560	1.263	1.784	1.413	yes	yes	yes	yes	yes	100/100
100ng/ul	9.19	999	870	568	1.148	1.759	1.532	yes	yes	yes	yes	yes	100/100
10ng/ul	9.198	999	796	551	1.255	1.813	1.445	yes	yes	yes	yes	yes	100/100
10ng/ul	9.198	999	818	573	1.221	1.743	1.428	yes	yes	yes	yes	yes	100/100
10ng/ul	9.198	999	745	489	1.341	2.043	1.524	yes	yes	yes	yes	yes	100/100
5ng/ul	9.198	999	772	496	1.294	2.014	1.556	yes	yes	yes	yes	yes	100/100
5ng/ul	9.198	999	780	522	1.281	1.914	1.494	yes	yes	yes	yes	yes	100/100
5ng/ul	9.194	999	862	623	1.159	**1.604**	1.384	yes	yes	**no**	yes	**no**	100/100
5ng/ul	9.189	999	793	480	1.260	2.081	1.652	yes	yes	yes	yes	yes	100/100
5ng/ul	9.185	999	727	439	1.374	2.276	1.656	yes	yes	yes	yes	yes	97.7/100
5ng/ul	*	*	*	*	*	*	*	*	*	*	*	**no**	*
3ng/ul	9.19	999	853	550	1.171	1.816	1.551	yes	yes	yes	yes	yes	100/100
3ng/ul	9.189	999	715	428	1.397	2.334	1.671	yes	yes	yes	yes	yes	100/100
3ng/ul	9.194	999	886	725	1.128	**1.378**	**1.222**	yes	yes	**no**	**no**	**no**	100/100
2ng/ul	9.19	999	844	562	1.184	1.778	1.502	yes	yes	yes	yes	yes	90.7/100
2ng/ul	9.194	999	729	464	1.370	2.153	1.571	yes	yes	yes	yes	yes	100/100
2ng/ul	*	*	*	*	*	*	*	*	*	*	*	**no**	*
1ng/ul	9.194	999	819	632	1.220	**1.581**	1.296	yes	yes	**no**	yes	**no**	**100/14**
1ng/ul	9.198	999	698	474	1.431	2.108	1.473	yes	yes	yes	yes	yes	**100/64**
1ng/ul	*	*	*	*	*	*	*	*	*	*	*	**no**	*
.5ng/ul	*	*	*	*	*	*	*	*	*	*	*	**no**	*
.5ng/ul	*	*	*	*	*	*	*	*	*	*	*	**no**	*
.5ng/ul	*	*	*	*	*	*	*	*	*	*	*	**no**	*
10ng/ul Cotton	9.198	999	805	595	1.241	1.679	1.353	yes	yes	yes	yes	yes	100/100
10ng/ul Cotton	9.194	999	862	685	1.159	**1.458**	**1.258**	yes	yes	**no**	**no**	**no**	100/100
10ng/ul Cotton	9.194	999	852	636	1.173	**1.571**	1.340	yes	yes	**no**	yes	**no**	**80/100**
5ng/ul Cotton	9.194	999	859	626	1.163	**1.596**	1.372	yes	yes	**no**	yes	**no**	100/100
5ng/ul Cotton	9.194	999	874	667	1.143	**1.498**	1.310	yes	yes	**no**	yes	**no**	100/100
5ng/ul Cotton	9.198	999	791	541	1.263	1.847	1.462	yes	yes	yes	yes	yes	100/100
10ng/ul Blood	9.198	999	853	658	1.171	**1.518**	1.296	yes	yes	**no**	yes	**no**	100/100
10ng/ul Blood	9.194	999	835	678	1.196	**1.473**	**1.232**	yes	yes	**no**	**no**	**no**	100/100
10ng/ul Blood	9.194	999	796	691	1.255	**1.446**	**1.152**	yes	yes	**no**	**no**	**no**	100/100
10ng/ul Blood	*	*	*	*	*	*	*	*	*	*	*	**no**	*
10ng/ul Blood	*	*	*	*	*	*	*	*	*	*	*	**no**	*
10ng/ul Blood	*	*	*	*	*	*	*	*	*	*	*	**no**	*
10ng/ul Blood	*	*	*	*	*	*	*	*	*	*	*	**no**	*
10ng/ul Blood	*	*	*	*	*	*	*	*	*	*	*	**no**	*
10ng/ul Blood	*	*	*	*	*	*	*	*	*	*	*	**no**	*
10ng/ul Blood	*	*	*	*	*	*	*	*	*	*	*	**no**	*
10ng/ul Blood	*	*	*	*	*	*	*	*	*	*	*	**no**	*
10ng/ul Blood	*	*	*	*	*	*	*	*	*	*	*	**no**	*

Table 5: GCMS results for 2-4 DNT

ATR-FTIR data, denoted in tables 6 to 32, shows available peak wavenumbers as compared to those identified in literature for each compound. It also lists the absorbance value associated with each wavenumber. The root mean squared (RMS) value was taken from noise close in proximity to the wavenumber of interest. This value, along with the absorbance value of the wavenumber, allows for the calculation of the number of standard deviations (STD) the wavenumber is above the noise. If the STD value is greater than 3, the data is sufficient for qualitative purposes. If the STD value is greater than 10, the data is sufficient for quantitative purposes.

Results drawn from the subjective interpretation of peak non-detection and the STD value indicate all but the STD value for DPA at 10,000 ug/mL are sufficient for quantitative purposes. The STD value for DPA at 10,000 ug/mL is 9. This indicates it may be used for qualitative purposes. For EC1, the number of relevant peaks ranged from 14 to 22 for values of solid EC1 to 400 ug/mL EC1. At 200 ug/mL, 1 relevant peak was available. The subtraction results from 100% cotton indicated 5 relevant peaks. Lastly, subtraction results from blood and 100% cotton samples indicated one relevant peak.

For DPA results, relevant peaks ranged in number from 14 to 17 peaks for values of solid DPA to 400 ug/mL DPA. At 200 ug/mL, 6 relevant peaks were available. The subtraction results from 100% cotton indicated 5 relevant peaks. Lastly, subtraction results from blood and 100% cotton samples indicated a complete non-detection of all relevant peaks.

For 2-4 DNT results, relevant peaks ranged from 9 to 10 peaks for values of solid 2-4 DNT to 400 ug/mL 2-4 DNT. At 200 ug/mL, 3 relevant peaks were available. The subtraction

results from 100% cotton indicated 4 relevant peaks. Lastly, subtraction results from blood and 100% cotton samples indicated 1 relevant peak.

EC1 Solid Peak Table	Column1	Column2	Column3
Wavenumber	Absorbance	Noise RMS	STD
3065	0.028	0.000227	123
2978	0.044	0.000227	194
2941	0.042	0.000227	185
2868	0.031	0.000227	137
1638	0.098	0.000227	432
1596	0.067	0.000227	295
1581	0.064	0.000227	282
1491	0.087	0.000227	383
1453	0.085	0.000227	374
1442	0.091	0.000227	401
1310	0.069	0.000227	304
1279	0.1	0.000227	441
1256	0.089	0.000227	392
1131	0.072	0.000227	317
1088	0.078	0.000227	344
1072	0.083	0.000227	366
1041	0.052	0.000227	229
1021	0.073	0.000227	322
752	0.128	0.000227	564
694	0.142	0.000227	626

EC1 10k ug/mL Peak Table	Column1	Column2	Column3
Wavenumber	Absorbance	Noise RMS	STD
3061	0.034	0.0003438	99
1595	0.094	0.0003438	273
1583	0.07	0.0003438	204
1495	0.124	0.0003438	361
1453	0.071	0.0003438	207
1389	0.099	0.0003438	288
1373	0.095	0.0003438	276
1311	0.062	0.0003438	180
1294	0.096	0.0003438	279
1278	0.092	0.0003438	268
1261	0.08	0.0003438	233
1131	0.063	0.0003438	183
1089	0.054	0.0003438	157
1074	0.054	0.0003438	157

1026	0.047	0.0003438	137
753	0.104	0.0003438	303
693	0.117	0.0003438	340

EC1 1k ug/mL Peak Table	Column1	Column2	Column3
Wavenumber	Absorbance	Noise RMS	STD
3066	0.012	0.000049	245
2989	0.013	0.000049	265
2978	0.0144	0.000049	294
2941	0.0139	0.000049	284
1641	0.0409	0.000567	72
1597	0.0195	0.000567	34
1494	0.0268	0.000567	47
1456	0.026	0.000567	46
1443	0.0252	0.000567	44
1394	0.0336	0.000567	59
1375	0.0242	0.000567	43
1355	0.0215	0.000567	38
1311	0.0229	0.000567	40
1297	0.0294	0.000567	52
1280	0.0246	0.000567	43
1259	0.0222	0.000567	39
1132	0.023	0.000567	41
1089	0.0259	0.000567	46
1073	0.0253	0.000567	45
1022	0.0253	0.000567	45
755	0.0378	0.000567	67
697	0.0425	0.000567	75

EC1 800 ug/mL Peak Table	Column1	Column2	Column3
Wavenumber	Absorbance	Noise RMS	STD
3065	0.0162	0.0000593	273
2989	0.0178	0.0000593	300
2978	0.0186	0.0000593	314
2942	0.0179	0.0000593	302
2868	0.0165	0.0000593	278
1641	0.0551	0.0007497	73
1596	0.0252	0.0007497	34
1493	0.0347	0.0007497	46
1454	0.0301	0.0007497	40
1443	0.0295	0.0007497	39
1394	0.0375	0.0007497	50
1375	0.0293	0.0007497	39

1311	0.0274	0.0007497	37
1297	0.0339	0.0007497	45
1280	0.0297	0.0007497	40
1259	0.0272	0.0007497	36
1132	0.0277	0.0007497	37
1089	0.0293	0.0007497	39
1073	0.0294	0.0007497	39
1022	0.0293	0.0007497	39
754	0.0473	0.0007497	63
696	0.0499	0.0007497	67

EC1 600 ug/mL Peak Table	Column1	Column2	Column3
Wavenumber	Absorbance	Noise RMS	STD
3063	0.0159	0.0000312	510
2976	0.0165	0.0000312	529
1495	0.0268	0.0000421	637
1457	0.0257	0.0000421	610
1394	0.0254	0.0000421	603
1294	0.0255	0.0000421	606
1277	0.0254	0.0000421	603
1261	0.0254	0.0000421	603
1130	0.0255	0.0000743	343
1074	0.0256	0.0000743	345
1088	0.0254	0.0000743	342
1024	0.0255	0.0000743	343
752	0.0314	0.0000743	423
693	0.033	0.0000743	444

EC1 400 ug/mL Peak Table	Column1	Column2	Column3
Wavenumber	Absorbance	Noise RMS	STD
2990	0.1313	0.0000321	4090
2977	0.0137	0.0000321	427
2942	0.0133	0.0000321	414
1642	0.0319	0.0002047	156
1596	0.02	0.0002047	98
1494	0.0242	0.0002047	118
1454	0.0228	0.0002047	111
1443	0.0226	0.0002047	110
1394	0.0263	0.0002047	128
1376	0.0223	0.0002047	109
1355	0.0208	0.0002047	102
1311	0.0218	0.0002047	106
1297	0.0253	0.0002047	124

1280	0.0232	0.0002047	113
1259	0.022	0.0002047	107
1132	0.0229	0.0000444	516
1089	0.0237	0.0000444	534
1073	0.0234	0.0000444	527
1042	0.0226	0.0000444	509
1022	0.0231	0.0000444	520
754	0.0332	0.0000444	748
696	0.0345	0.0000444	777

EC1 200ug/mL Peak Table	Column1	Column2	Column3
Wavenumber	Absorbance	Noise RMS	STD
753	0.029	0.0000904	321

EC1 10k Cotton Peak Table	Column1	Column2	Column3
Wavenumber	Absorbance	Noise RMS	STD
1582	0.0049	0.000149	33
1495	0.0063	0.000149	42
1296	0.0028	0.000149	19
752	0.0082	0.000149	55
693	0.0087	0.000149	58

EC1 10k Blood/Cotton Peak Table	Column1	Column2	Column3
Wavenumber	Absorbance	Noise RMS	STD
1310	0.0261	0.0001327	197

Tables 6-14: ATR-FTIR data for EC1

DPA Solid Peak Table	Column1	Column2	Column3
Wavenumber	Absorbance	Noise RMS	STD
3406	0.222	0.00242	92
3382	0.409	0.00242	169
1594	0.508	0.00242	210
1493	0.59	0.00242	244
1458	0.566	0.00242	234
1418	0.436	0.00242	180
1316	0.494	0.00242	204
1242	0.338	0.00242	140
1219	0.258	0.00242	107
1172	0.396	0.00242	164
875	0.424	0.00242	175
700	0.537	0.00242	222

748	0.702	0.00242	290
642	0.341	0.00242	141
612	0.296	0.00242	122
568	0.249	0.00242	103

DPA 10k ug/mL Peak Table	Column1	Column2	Column3
Wavenumber	Absorbance	Noise RMS	STD
3407	0.086	0.00114	75
3383	0.149	0.00114	131
1596	0.161	0.00114	141
1519	0.159	0.00114	139
1495	0.173	0.00114	152
1458	0.126	0.00114	111
1418	0.112	0.00114	98
1243	0.086	0.00114	75
1220	0.068	0.00114	60
1173	0.099	0.00114	87
876	0.099	0.00114	87
748	0.211	0.00114	185
701	0.113	0.00114	99
689	0.227	0.00114	199
642	0.067	0.00114	59
613	0.063	0.00114	55
567	0.06	0.00114	53

DPA 1k ug/mL Peak Table	Column1	Column2	Column3
Wavenumber	Absorbance	Noise RMS	STD
3407	0.026	0.0003815	68
3384	0.0413	0.0003815	108
1597	0.0493	0.0003815	129
1520	0.0473	0.0003815	124
1496	0.0509	0.0003815	133
1458	0.0334	0.0003815	88
1418	0.0306	0.0003815	80
1243	0.0268	0.0003815	70
1220	0.0255	0.0003815	67
1173	0.0305	0.0003815	80
1024	0.0276	0.0003815	72
876	0.0324	0.0003815	85
743	0.0717	0.0003815	188
701	0.0402	0.0003815	105
689	0.0652	0.0003815	171
643	0.031	0.0003815	81

DPA 800 ug/mL Peak Table	Column1	Column2	Column3
Wavenumber	Absorbance	Noise RMS	STD
3406	0.0188	0.0000974	193
3384	0.0256	0.0000974	263
1597	0.0323	0.0000974	332
1520	0.0321	0.0000974	330
1496	0.0344	0.0000974	353
1458	0.025	0.0000974	257
1418	0.0248	0.0000974	255
1243	0.0235	0.0000974	241
1220	0.0231	0.0000974	237
1173	0.0256	0.0000974	263
1024	0.0258	0.0000974	265
876	0.0289	0.0000974	297
744	0.0467	0.0000974	479
701	0.0333	0.0000974	342
689	0.0448	0.0000974	460

DPA 600 ug/mL Peak Table	Column1	Column2	Column3
Wavenumber	Absorbance	Noise RMS	STD
3406	0.0159	0.0000508	313
3384	0.0203	0.0000508	400
1597	0.0275	0.000276	100
1520	0.0283	0.000276	103
1496	0.0296	0.000276	107
1458	0.0224	0.000276	81
1418	0.023	0.000276	83
1243	0.0223	0.000276	81
1220	0.0224	0.000276	81
1173	0.0239	0.000276	87
876	0.0276	0.000276	100
744	0.0403	0.000276	146
701	0.0322	0.000276	117
689	0.0402	0.000276	146

DPA 400 ug/mL Peak Table	Column1	Column2	Column3
Wavenumber	Absorbance	Noise RMS	STD
3406	0.0141	0.0000642	220
3384	0.0168	0.0000642	262
1597	0.0239	0.000356	67
1520	0.0246	0.000356	69
1496	0.0257	0.000356	72

1459	0.0201	0.000356	56
1418	0.0211	0.000356	59
1243	0.0211	0.000356	59
1219	0.0211	0.000356	59
1173	0.0224	0.000356	63
876	0.0265	0.0000762	348
743	0.0352	0.0000762	462
701	0.0306	0.0000762	402
689	0.0359	0.0000762	471

DPA 200 ug/mL Peak Table	Column1	Column2	Column3
Wavenumber	Absorbance	Noise RMS	STD
3382	0.0117	0.0000503	233
1595	0.0185	0.000103	180
1495	0.0195	0.000103	189
1312	0.02	0.000103	194
744	0.0267	0.0000906	295
689	0.0271	0.0000906	299

DPA 10k Cotton Peak Table	Column1	Column2	Column3
Wavenumber	Absorbance	Noise RMS	STD
1495	0.0084	0.000271	31
1311	0.0067	0.000271	25
1080	0.0025	0.000271	9
747	0.0104	0.000271	38
689	0.008	0.000271	30

Column1	Column2	Column3	Column4
DPA 10k Blood Peak Table			
Wavenumber	Absorbance	Noise RMS	STD
N/A	N/A	N/A	N/A

Tables 15-23: ATR-FTIR data for DPA

2-4 DNT Solid Peak Table	Column1	Column2	Column3
Wavenumber	Absorbance	Noise RMS	STD
1607	0.282	0.00214	132
1343	0.614	0.00214	287
1203	0.178	0.00214	83
1153	0.26	0.00214	121
1068	0.245	0.00214	114

835	0.409	0.00214	191
790	0.337	0.00214	157
731	0.531	0.00214	248
704	0.35	0.00214	164

2-4 DNT 10k ug/mL Peak Table	Column1	Column2	Column3
Wavenumber	Absorbance	Noise RMS	STD
1607	0.052	0.0000408	1275
1528	0.123	0.0000408	3015
1347	0.114	0.0000408	2794
1153	0.038	0.0000408	931
1069	0.035	0.0000408	858
836	0.052	0.0000408	1275
790	0.043	0.0000408	1054
732	0.0758	0.0000408	1858
708	0.0401	0.0000408	983

2-4 DNT 1k ug/mL Peak Table	Column1	Column2	Column3
Wavenumber	Absorbance	Noise RMS	STD
1607	0.0278	0.0003362	83
1528	0.0507	0.0003362	151
1348	0.0501	0.0003362	149
1203	0.0231	0.0003362	69
1153	0.026	0.0003362	77
1068	0.0261	0.0003362	78
836	0.0324	0.0003362	96
791	0.0307	0.0003362	91
734	0.0402	0.0003362	120
708	0.0311	0.0003362	93

2-4 DNT 800ug/mL Peak Table	Column1	Column2	Column3
Wavenumber	Absorbance	Noise RMS	STD
1607	0.0278	0.0000558	498
1528	0.0462	0.0000558	828
1348	0.0457	0.0000558	819
1153	0.0269	0.0000558	482
1068	0.0271	0.0000558	486
836	0.0326	0.0000558	584
790	0.031	0.0000558	556
733	0.0385	0.0000558	690
708	0.0315	0.0000558	565

2-4 DNT 600 ug/mL Peak Table	Column1	Column2	Column3

Wavenumber	Absorbance	Noise RMS	STD
1607	0.0245	0.000039	628
1528	0.0388	0.000039	995
1347	0.0386	0.000039	990
1153	0.0247	0.000039	633
1069	0.025	0.000039	641
836	0.0311	0.000039	797
790	0.0292	0.000039	749
733	0.0379	0.000039	972
705	0.0303	0.000039	777

2-4 DNT 400 ug/mL Peak Table	Column1	Column2	Column3
Wavenumber	Absorbance	Noise RMS	STD
1607	0.0213	0.0000714	298
1529	0.0275	0.0000714	385
1347	0.029	0.0000714	406
1153	0.0233	0.000035	666
1068	0.0239	0.000035	683
835	0.0276	0.000035	789
791	0.0273	0.000035	780
733	0.0311	0.000035	889
702	0.0288	0.000035	823

2-4 DNT 200 ug/mL Peak Table	Column1	Column2	Column3
Wavenumber	Absorbance	Noise RMS	STD
1347	0.022	0.0000372	591
835	0.0253	0.000045	562
733	0.0277	0.0000676	410

2-4 DNT Cotton Peak Table	Column1	Column2	Column3
Wavenumber	Absorbance	Noise RMS	STD
1346	0.0055	0.0000736	75
835	0.0032	0.0000736	43
790	0.0026	0.0000736	35
732	0.0039	0.0000736	53

2-4 DNT Blood Peak Table	Column1	Column2	Column3
Wavenumber	Absorbance	Noise RMS	STD
1204	0.0229	0.000223	103

Tables 24-32: ATR-FTIR data for 2-4 DNT

Discussion

Blood is a common contaminant present at crime scenes and its effect on the OGSR compounds of gunshot residue remain unclear. Because of the detrimental effects blood has on IGSR, this study hypothesized that blood at a crime scene would have a masking effect on the analysis of OGSR compounds. In this study, we analyzed the results of GCMS, Raman, and ATR-FTIR qualitative results on four highly selective compounds associated with OGSR with the application of 100% cloth substrate and pigs' blood.

Through this study, it was determined blood may have a significant impact on the analysis of OGSR compounds. In GCMS analysis, 2-4 DNT elution became hindered with a reduction in concentration and with the application of 2% EDTA pigs' blood. In ATR-FTIR analysis, EC1, DPA, and 2-4 DNT experienced non-detected peaks with the addition of 100% cloth substrate and non-EDTA pigs' blood. This research aids in determining the limiting factors blood may present in GCMS and ATR-FTIR instrumentation regarding OGSR analysis, aiding current research into instrumentational efficacy for OGSR.

Findings for ATR-FTIR correlate with previous findings in which 100% cotton substrate interfered with the peaks of the compounds of interest [39]. These results are not surprising, as ATR-FTIR is a surface scanning instrumentation. Because both 100% cotton and blood would act to create a layer over that of deposited analytes, the finding of a masking effect are expected. This finding calls into question what advantages ATR-FTIR would provide over the use of chromatography techniques as it applies to individual OGSR compounds. In general, ATR-FTIR, as compared to GCMS, allows for minimal sample preparation and expedient results. If samples were to be further extracted to avoid the masking effects of the fabric and blood, an examiner

would utilize GCMS due to its increased sensitivity and separation capabilities. Results would also indicate nitrocellulose, which is in a much higher concentration than the four compounds of interest for this study, may be a better analyte target for spectroscopy methods. However, nitrocellulose is a common compound found in sources outside of gunshot powder and residue. Application of the methodology of this study with nitrocellulose for ATR-FTIR could aid in determining a presumptive analysis method for OGSR.

Unlike the results of ATR-FTIR, Raman spectroscopy results were inconclusive due to the inability to visualize the locations of the analytes on the substrates utilized. The use of a visualization technique such as hyperspectral imaging may have allowed for additional results. Hyperspectral imaging produces a reflectance spectrum based on every pixel in an image through multiple different wavelengths of light, both visual and non-visual. This allows for the characterization and mapping of the surface of an image to provide visualization of areas of interest. Using hyperspectral imaging as an initial technique allows for the guidance of Raman spectroscopy to specific locations on a substrate, which provides a more detailed analysis than that of hyperspectral imaging [40].

This study had limitations with sample sizes, sample representation as compared to scene samples, and the lack of an internal standard for GCMS analysis. Sample size for GCMS analysis consisted of triplicate sample runs as well as triplicate sample preparation for samples with the addition of 2% EDTA blood. However, ATR-FTIR samples were only run in triplicate instead of the intended 15 replicates. Overall, the lack of representative data makes the findings for ATR-FTIR difficult to generalize. In addition, the lack of a sample set consisting of range fired gunshot residue limits the data set provided in this study to theoretical results based on the four OGSR compounds alone. Also, it should be noted that although pigs' blood does share

similarities to human whole blood, it cannot be said that the results of these studies are representative to the use of human blood. Lastly, using an internal standard during GCMS analysis allows for interpretation of instrumental effects during analysis. Because this study did not use one, it cannot be determined what degree of interference may have occurred between analysis. However, the use of ranges for ion ratios and retention time in data interpretation alleviates this limitation qualitatively.

Future research should look to alleviate the limitations denoted for this research as well as apply the findings in this study to further research. Applying the study of blood contamination to fired gunshot residue in which the OGSR compounds available in that GSR is known would give crime scene value to the results based in this study. To further the value of the results, the use of whole, human blood would eliminate any interference aspects that may arise between pigs' blood and human blood. Additionally, a more robust sample set consisting of more samples and analysis replicates would enhance the results of future work. For Chromatography studies, a reliable internal standard should be used. The use of Undecane has been discussed and future studies should apply its use or seek an alternative that would work for a wide range of the OGSR compounds identified as specific for GSR.

In addition to the above recommendations based on the limitations of this study regarding future research, current literature has not addressed the average concentrations of OGSR compounds regarding the manufacture of smokeless gunpowder. OGSR compounds are applied as a lacquer during the manufacture of smokeless gunpowder [35]. Though estimates do exist as wide ranges for some compounds, a compendium of lacquers detailing the concentrations of OGSR compounds would benefit the field as to what to expect from gunshot residue from smokeless powder manufactured with a specific lacquer. However, complications with the

release of that information may arise due to how much information the individual manufactures would be willing to provide. Additionally, studies into the overall loss in concentration once the smokeless gunpowder has gone through the manufacturing process may allow for interpretation of what can be expected from average OGSR concentrations found at crime scenes. This information would be beneficial to the selection of instrumentation with a target sensitivity for OGSR analysis.

Conclusions

This study was designed to estimate the masking effects of blood on relevant compounds of OGSR. Using four of the most common, relevant, and analytically distinguishing compounds associated with OGSR, samples were created and evaluated using GCMS and ATR-FTIR instrumentation. The hypothesis was that blood would have a noticeable masking effect on EC1, MC1, DPA, and 2-4 DNT. Results indicate the hypothesis partially holds true for 2-4 DNT using GCMS, while holding wholly true for ATR-FTIR instrumentation.

Based on the results of the GCMS data (at ng/ul on column), the data supports the conclusion that compounds EC1, MC1, and DPA elute down to .5 ng/µL. For EC1, one sample did not elute at 10 ng/µL in blood. For MC1, three samples did not elute at 5 ng/µL, 10 ng/µL on cotton, and 5 ng/µL on cotton. For DPA, one sample did not elute at 100 ng/µL. 2-4 DNT had most samples not elute after 10 ng/µL.

Interpretation of these results would suggest blood does not have a masking effect on EC1, MC1, and DPA when analyzed by GCMS instrumentation. Results of the limit of detection study indicates that these compounds can be detected as low as 0.5 ng/µL. The results of 2-4 DNT suggest something caused elution hindrance after 10 ng/µL during limit of detection studies. Results also indicate the addition of blood or 100% cotton substrate may also hinder 2-4 DNT elution. However, it cannot be stated to be only due to the presence of blood or 100% cotton. Other possibilities exist such as degradation during storage times, or inlet temperature causing thermolabile degradation. Further research into the storage capabilities of 2-4 DNT over time as well as thermolabile properties under varying conditions of GCMS instrumentation would give more weight to these results.

If ATR-FTIR results are examined, results indicate that EC1, DPA, and 2-4 DNT samples have a limit of detection between 400 ng/µL to 200 ng/ul concentration. However, this is a subjective interpretation based on the number of detected peaks associated between those two concentrations. EC1 contains 22 relevant peaks at 400 ng/µL, DPA contains 14 relevant peaks at 400 ng/µL, and 2-4 DNT contains 9 relevant peaks at 400 ng/µL. These all drop to 1 relevant peak, 6 relevant peaks, and 3 relevant peaks, respectively.

The hypothesis that blood will have a masking effect on the compounds of interest hold true based on the analysis of ATR-FTIR samples. Interestingly, 100% cotton cloth substrate also seemed to have a direct correlation with peaks not being detected as well. In 100% cotton substrate subtractions with sample concentration at 10,000 ug/ml, EC1 retained 5 relevant peaks, DPA retained 5 relevant peaks, and 2-4 DNT retained 4 relevant peaks. This would indicate the presence of 100% cotton as a substrate can hamper the presence of literature-denoted relevant peaks of these compounds. When non-EDTA treated pigs' blood was added to 10,000 ug/ml samples, this dropped even further. For EC1, subtraction results for blood samples retained 1 relevant peak, DPA retained no relevant peaks, and 2-4 Dinitrotoluene retained no relevant peaks. All peaks obtained were relevant based on the STD values associated with them.

Interpretation of the peak non-detection that occurred would indicate that 100% cotton cloth substrate caused interference with peak detection. Further, the presence of non EDTA treated pigs' blood over the surface interference with peak detection even further. The results would indicate 100% cotton caused peak non-detection and that the addition of non-EDTA treated pigs' blood further caused peak non-detection to occur. The near complete masking of peaks of interest supports the hypothesis proposed in this study. Another finding is that the

overall sensitivity of GCMS is greater than that of ATR-FTIR for the three compounds of interest analyzed through ATR-FTIR.

In summary, this study provided context to current literature in that blood may have a masking effect on OGSR compounds in the context of GCMS and ATR-FTIR analysis. Though limitations exist, this study provides a foundation for contaminant analysis for future research into OGSR. Overall, this study highlights the importance of acknowledgement of contamination, blood specifically, regarding OGSR and addressing it accordingly as a possible limitation.

```
File       :C:\msdchem\1\data\TWW_Explosives\Ethyl Centralite\EC1 061318
...          UNI1.D
Operator   :
Instrument :    5975 MSD
Acquired   : 13 Jun 2018  14:41     using AcqMethod TWW_UNI1.M
Sample Name: 100 ng/uL ~~MC1~~ EC1
Misc Info  :
```

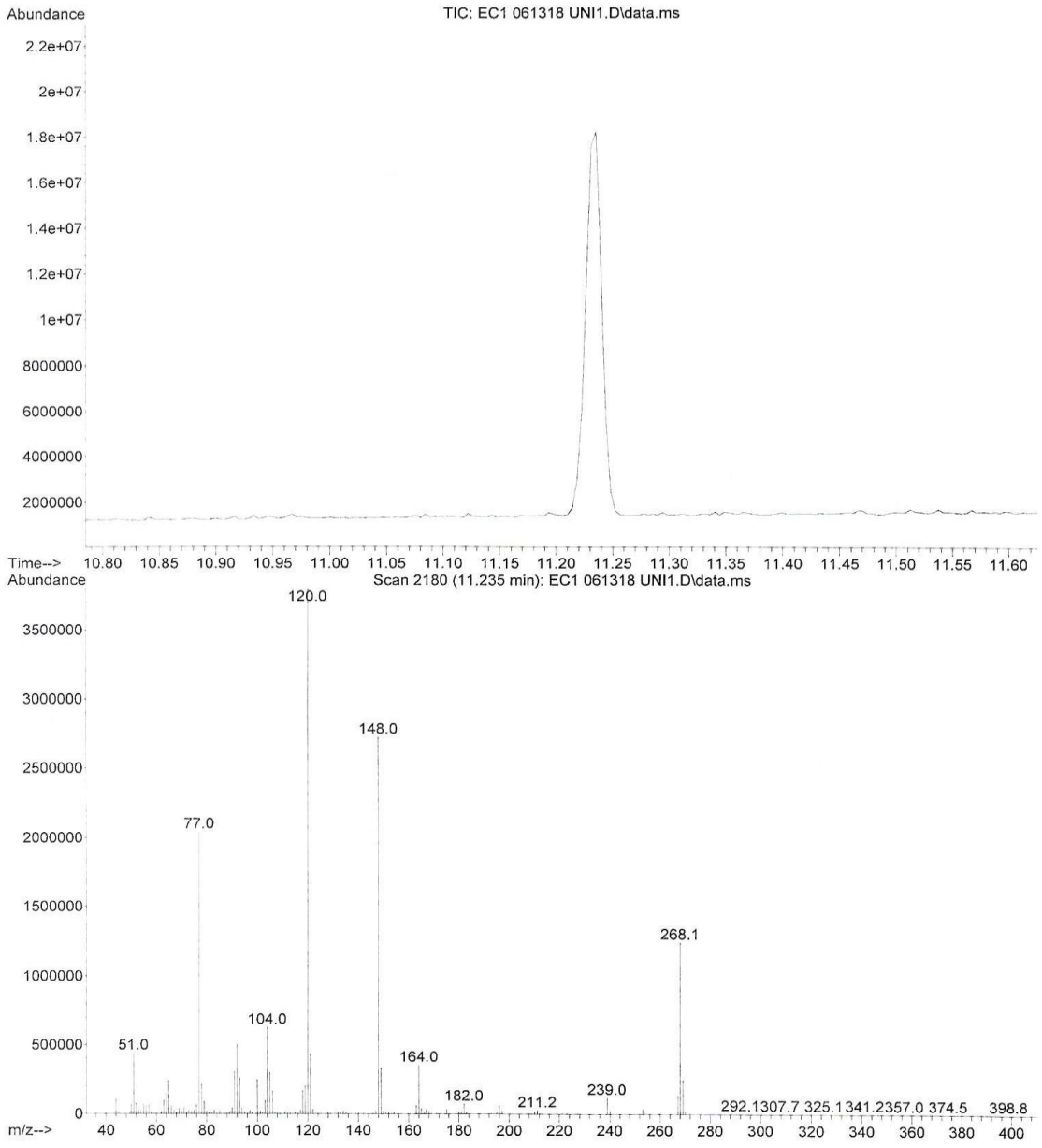

```
File       :C:\msdchem\1\data\TWW_Explosives\Ethyl Centralite\EC1 82019
...         SIM NO F 80MSEC REP1 S1.D
Operator   :
Instrument :    5975 MSD
Acquired   : 20 Jun 2018  12:26     using AcqMethod TWW_UNI1 SIM TEST EC1 80MSEC
Sample Name: 10 ng/uL EC1 no fabric
Misc Info  :
```

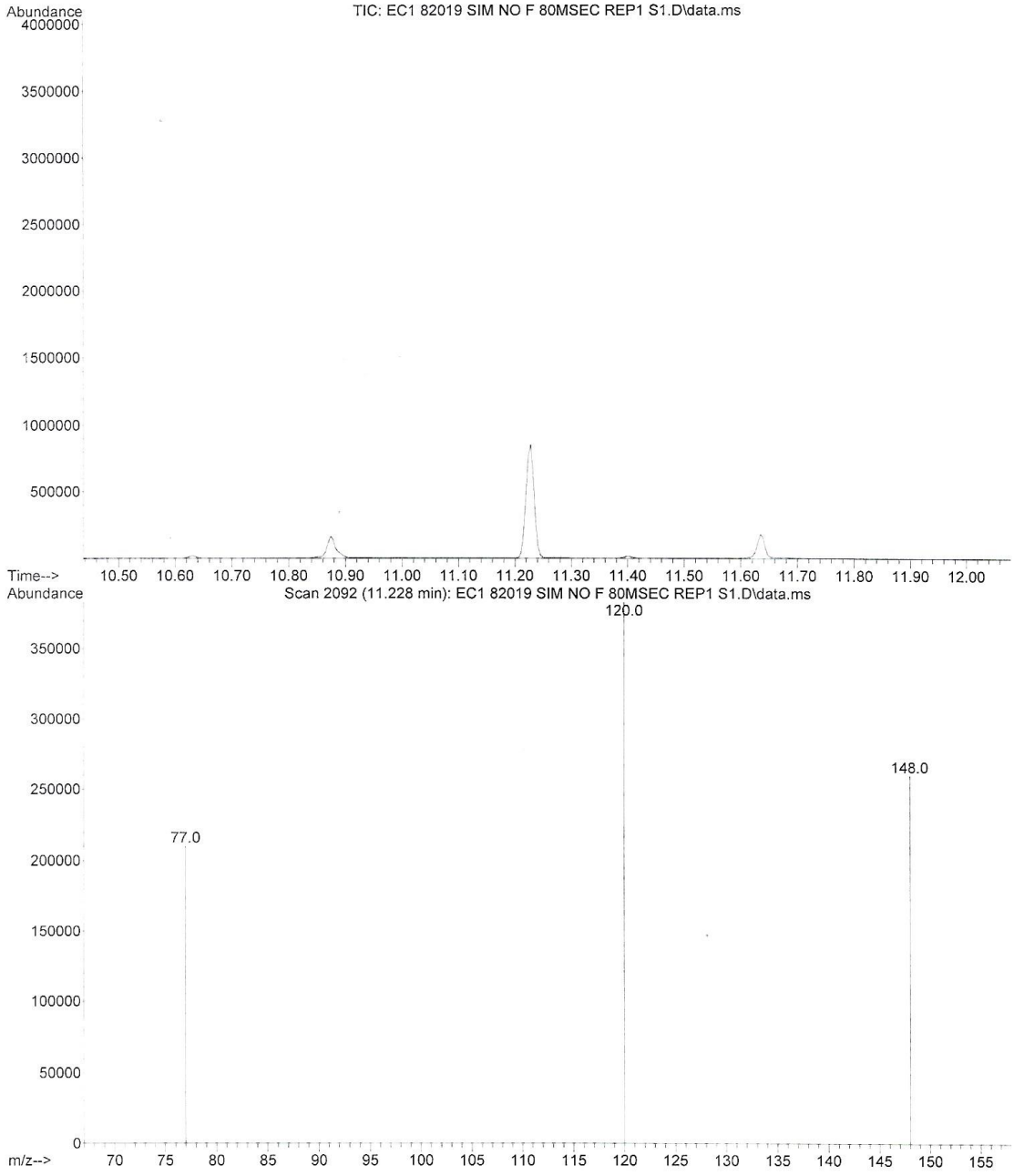

```
File       :C:\msdchem\1\data\TWW_Explosives\ALS Run 080818\EC1 5 ng rep
...          1.D
Operator   :
Instrument :    5975 MSD
Acquired   :  8 Aug 2018  16:03     using AcqMethod TWW SIM EC1 DEFAULT.M
Sample Name: EC1 5 ng
Misc Info  :
```

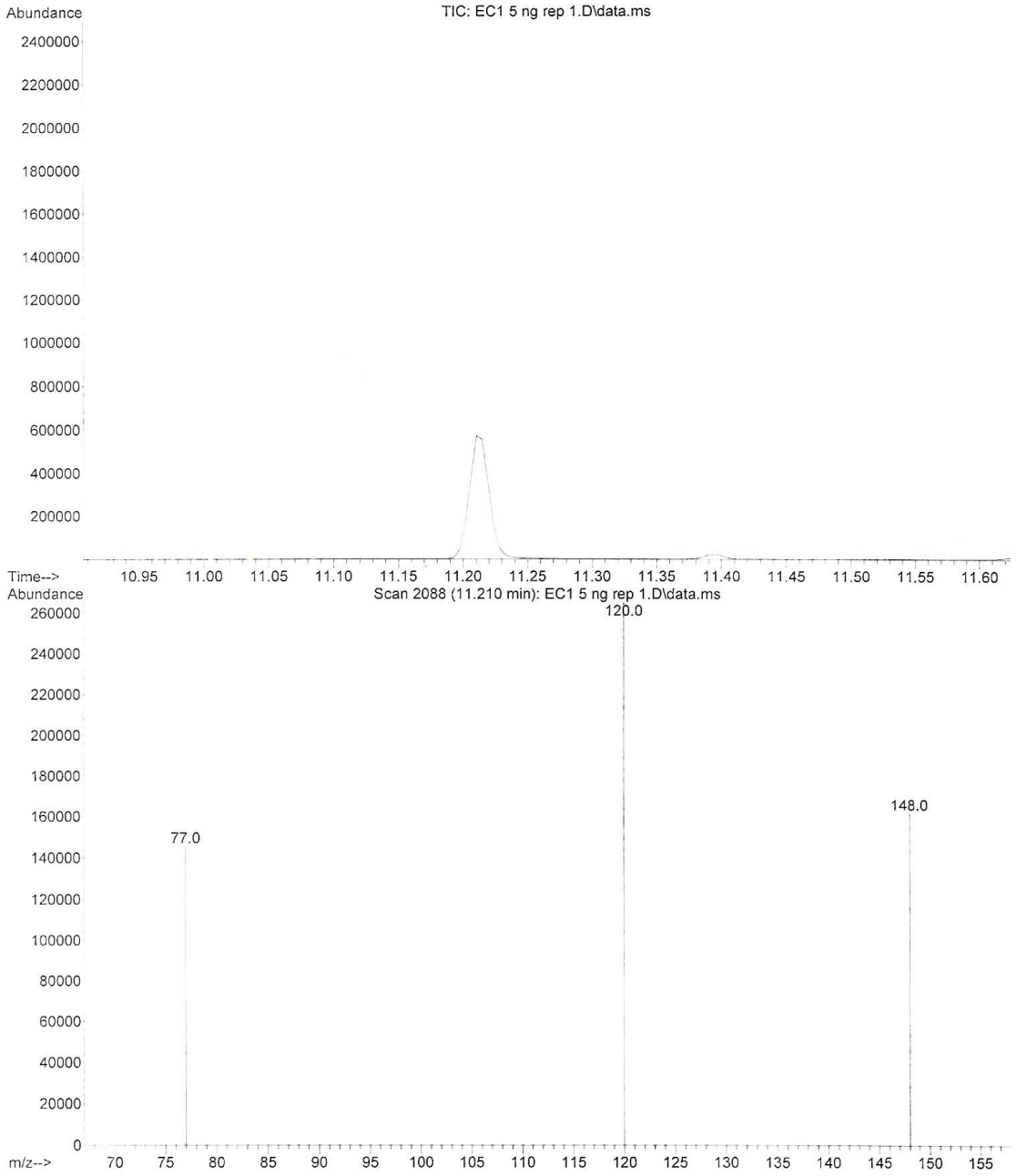

```
File       :C:\msdchem\1\data\TWW_Explosives\ALS Run 080818\EC1 3 ng rep
...          1.D
Operator   :
Instrument :    5975 MSD
Acquired   :  8 Aug 2018  16:25     using AcqMethod TWW SIM EC1 DEFAULT.M
Sample Name: EC1 3 ng
Misc Info  :
```

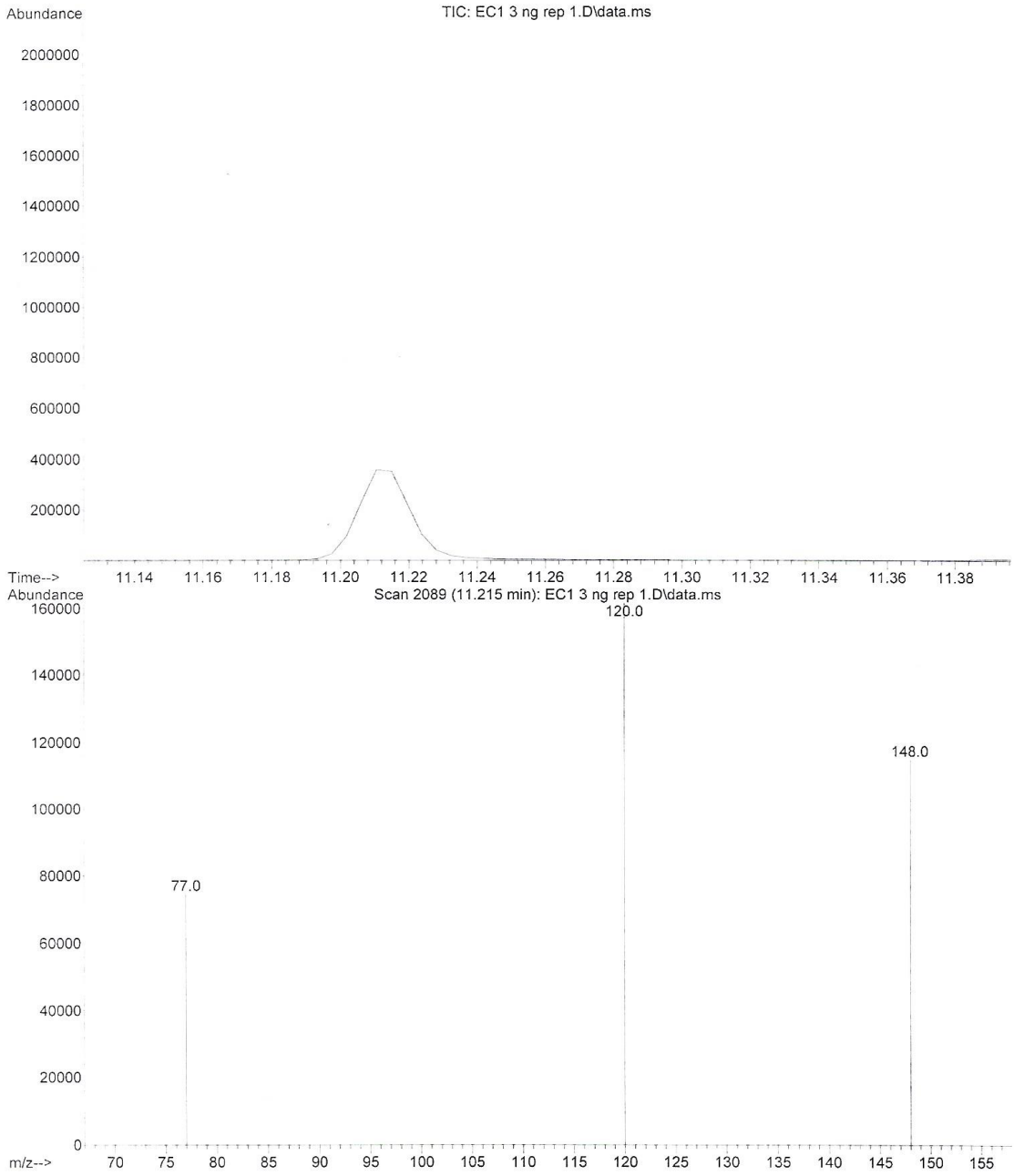

```
File       :C:\msdchem\1\data\TWW_Explosives\ALS Run 080918\EC1 2 ng rep
...          1.D
Operator   :
Instrument :    5975 MSD
Acquired   :  9 Aug 2018  17:32     using AcqMethod TWW SIM EC1 DEFAULT.M
Sample Name: EC1 2 ng
Misc Info  :
```

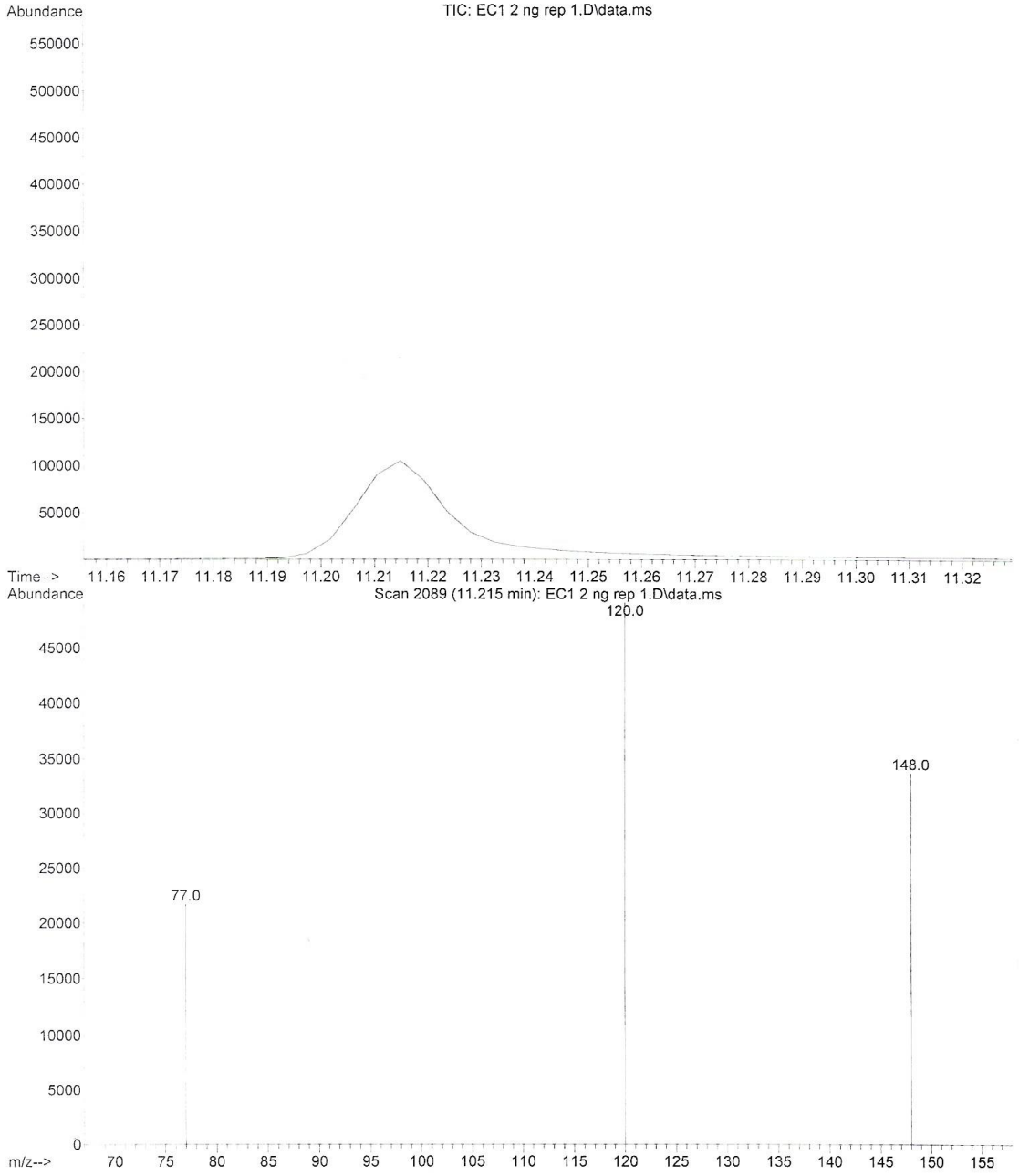

```
File       :C:\msdchem\1\data\TWW_Explosives\ALS Run 080818\EC1 1 ng rep
...          1.D
Operator   :
Instrument :    5975 MSD
Acquired   :  8 Aug 2018  17:09     using AcqMethod TWW SIM EC1 DEFAULT.M
Sample Name: EC1 1 ng
Misc Info  :
```

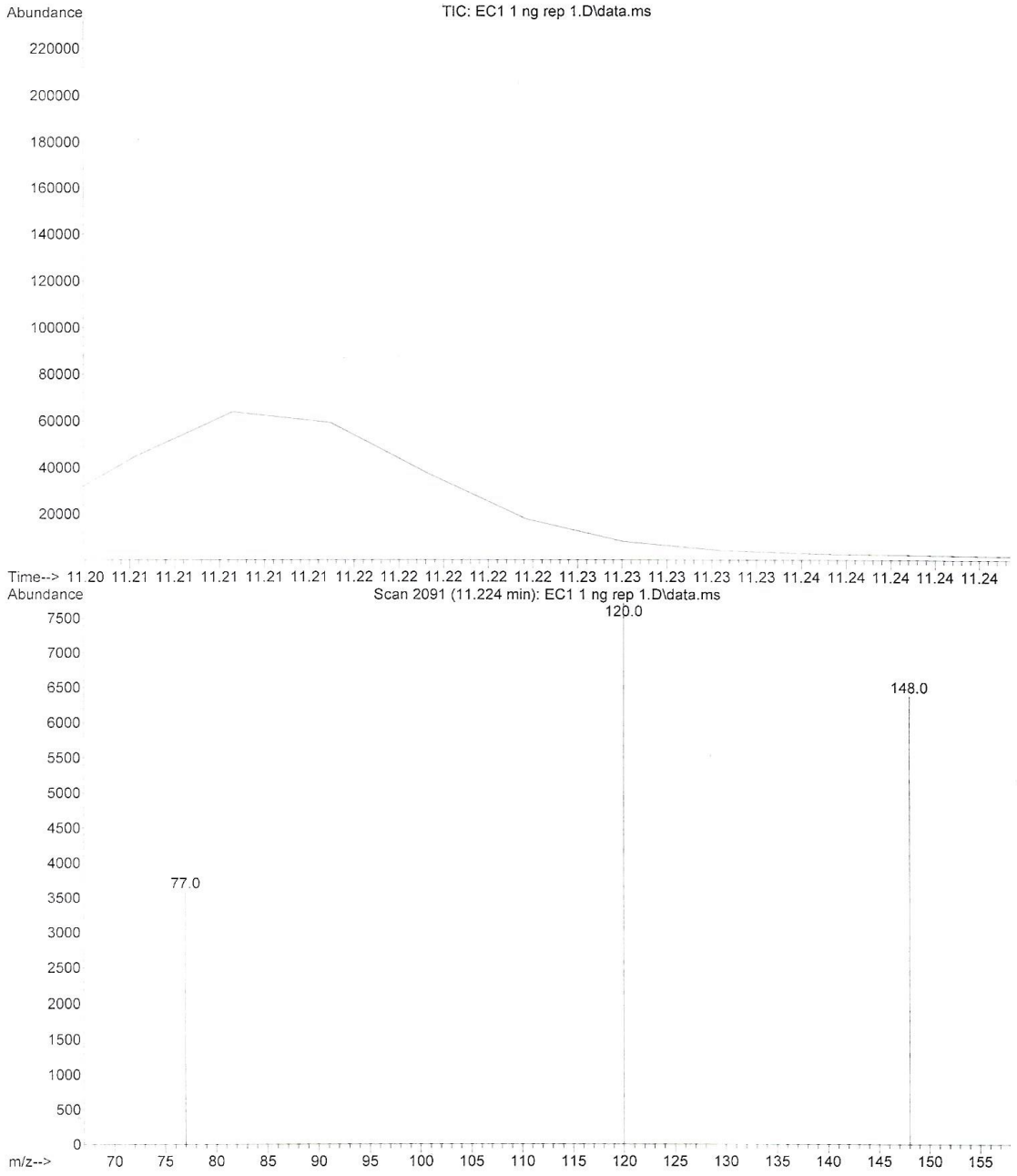

```
File       :C:\msdchem\1\data\TWW_Explosives\ALS Run 080818\EC1 half ng
...         rep 1.D
Operator   :
Instrument :    5975 MSD
Acquired   :  8 Aug 2018  17:30     using AcqMethod TWW SIM EC1 DEFAULT.M
Sample Name: EC1 .5 ng
Misc Info  :
```

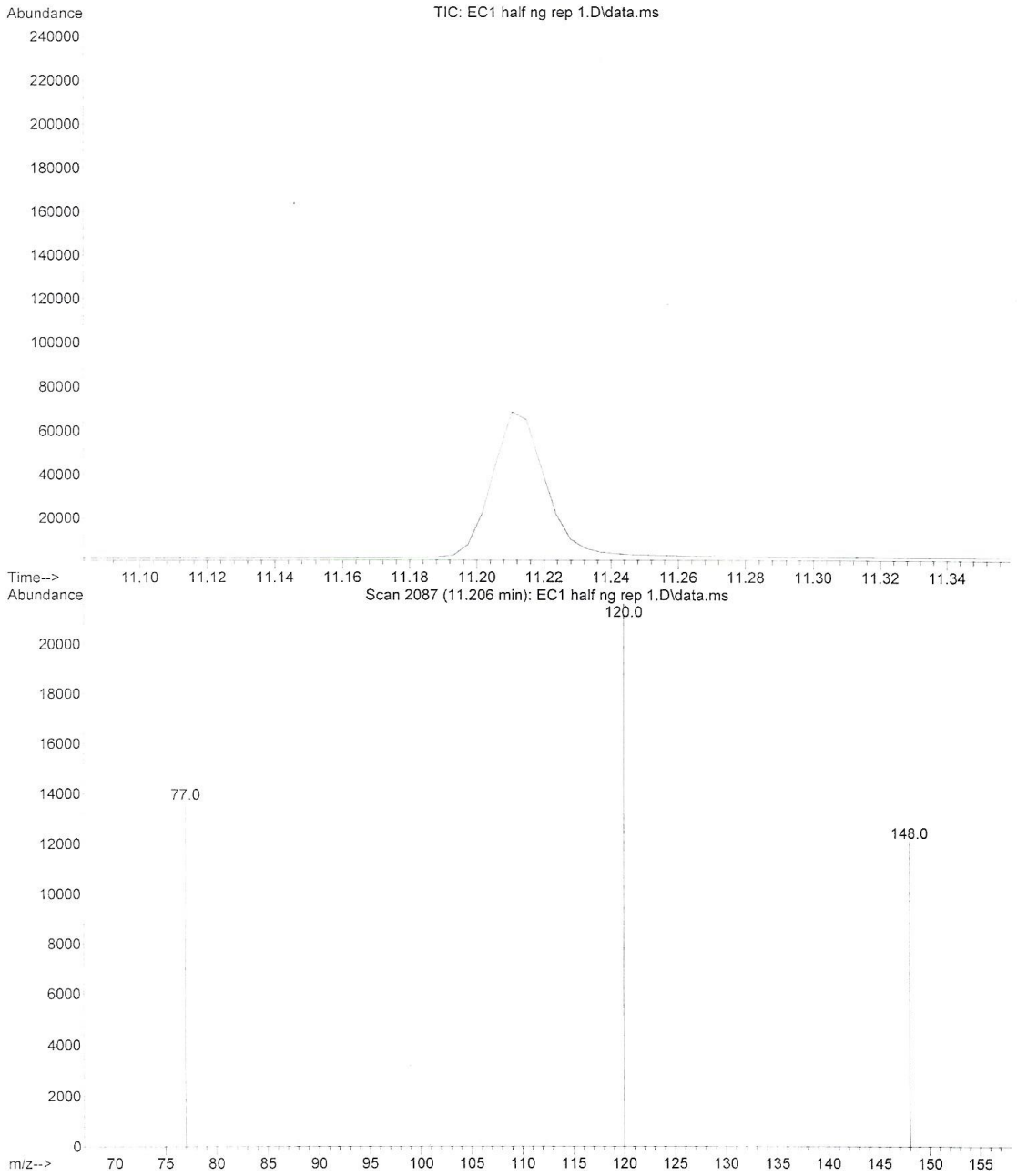

```
File       :C:\msdchem\1\data\TWW_Explosives\Ethyl Centralite\EC1 62018
...         SIM 80MSEC COTTON REP1 S1.D
Operator   :
Instrument :    5975 MSD
Acquired   : 20 Jun 2018  14:18     using AcqMethod TWW_UNI1 SIM TEST EC1 80MSEC
Sample Name: 10 ng/uL EC1 COTTON 80MSEC
Misc Info  :
```

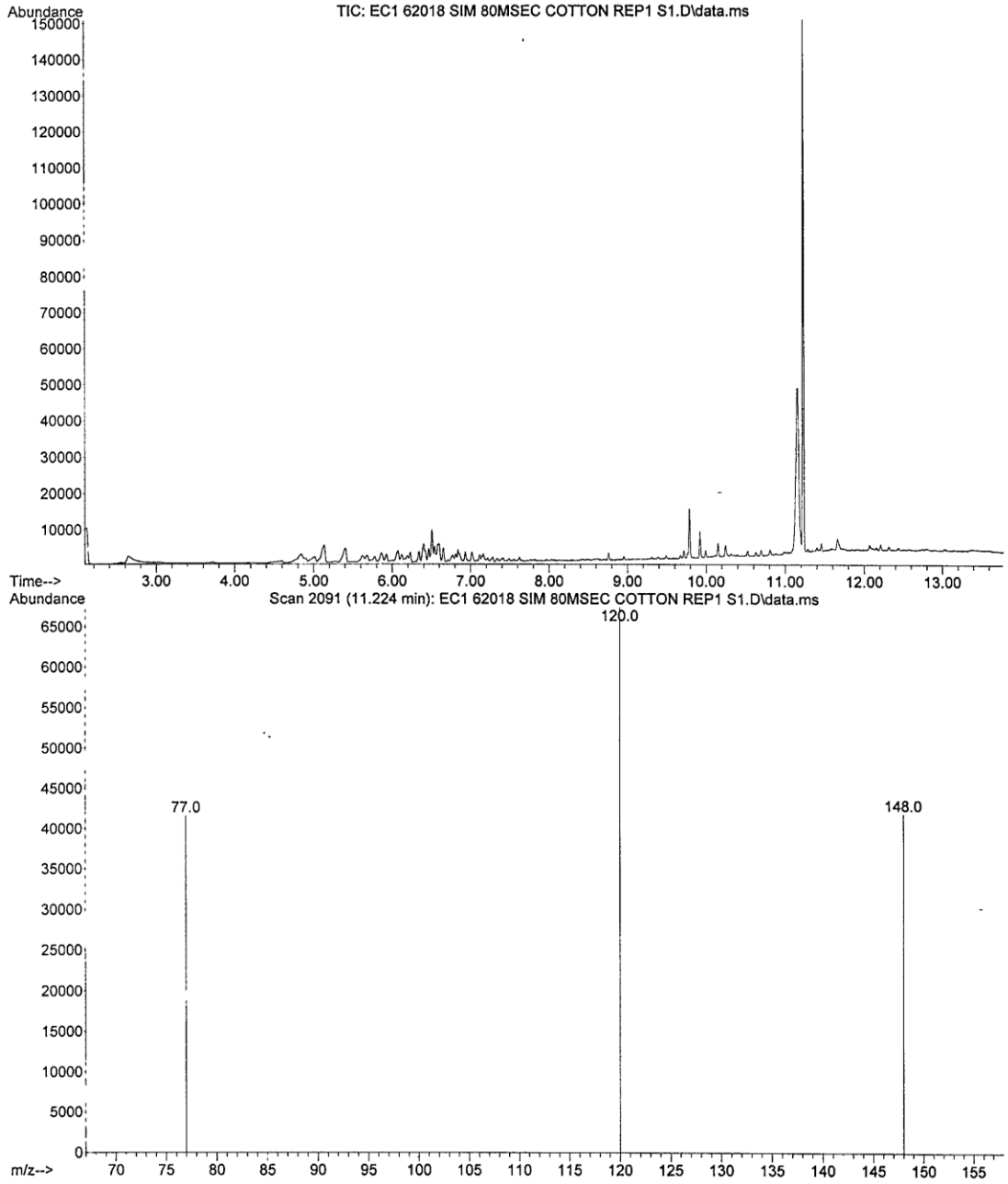

```
File       :C:\msdchem\1\data\TWW_Explosives\Ethyl Centralite\EC1 071118
...          SIM COTN 5NG REP1 S1.D
Operator   :
Instrument :    5975 MSD
Acquired   : 11 Jul 2018  14:10     using AcqMethod TWW_UNI1 SIM TEST EC1 80MSEC
Sample Name: EC1 5 ng/ul 100% COTTON REP1 S1
Misc Info  :
```

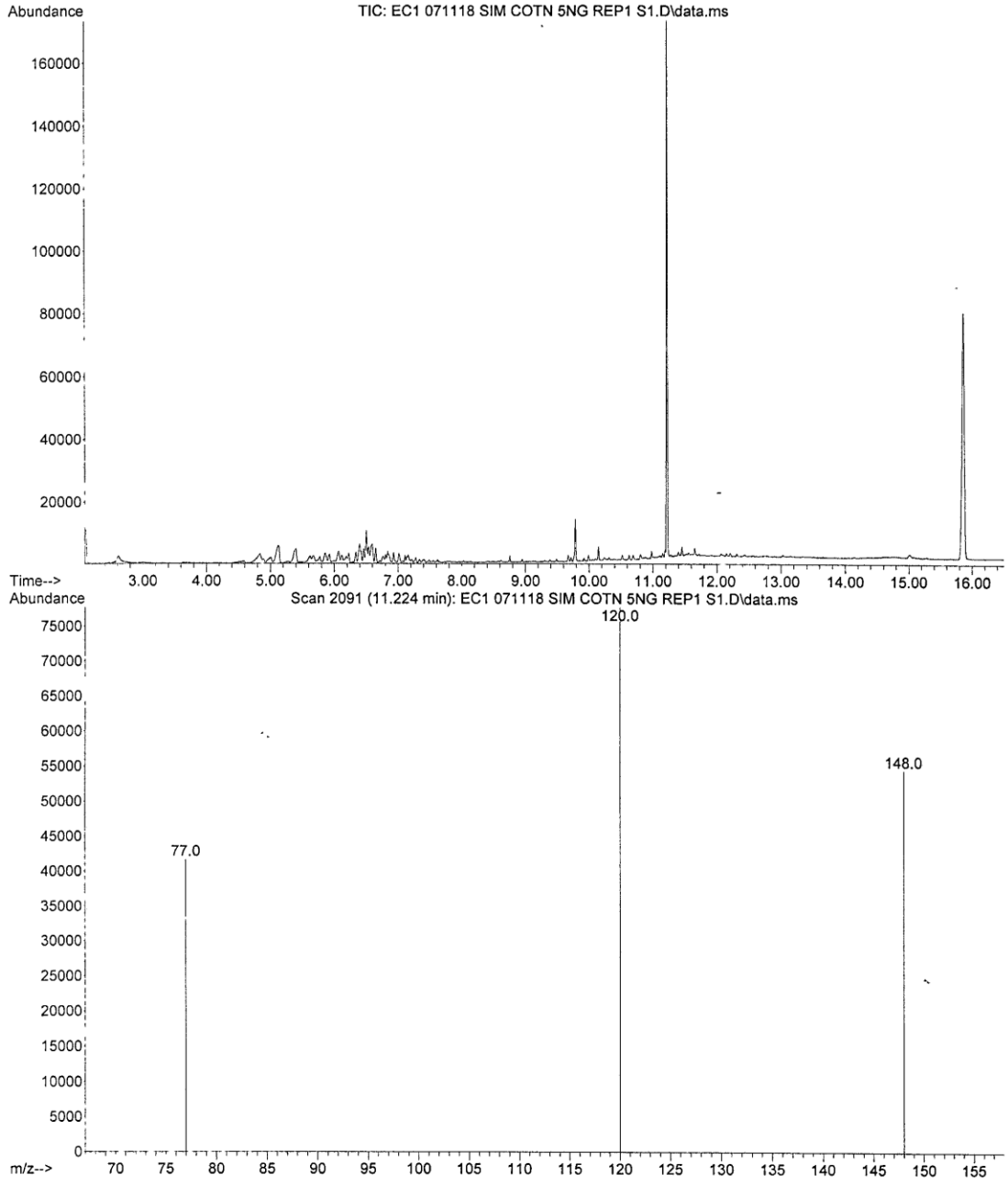

```
File       :C:\msdchem\1\data\TWW_Explosives\Ethyl Centralite\EC1 71318
...         10 NGUL BLOOD REP1 S1.D
Operator   :
Instrument :    5975 MSD
Acquired   : 13 Jul 2018  12:32     using AcqMethod TWW_UNI1 SIM TEST EC1 80MSEC
Sample Name: EC1 10ng/ul BLOOD REP1 S1
Misc Info  :
```

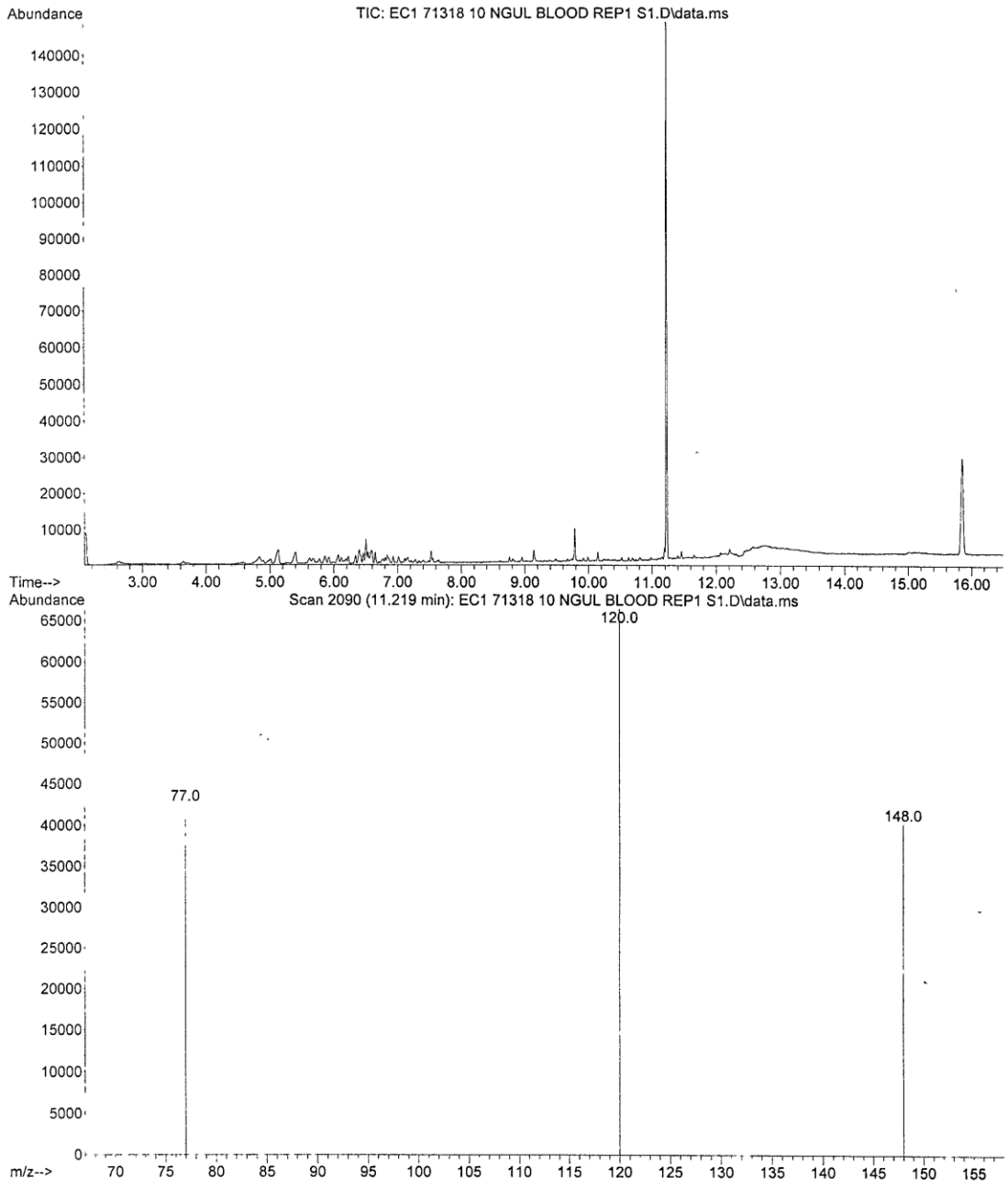

```
File       :C:\msdchem\1\data\TWW_Explosives\Methyl Centralite\MC1 06131
...         8 UNI1.D
Operator   :
Instrument :    5975 MSD
Acquired   : 13 Jun 2018  14:20     using AcqMethod TWW_UNI1.M
Sample Name: 100 ng/uL MC1
Misc Info  :
```

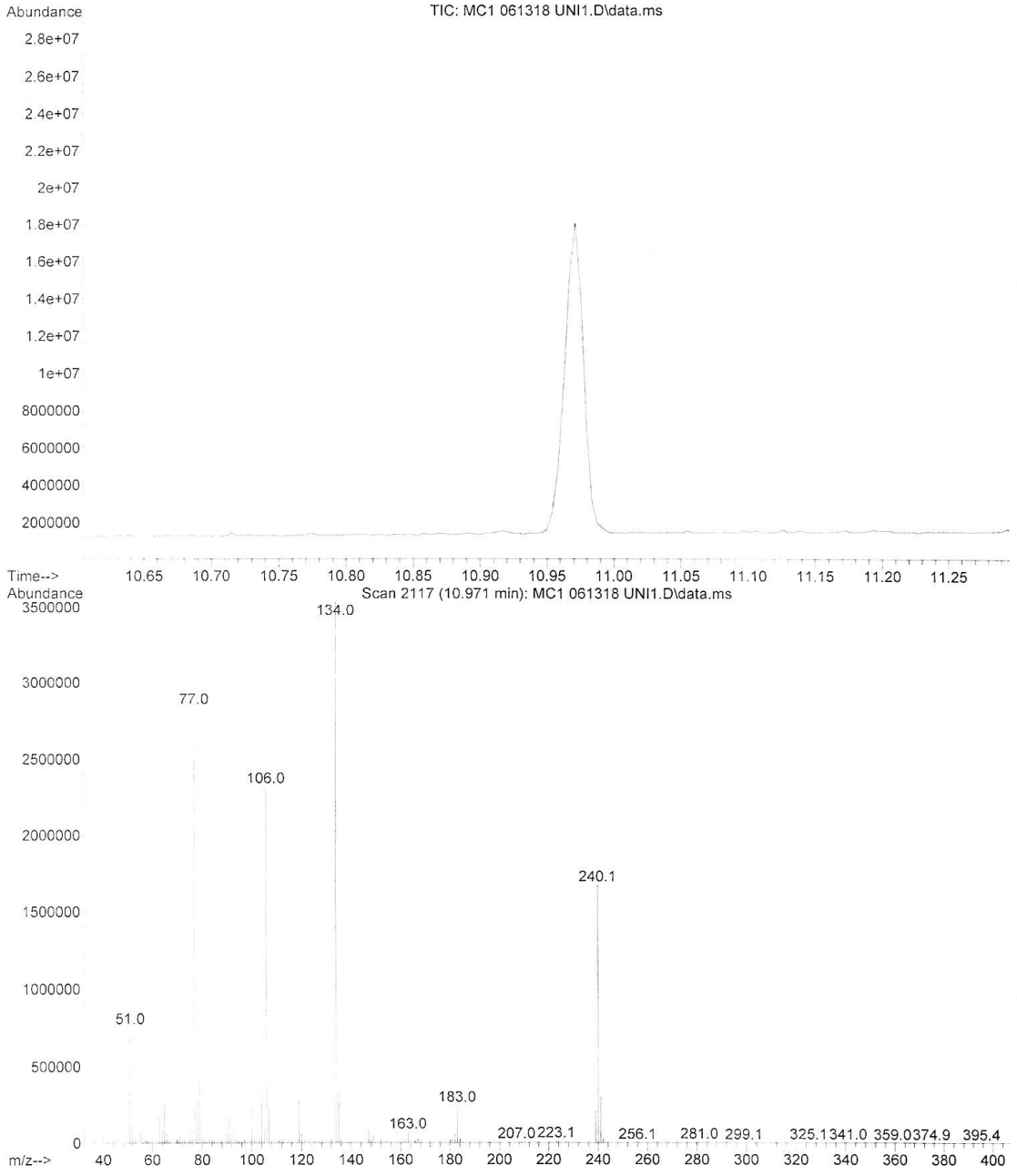

```
File       :C:\msdchem\1\data\TWW_Explosives\Methyl Centralite\MC1 06141
...         8 SIM REP1.D
Operator   :
Instrument :     5975 MSD
Acquired   : 14 Jun 2018  14:01      using AcqMethod TWW_UNI1 SIM TEST MC1.M
Sample Name: 10 ng/uL MC1
Misc Info  :
```

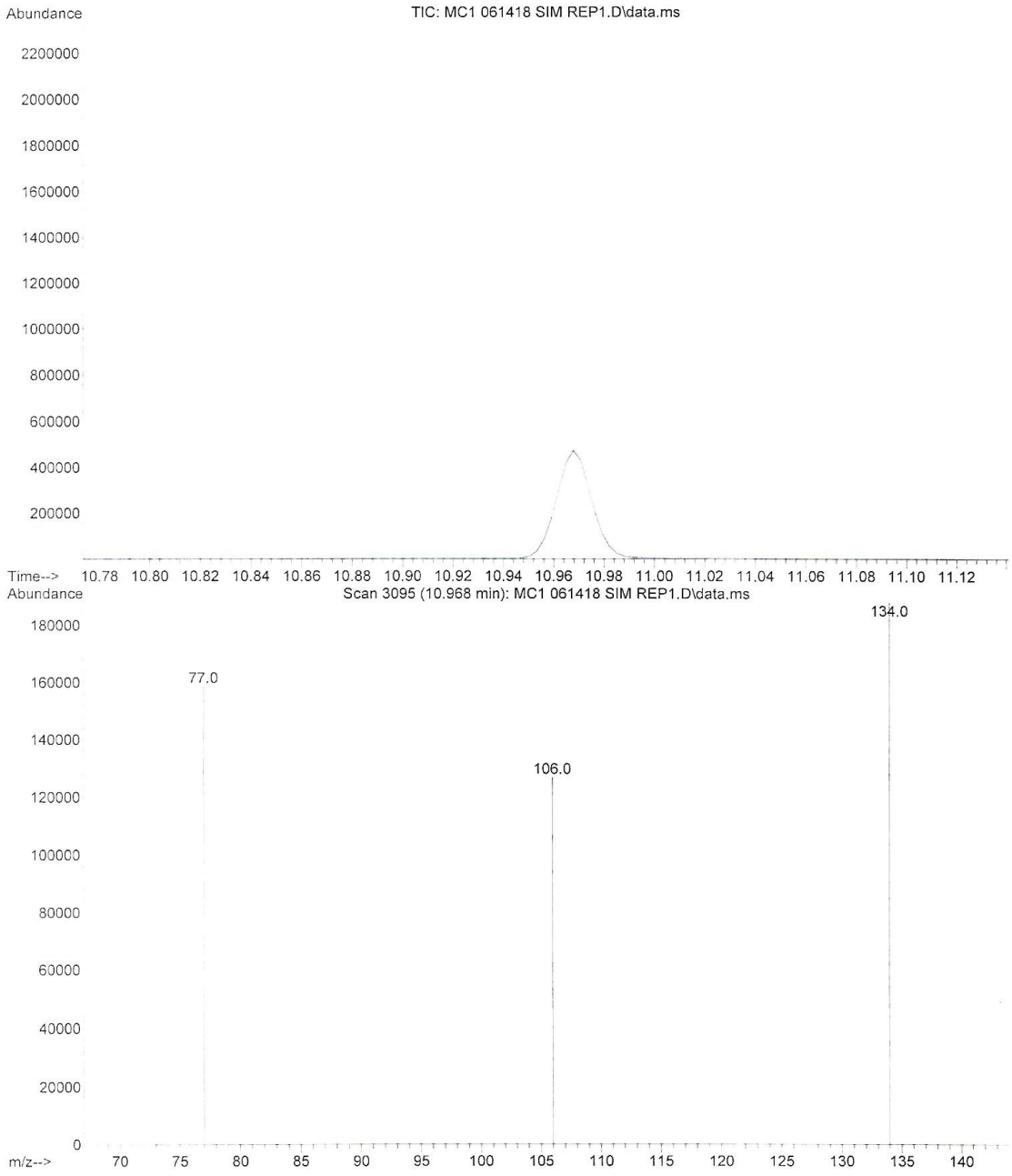

```
File       :C:\msdchem\1\data\TWW_Explosives\Methyl Centralite\MC1 06291
...         8 SIM NO F REP1 S1.D
Operator   :
Instrument :     5975 MSD
Acquired   : 29 Jun 2018  10:44      using AcqMethod TWW_UNI1 SIM TEST MC1 80MSEC
Sample Name: MC1 5 ng/ul NO FABRIC
Misc Info  :
```

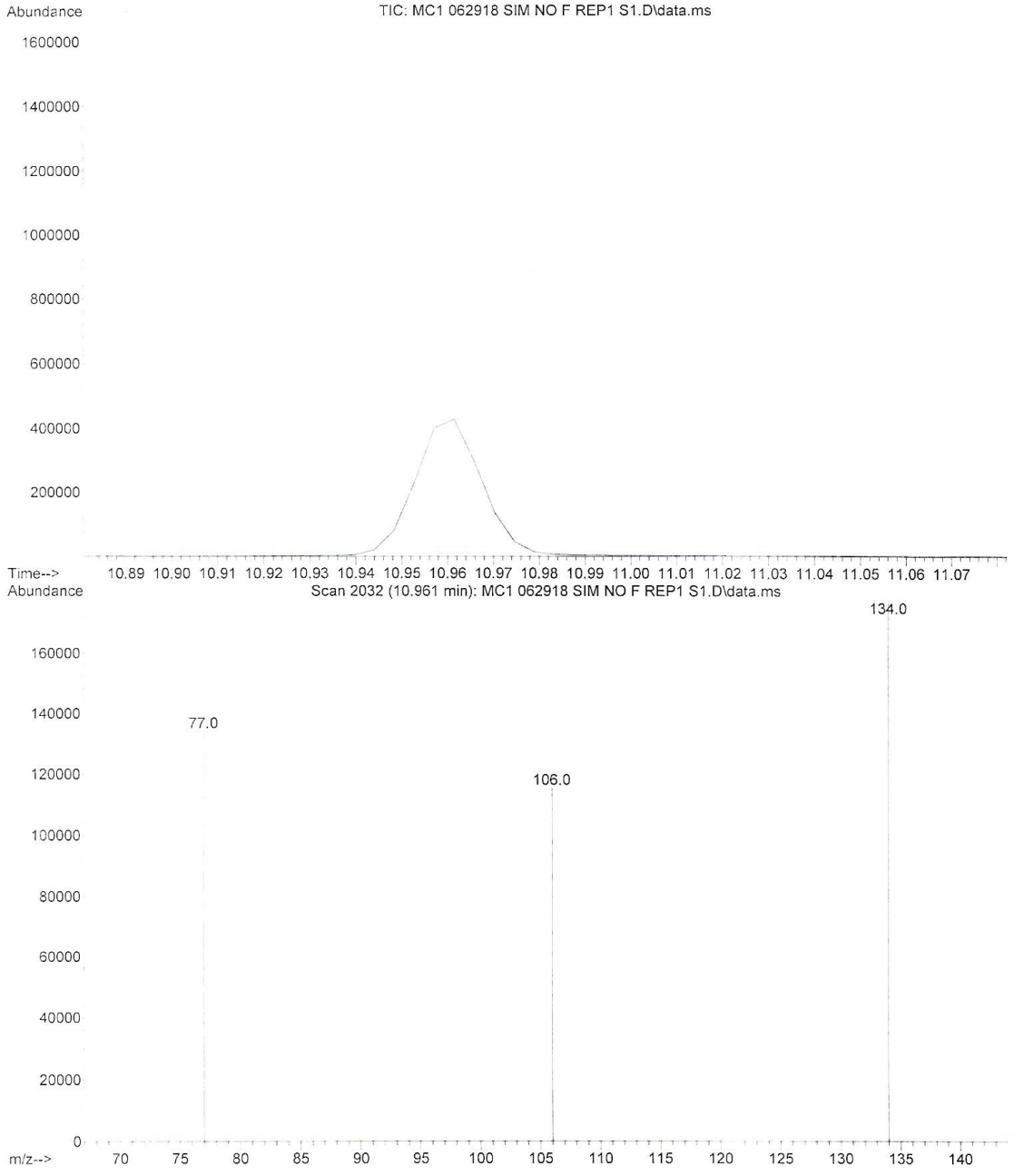

```
File       :C:\msdchem\1\data\TWW_Explosives\ALS Run 080818\MC1 3 ng rep
...          1.D
Operator   :
Instrument :    5975 MSD
Acquired   :  8 Aug 2018  18:57     using AcqMethod TWW MC1 SIM DEFAULT.M
Sample Name: MC1 3 ng
Misc Info  :
```

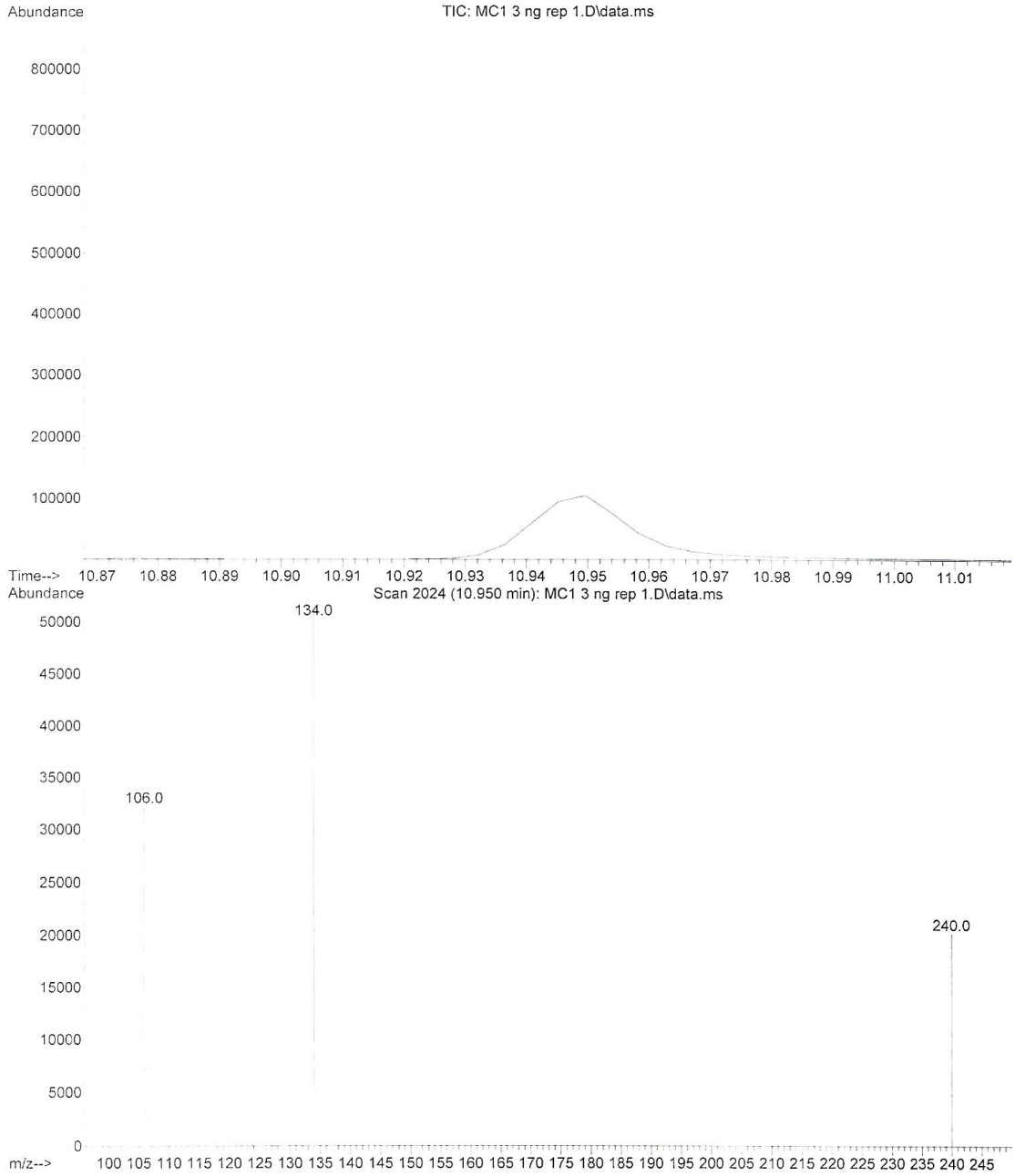

```
File        :C:\msdchem\1\data\TWW_Explosives\ALS Run 080818\MC1 2 ng rep
...           1.D
Operator    :
Instrument  :     5975 MSD
Acquired    :   8 Aug 2018   19:19      using AcqMethod TWW MC1 SIM DEFAULT.M
Sample Name: MC1 2 ng
Misc Info   :
```

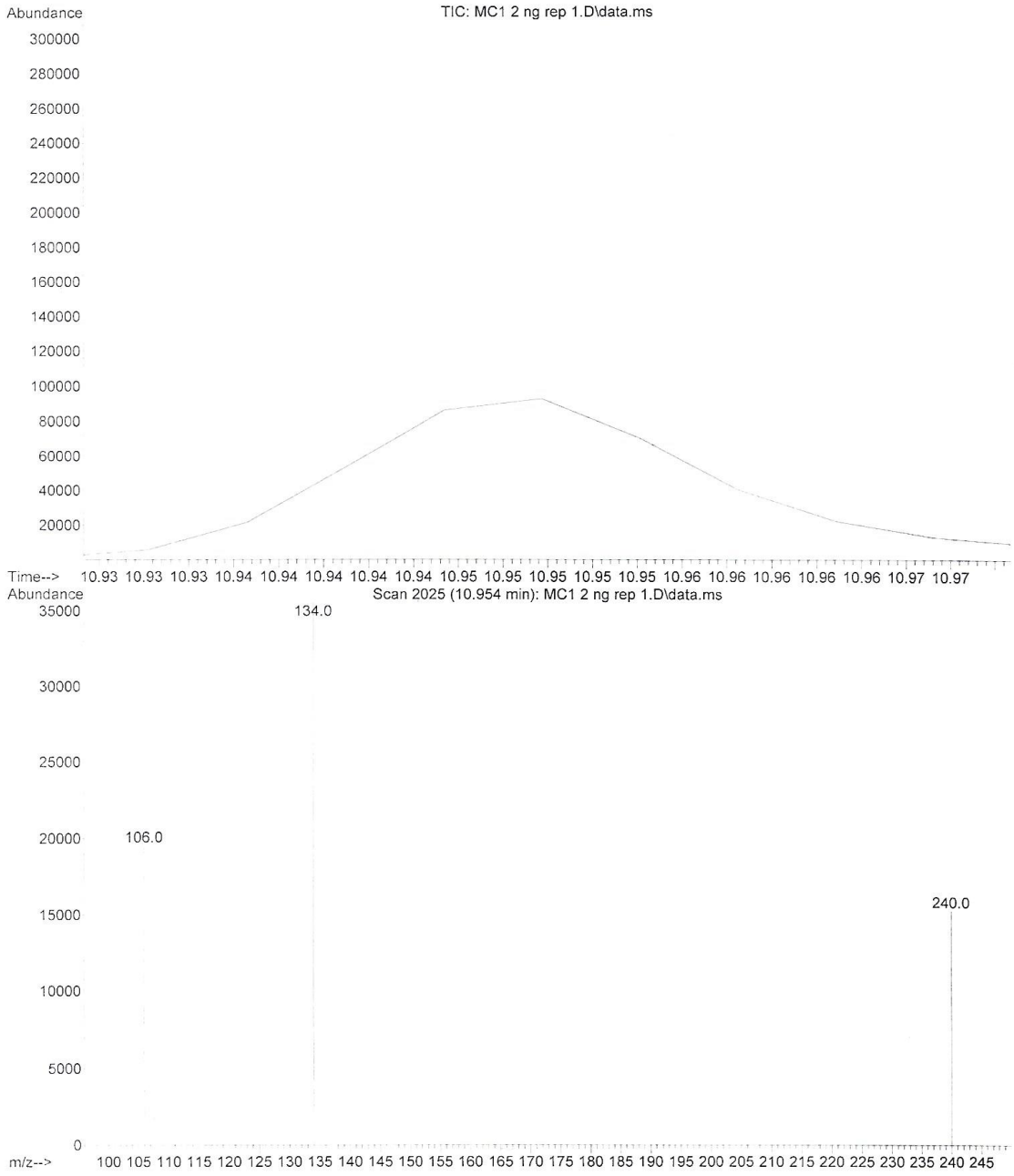

```
File        :C:\msdchem\1\data\TWW_Explosives\ALS Run 080818\MC1 1 ng rep
...           1.D
Operator    :
Instrument  :     5975 MSD
Acquired    :  8 Aug 2018  19:41      using AcqMethod TWW MC1 SIM DEFAULT.M
Sample Name: MC1 1 ng
Misc Info   :
```

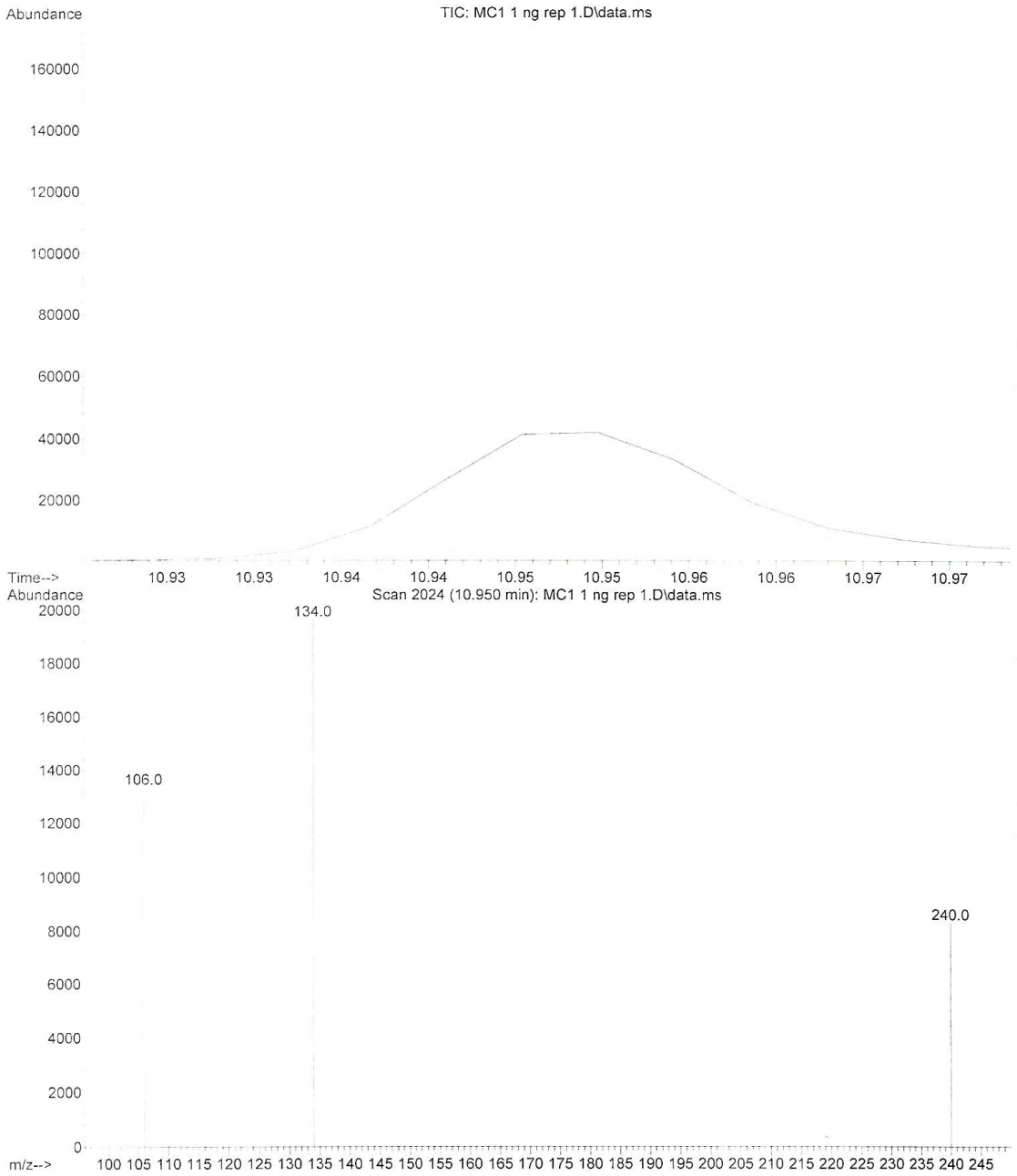

```
File       :C:\msdchem\1\data\TWW_Explosives\ALS Run 080818\MC1 half ng
...         rep 1.D
Operator   :
Instrument :    5975 MSD
Acquired   :  8 Aug 2018  20:02     using AcqMethod TWW MC1 SIM DEFAULT.M
Sample Name: MC1 .5 ng
Misc Info  :
```

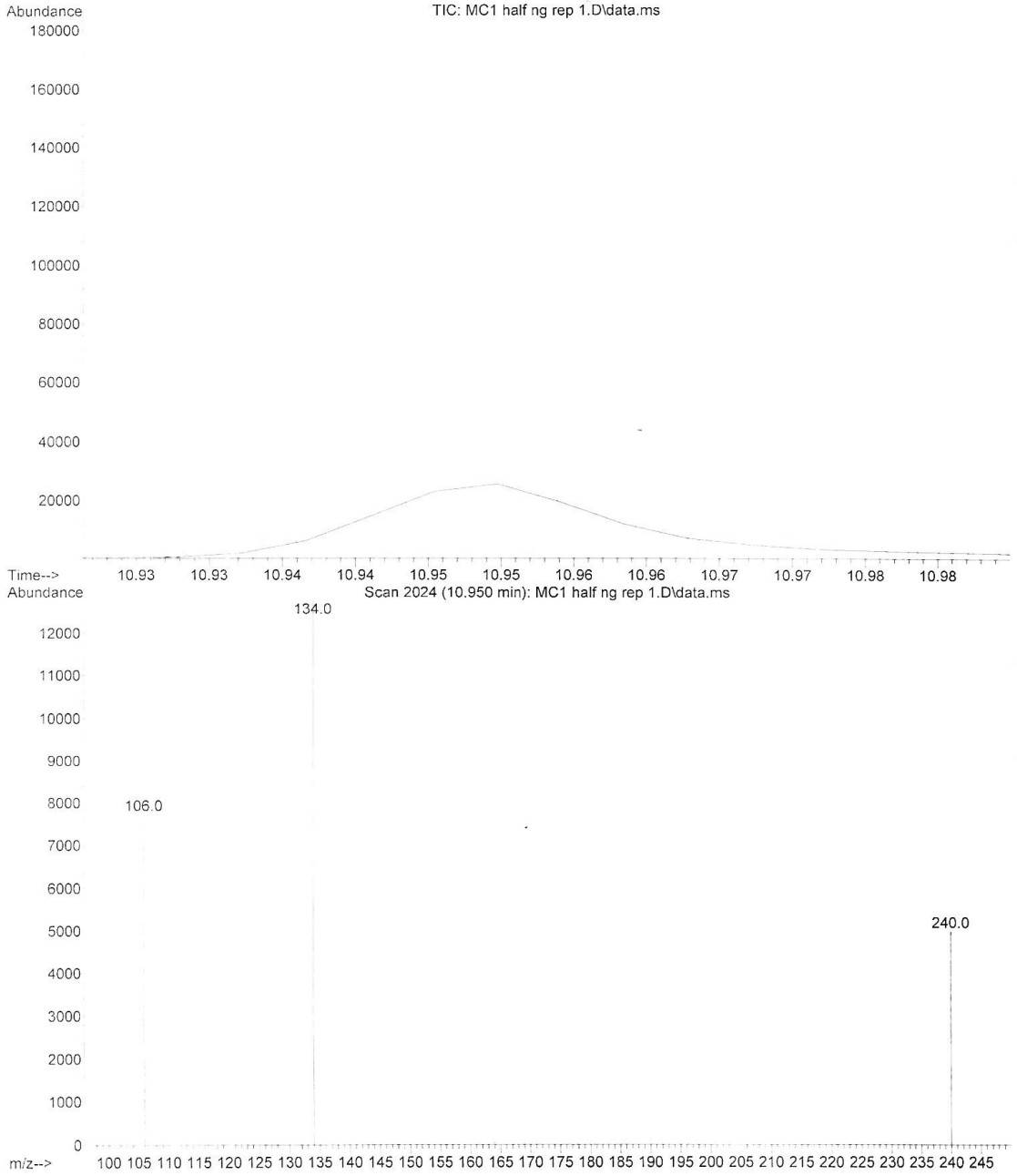

```
File       :C:\msdchem\1\data\TWW_Explosives\Methyl Centralite\MC1 62018
...          SIM 80MSEC COTTON REP1 S1.D
Operator   :
Instrument :    5975 MSD
Acquired   : 20 Jun 2018  14:36     using AcqMethod TWW_UNI1 SIM TEST MC1 80MSEC
Sample Name: 10 ng/uL MC1 COTTON 80MSEC
Misc Info  :
```

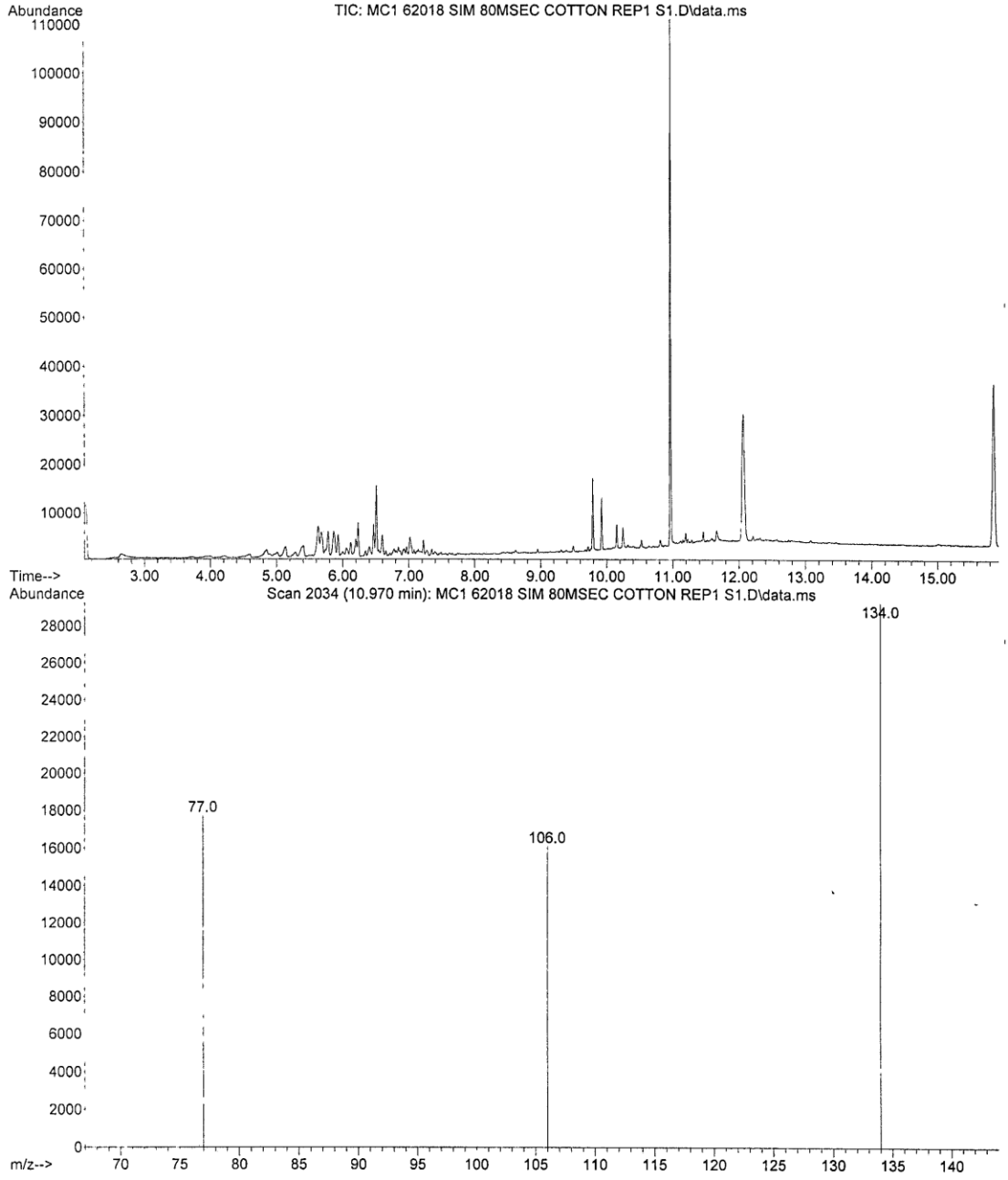

```
File       :C:\msdchem\1\data\TWW_Explosives\Methyl Centralite\MC1 07111
...         8 SIM COTN 5NG REP1 S1.D
Operator   :
Instrument :     5975 MSD
Acquired   : 11 Jul 2018  15:15     using AcqMethod TWW_UNI1 SIM TEST MC1 80MSEC
Sample Name: MC1 5 ng/ul 100% COTTON REP1 S1
Misc Info  :
```

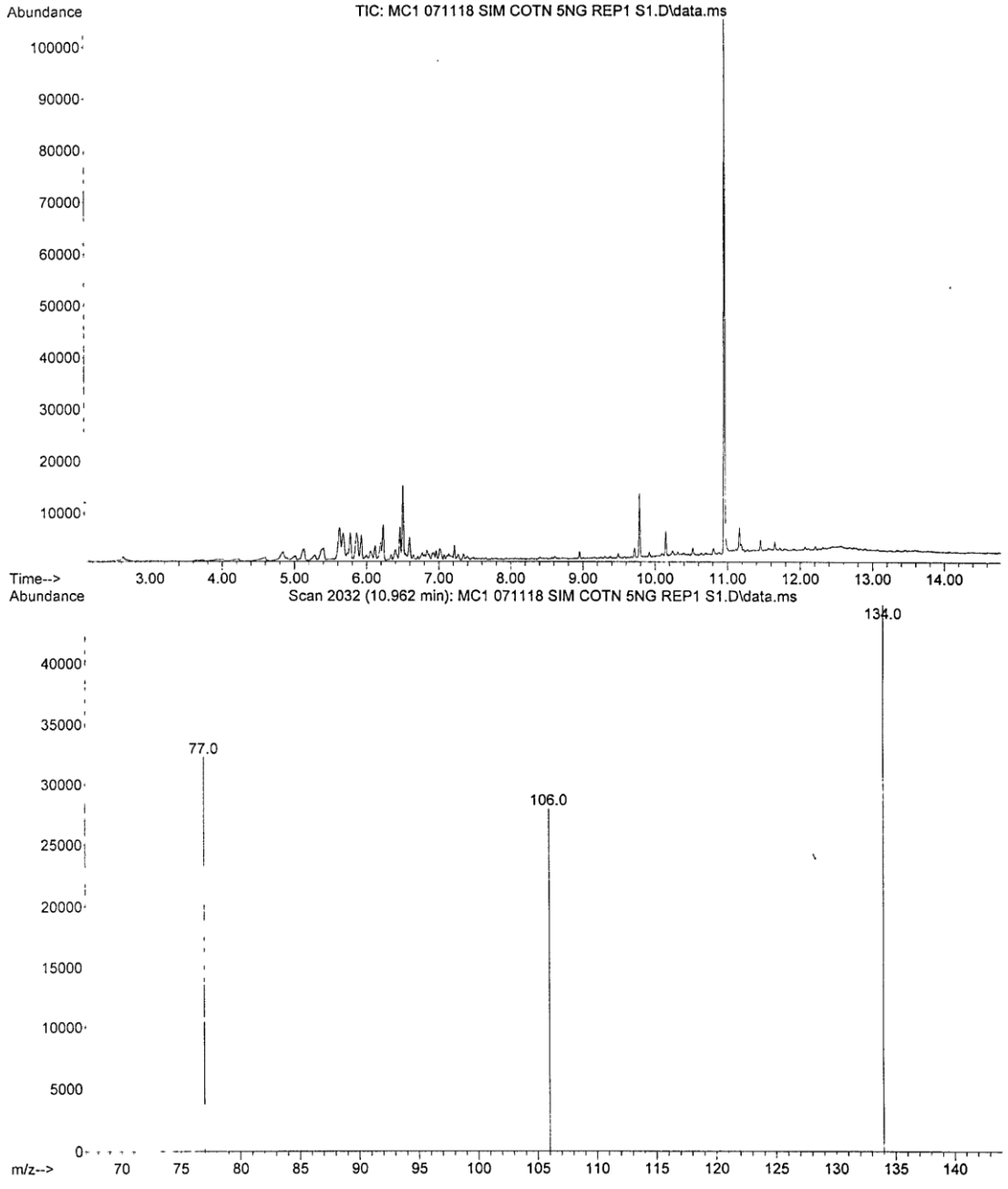

```
File       :C:\msdchem\1\data\TWW_Explosives\Methyl Centralite\MC1 07181
...         8 10NGUL BLOOD REP1 S1.D
Operator   :
Instrument :    5975 MSD
Acquired   : 18 Jul 2018  14:19     using AcqMethod TWW_UNI1 SIM TEST MC1 80MSEC
Sample Name: MC1 10ng/ul BLOOD REP1 S1
Misc Info  :
```

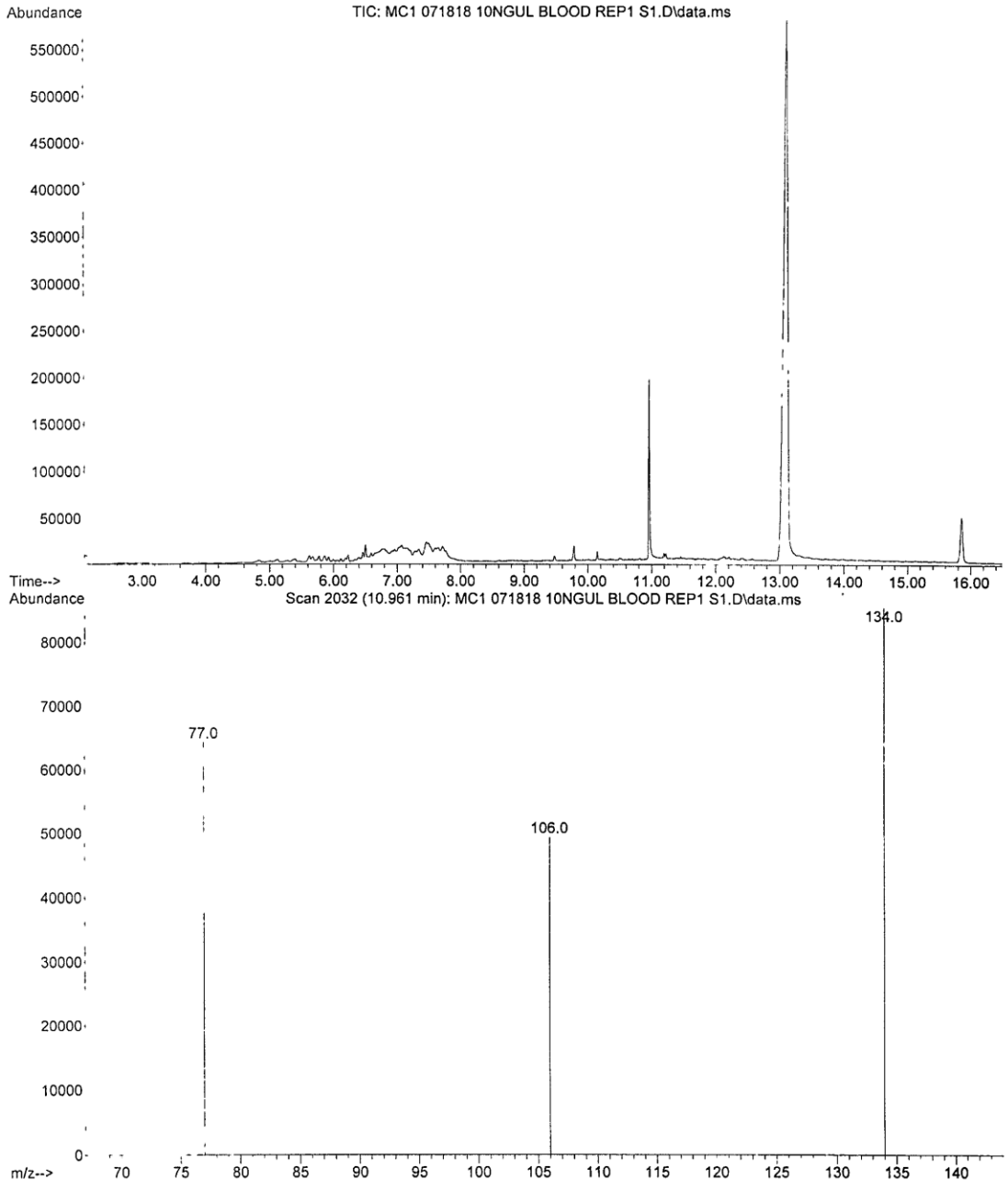

```
File       :C:\msdchem\1\data\TWW_Explosives\Diphenylamine\DPA 100 NG RE
...         P2 SIM AND SCAN.D
Operator   :
Instrument :    5975 MSD
Acquired   : 17 Aug 2018  11:11     using AcqMethod TWW DPA SIM DEFAULT.M
Sample Name: DPA 100 ng rep2 SIM and SCAN
Misc Info  :
```

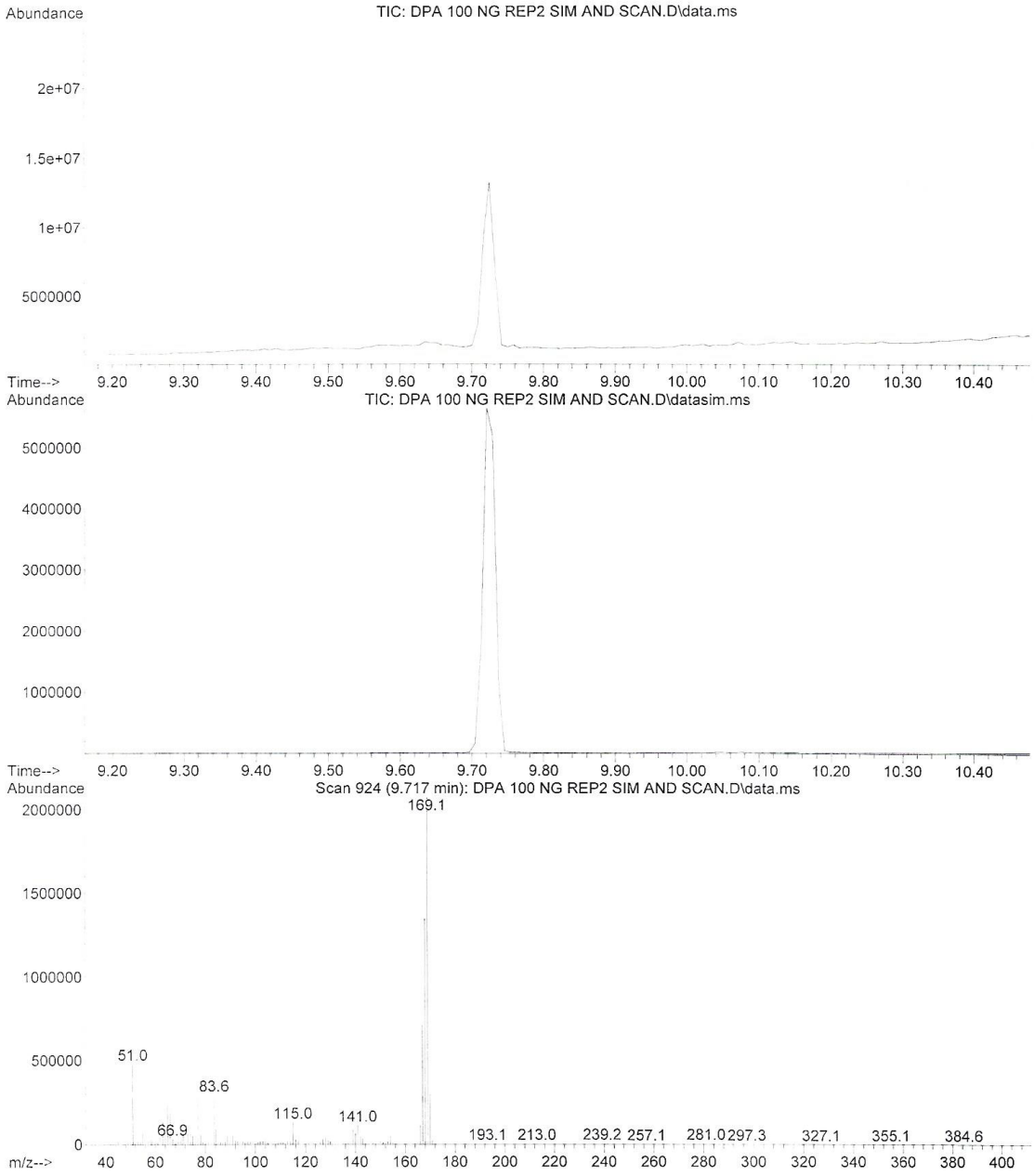

```
File       :C:\msdchem\1\data\TWW_Explosives\Diphenylamine\DPA 062218 SI
...         M 80MSEC REP2 S1.D
Operator   :
Instrument :    5975 MSD
Acquired   : 22 Jun 2018   8:54     using AcqMethod TWW_UNI1 SIM TEST DPA 80 MSE
Sample Name: 10 ng/ul DPA no fabric
Misc Info  :
```

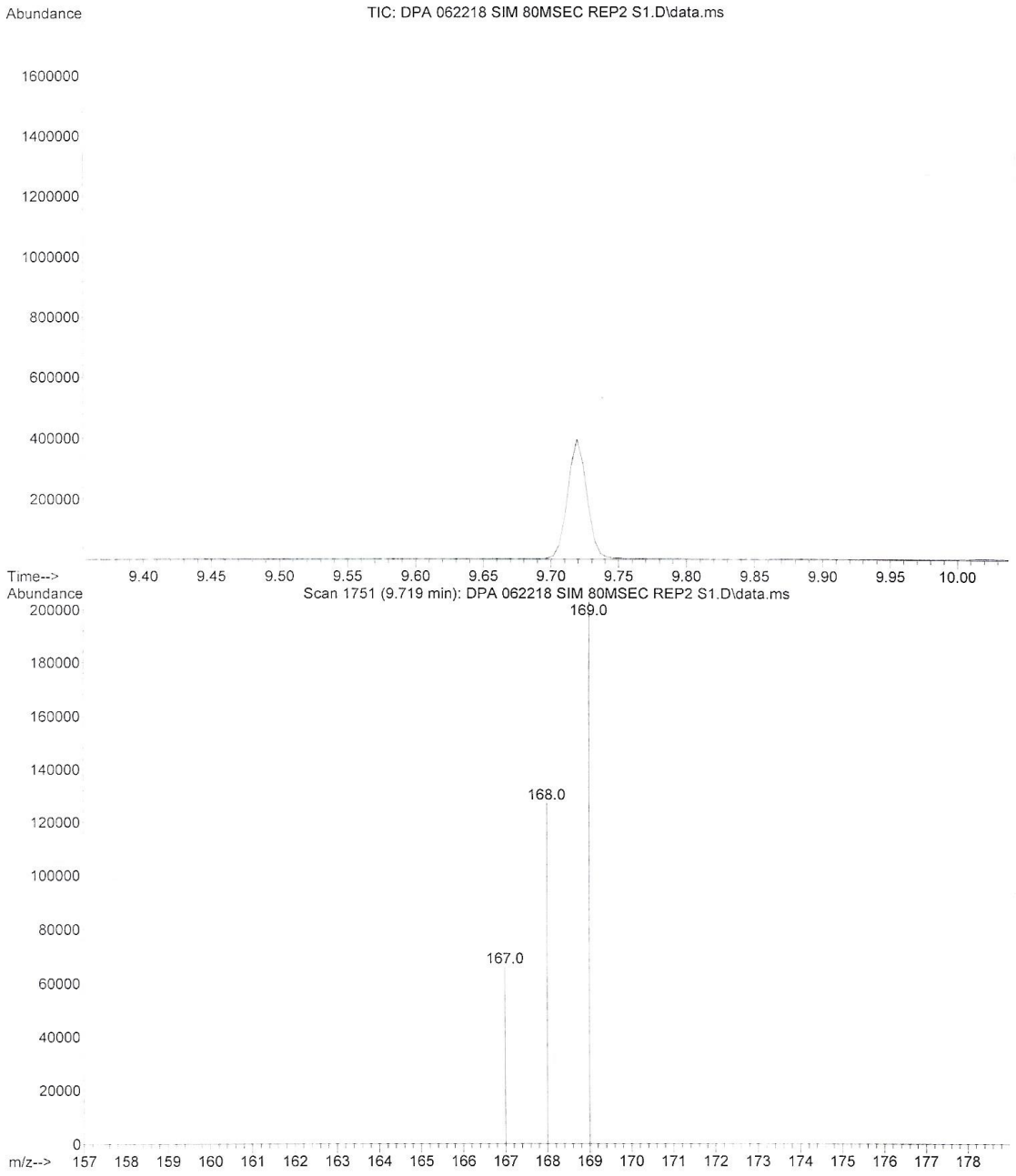

```
File       :C:\msdchem\1\data\TWW_Explosives\Diphenylamine\DPA 062918 SI
...         M NO F REP2 S1.D
Operator   :
Instrument :    5975 MSD
Acquired   : 29 Jun 2018  11:31     using AcqMethod TWW_UNI1 SIM TEST DPA 80 MSE
Sample Name: DPA 5 ng/ul NO FABRIC
Misc Info  :
```

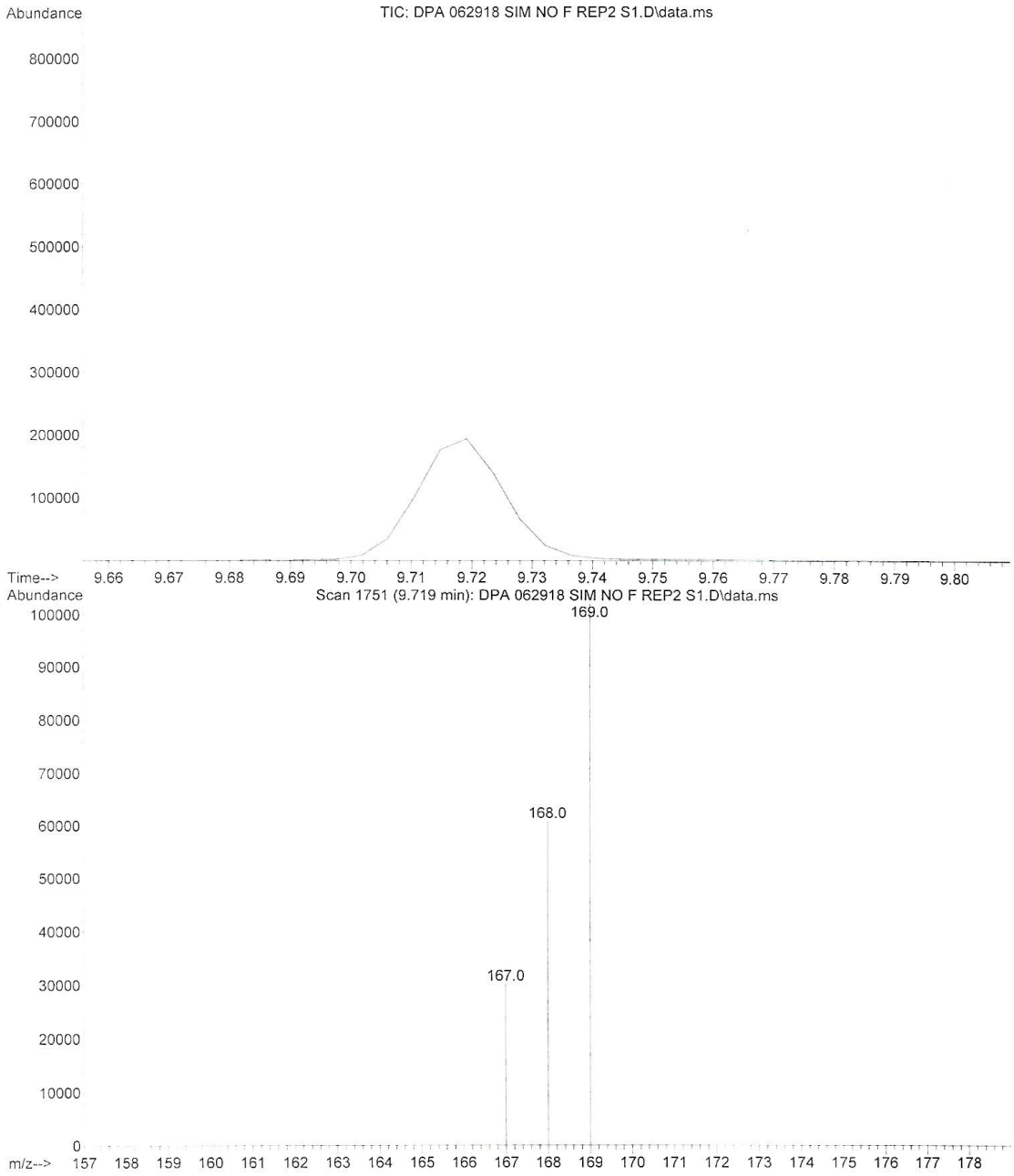

```
File       :C:\msdchem\1\data\TWW_Explosives\ALS Run 080818\DPA 3 ng rep
...          1.D
Operator   :
Instrument :    5975 MSD
Acquired   :  8 Aug 2018  13:53     using AcqMethod TWW DPA SIM DEFAULT.M
Sample Name: DPA 3 ng
Misc Info  :
```

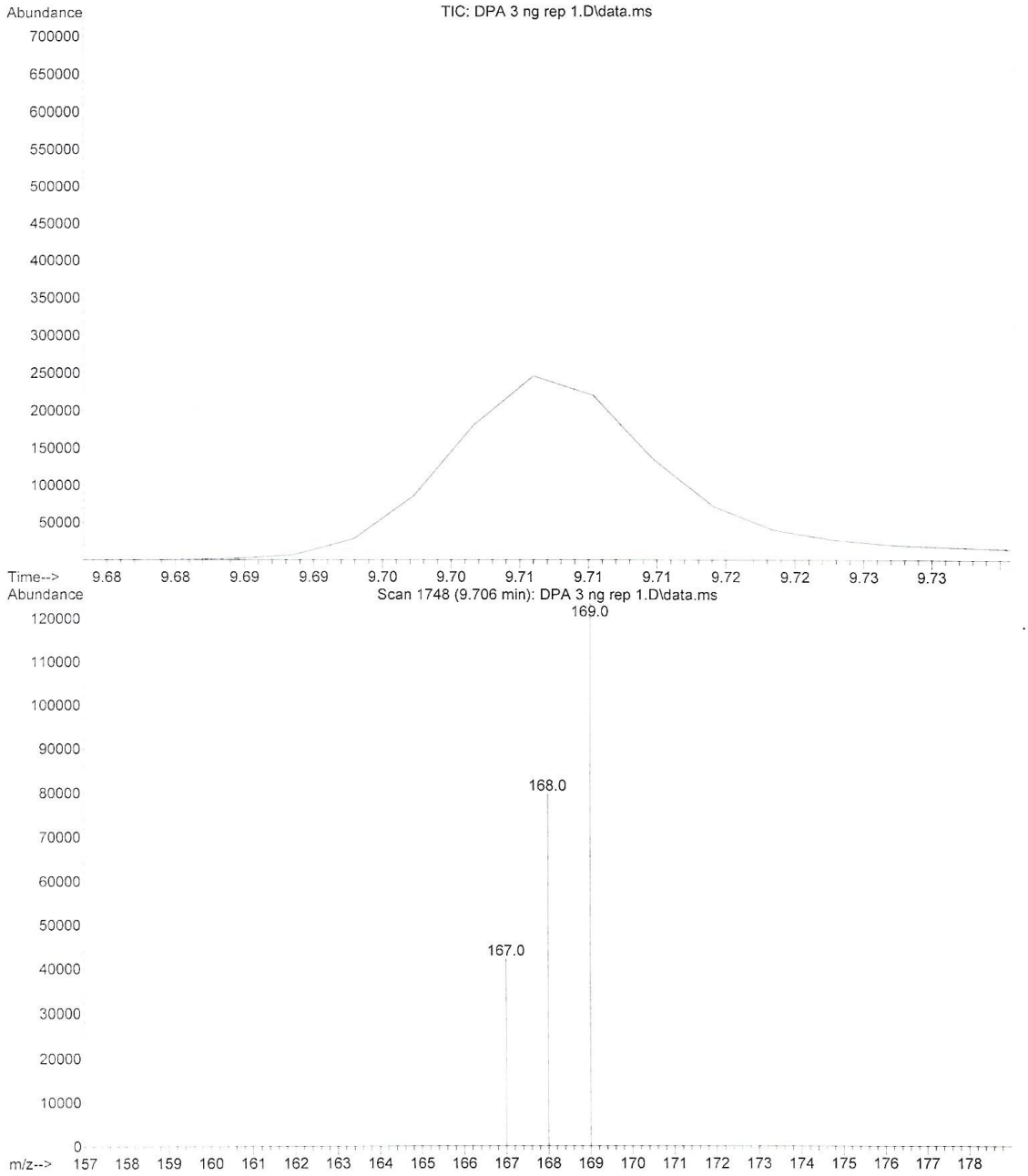

```
File       :C:\msdchem\1\data\TWW_Explosives\ALS Run 080818\DPA 2 ng rep
...          1.D
Operator   :
Instrument :    5975 MSD
Acquired   :  8 Aug 2018  14:15     using AcqMethod TWW DPA SIM DEFAULT.M
Sample Name: DPA 2 ng
Misc Info  :
```

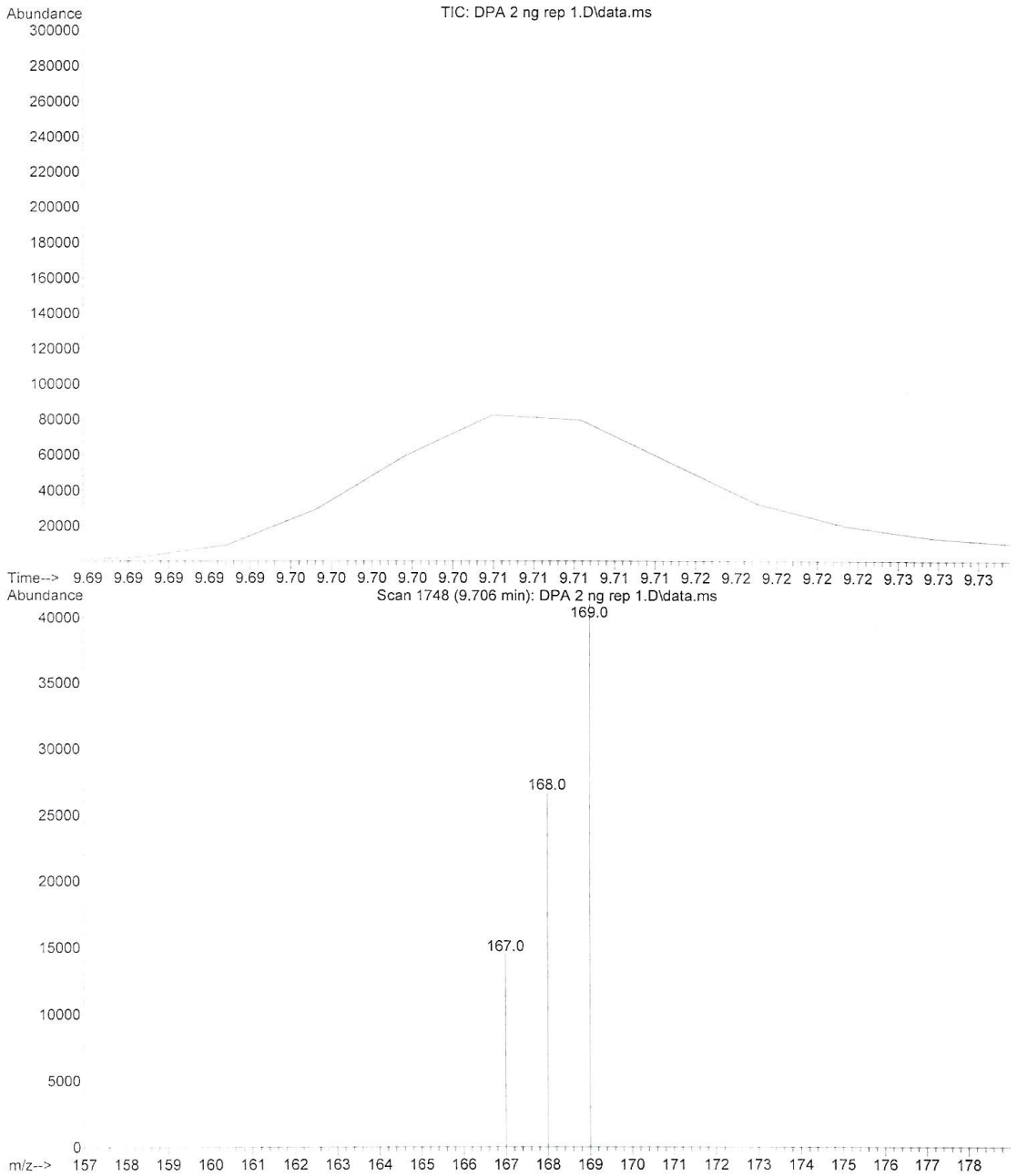

```
File       :C:\msdchem\1\data\TWW_Explosives\ALS Run 080818\DPA 1 ng rep
...          1.D
Operator   :
Instrument :    5975 MSD
Acquired   :  8 Aug 2018  14:37     using AcqMethod TWW DPA SIM DEFAULT.M
Sample Name: DPA 1 ng
Misc Info  :
```

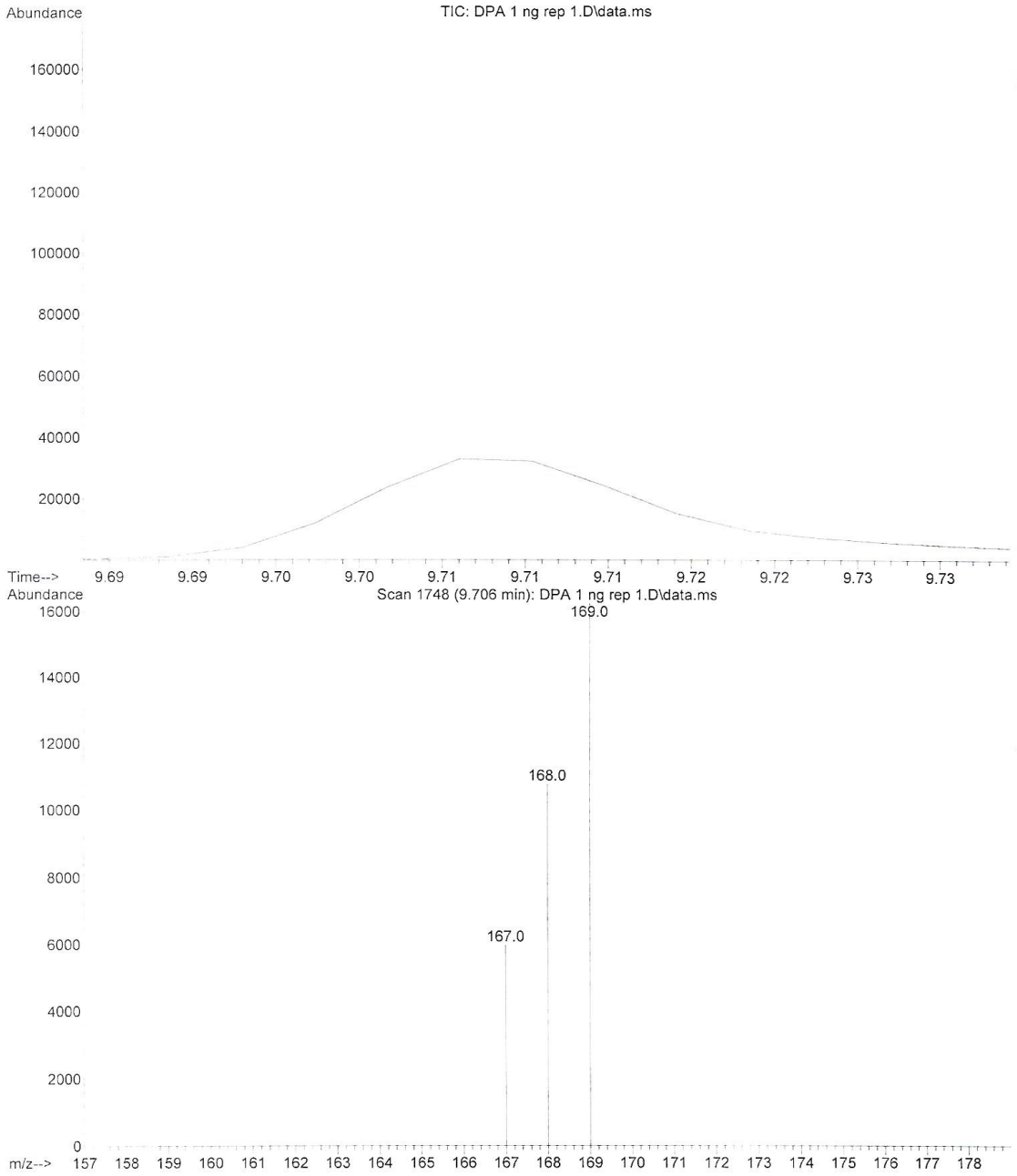

```
File        :C:\msdchem\1\data\TWW_Explosives\ALS Run 080818\DPA half ng
...          rep 1.D
Operator    :
Instrument  :    5975 MSD
Acquired    :  8 Aug 2018  14:58     using AcqMethod TWW DPA SIM DEFAULT.M
Sample Name: DPA .5 ng
Misc Info   :
```

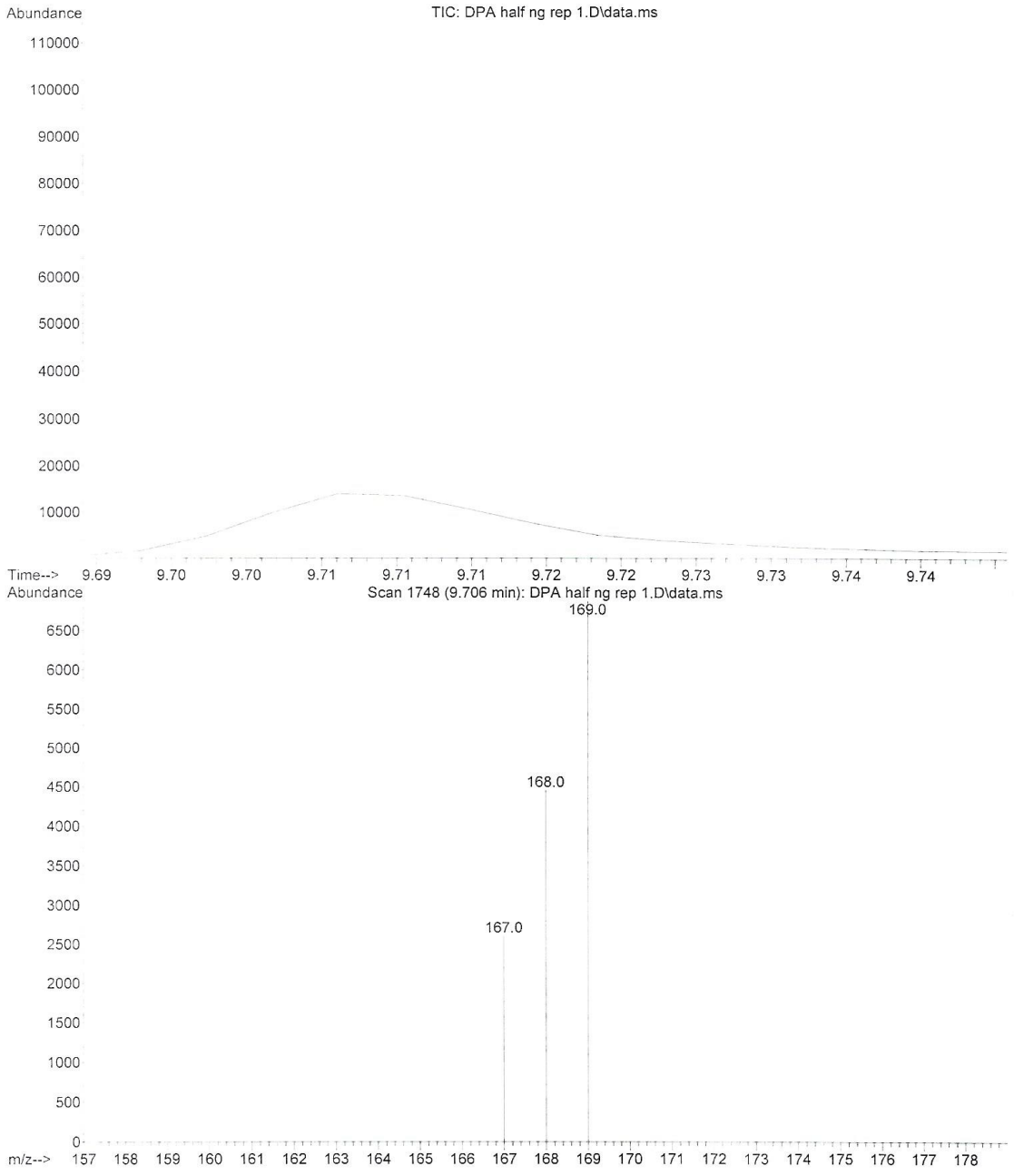

```
File       :C:\msdchem\1\data\TWW_Explosives\Diphenylamine\DPA 71318 10
...         NGUL COTN REP1 S1.D
Operator   :
Instrument :    5975 MSD
Acquired   : 13 Jul 2018  10:06     using AcqMethod TWW_UNI1 SIM TEST DPA 80 MSE
Sample Name: DPA 10ng/ul 100% Cotton REP1 S1
Misc Info  :
```

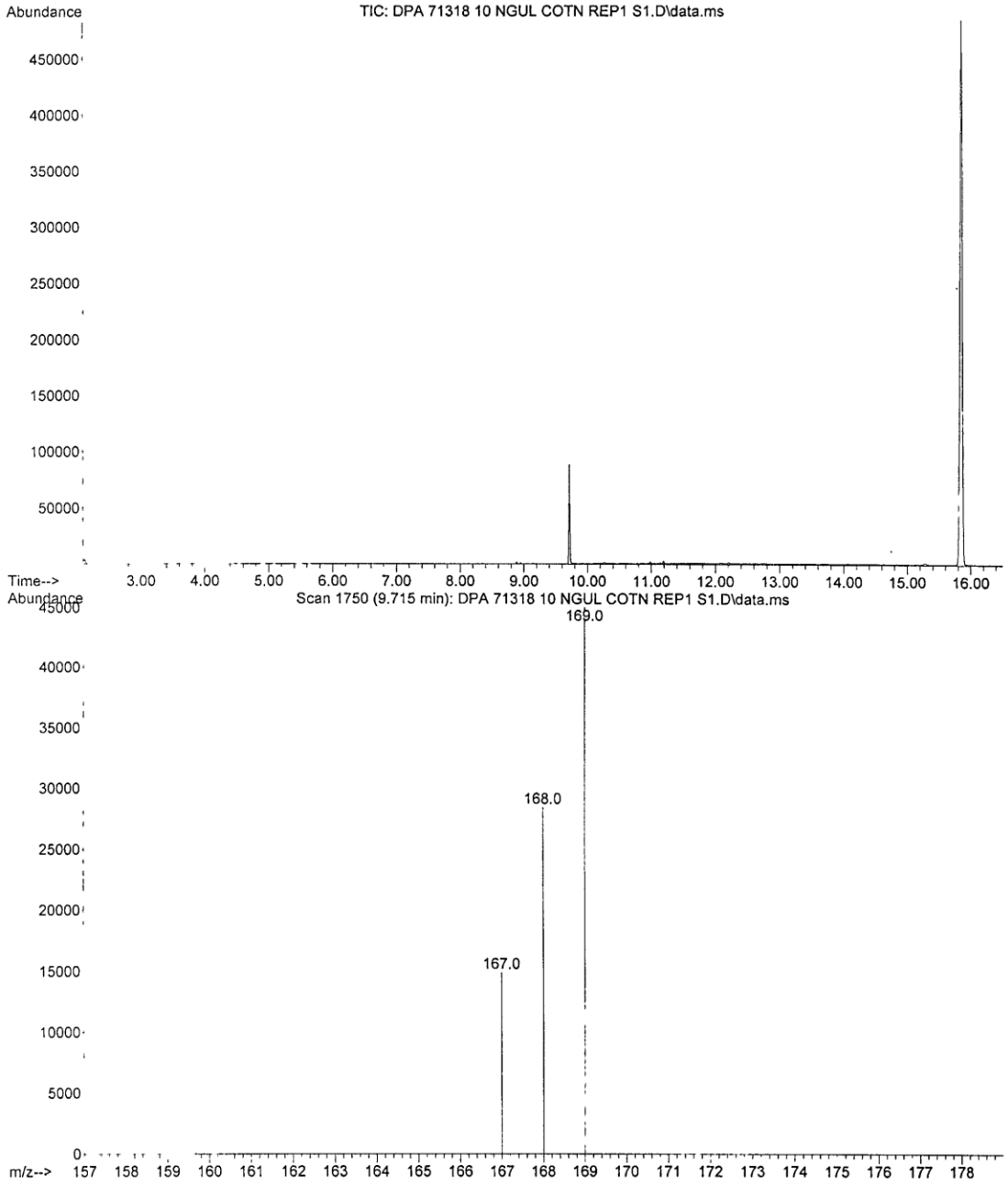

```
File        :C:\msdchem\1\data\TWW_Explosives\Diphenylamine\DPA 071118 SI
...          M COTN 5NG REP1 S1.D
Operator    :
Instrument  :     5975 MSD
Acquired    : 11 Jul 2018  13:02     using AcqMethod TWW_UNI1 SIM TEST DPA 80 MSE
Sample Name: DPA 5 ng/ul 100% COTTON REP1 S1
Misc Info   :
```

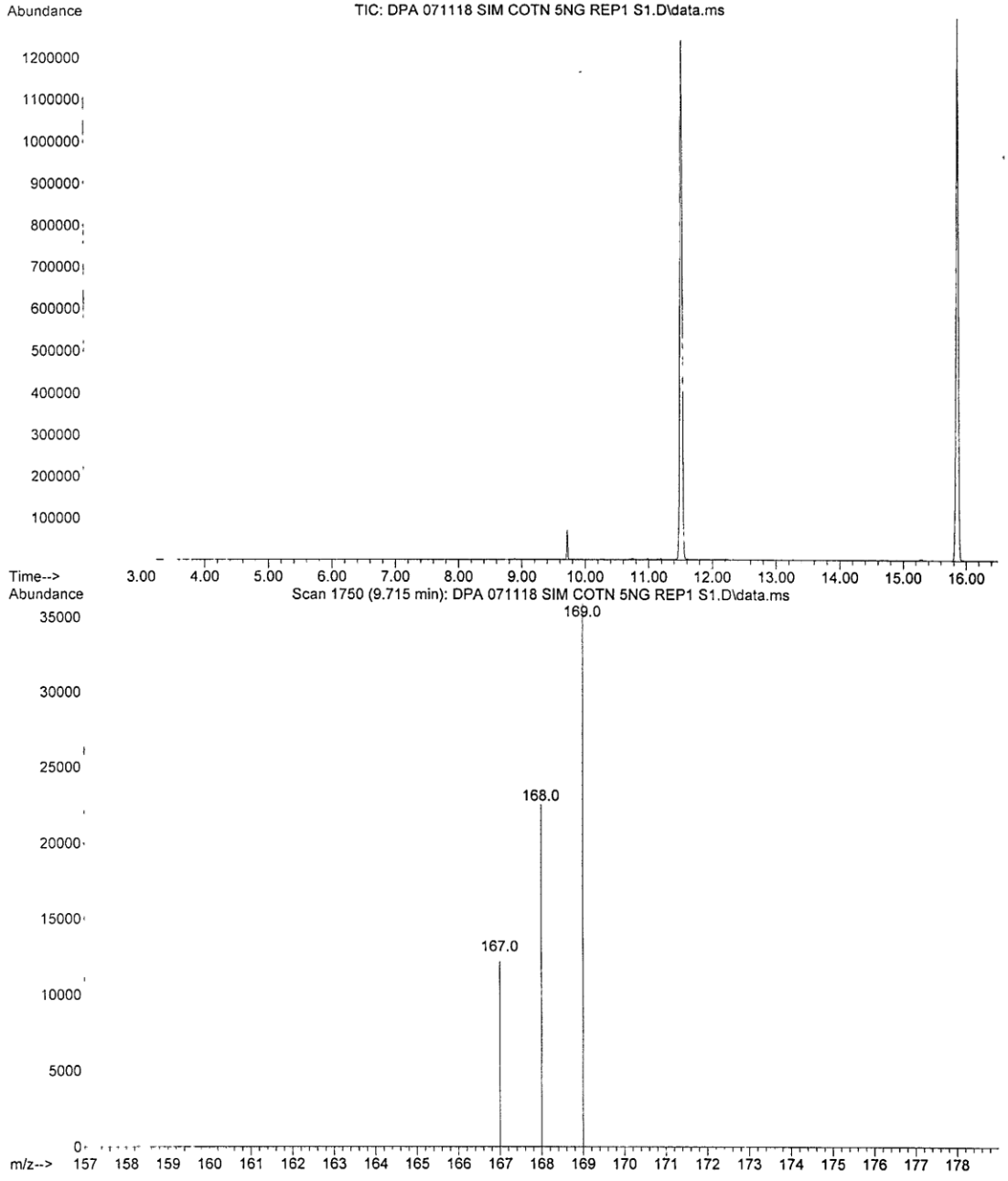

```
File       :C:\msdchem\1\data\TWW_Explosives\Diphenylamine\DPA 71318 10
...         NGUL BLOOD REP2 S1.D
Operator   :
Instrument :    5975 MSD
Acquired   : 13 Jul 2018  10:31     using AcqMethod TWW_UNI1 SIM TEST DPA 80 MSE
Sample Name: DPA 10ng/ul BLOOD REP2 S1
Misc Info  :
```

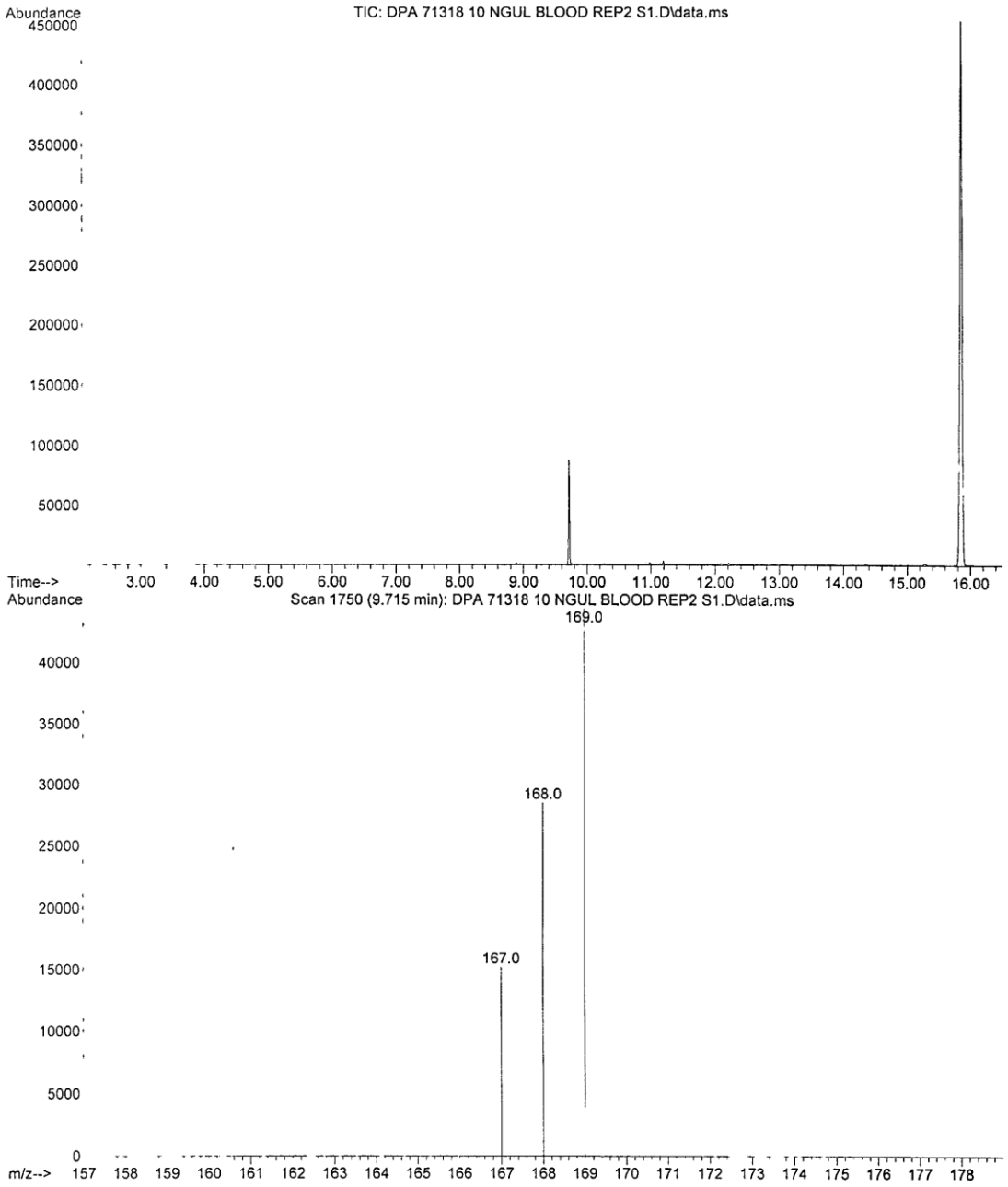

```
File       :C:\msdchem\1\data\TWW_Explosives\2-4 Dinotrotoluene\2-4 DNL
...         061318 UNI1.D
Operator   :
Instrument :     5975 MSD
Acquired   : 13 Jun 2018  15:08      using AcqMethod TWW_UNI1.M
Sample Name: 100 ng/uL MC1
Misc Info  :
```

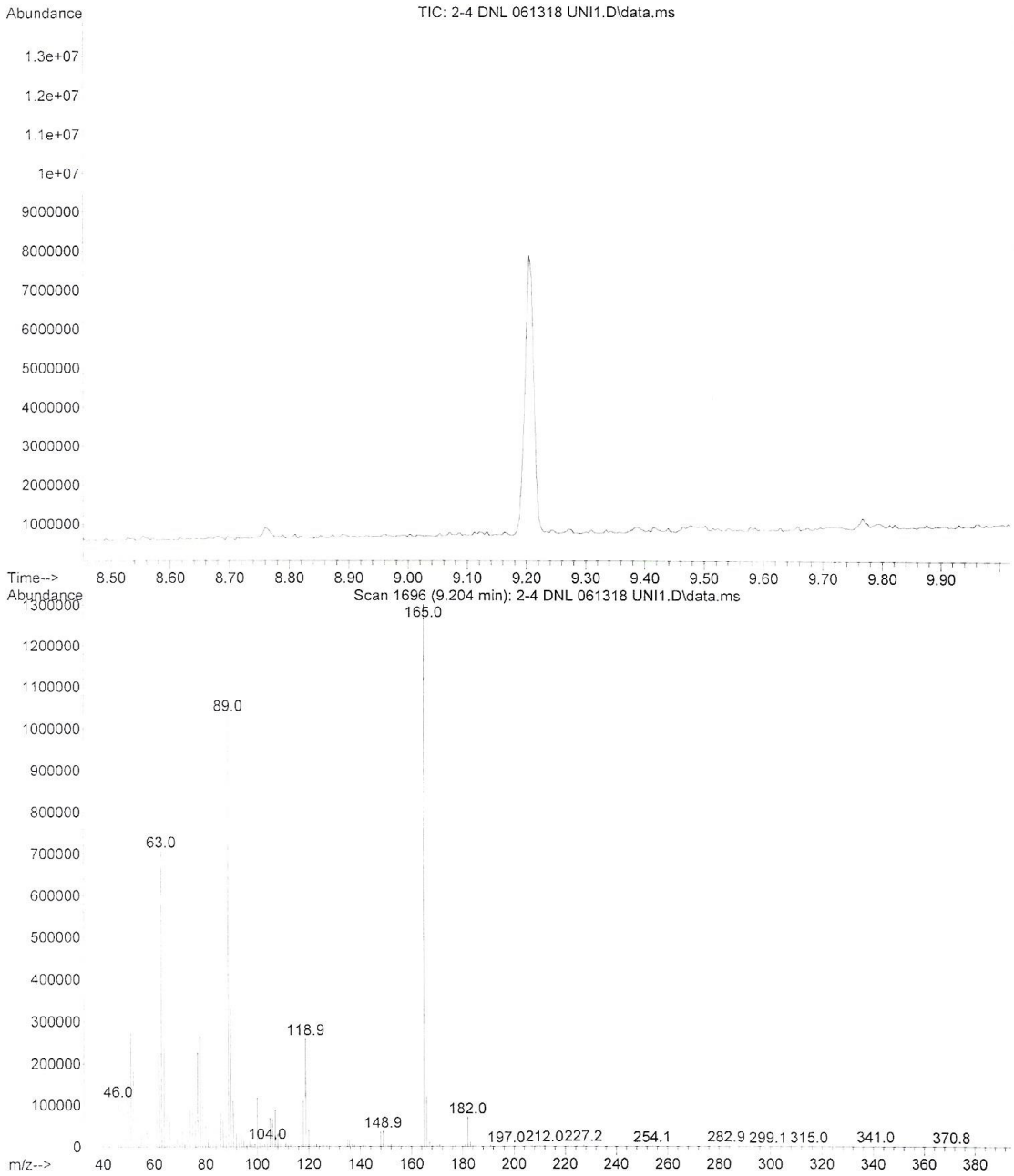

```
File       :C:\msdchem\1\data\TWW_Explosives\2-4 Dinotrotoluene\2-4 DNL
...         82018 SIM 80MSEC NO F REP1 S1.D
Operator   :
Instrument :     5975 MSD
Acquired   : 20 Jun 2018  13:16      using AcqMethod TWW_UNI1 SIM TEST 2-4 DNL 80
Sample Name: 10 ng/uL 2-4 DNL no fabric 80MSEC
Misc Info  :
```

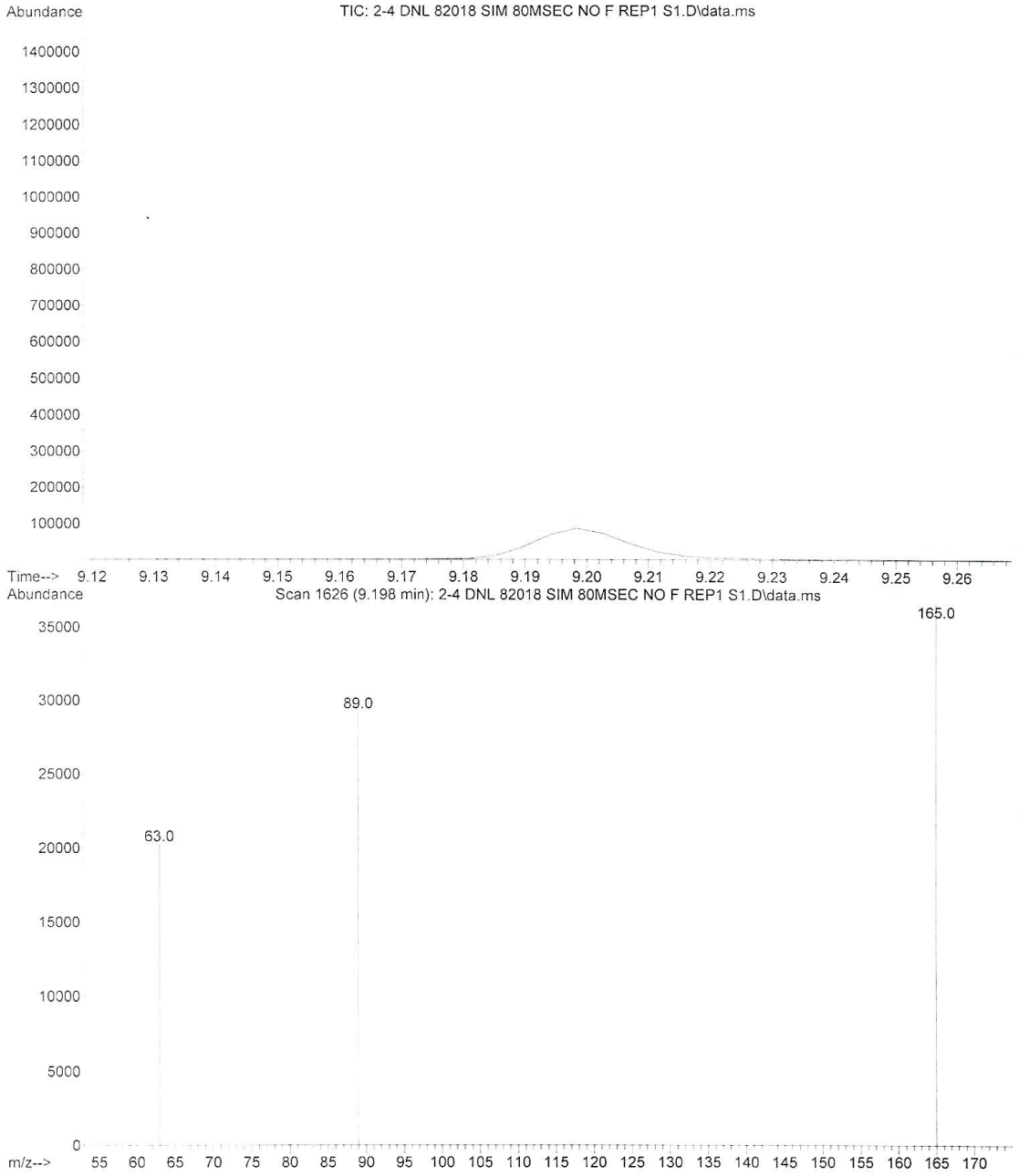

```
File       :C:\msdchem\1\data\TWW_Explosives\2-4 Dinotrotoluene\DNL 0629
...         18 SIM NO F REP1 S1.D
Operator   :
Instrument :     5975 MSD
Acquired   : 29 Jun 2018  12:14      using AcqMethod TWW_UNI1 SIM TEST 2-4 DNL 80
Sample Name: 2-4 DNL 5 ng/ul NO FABRIC
Misc Info  :
```

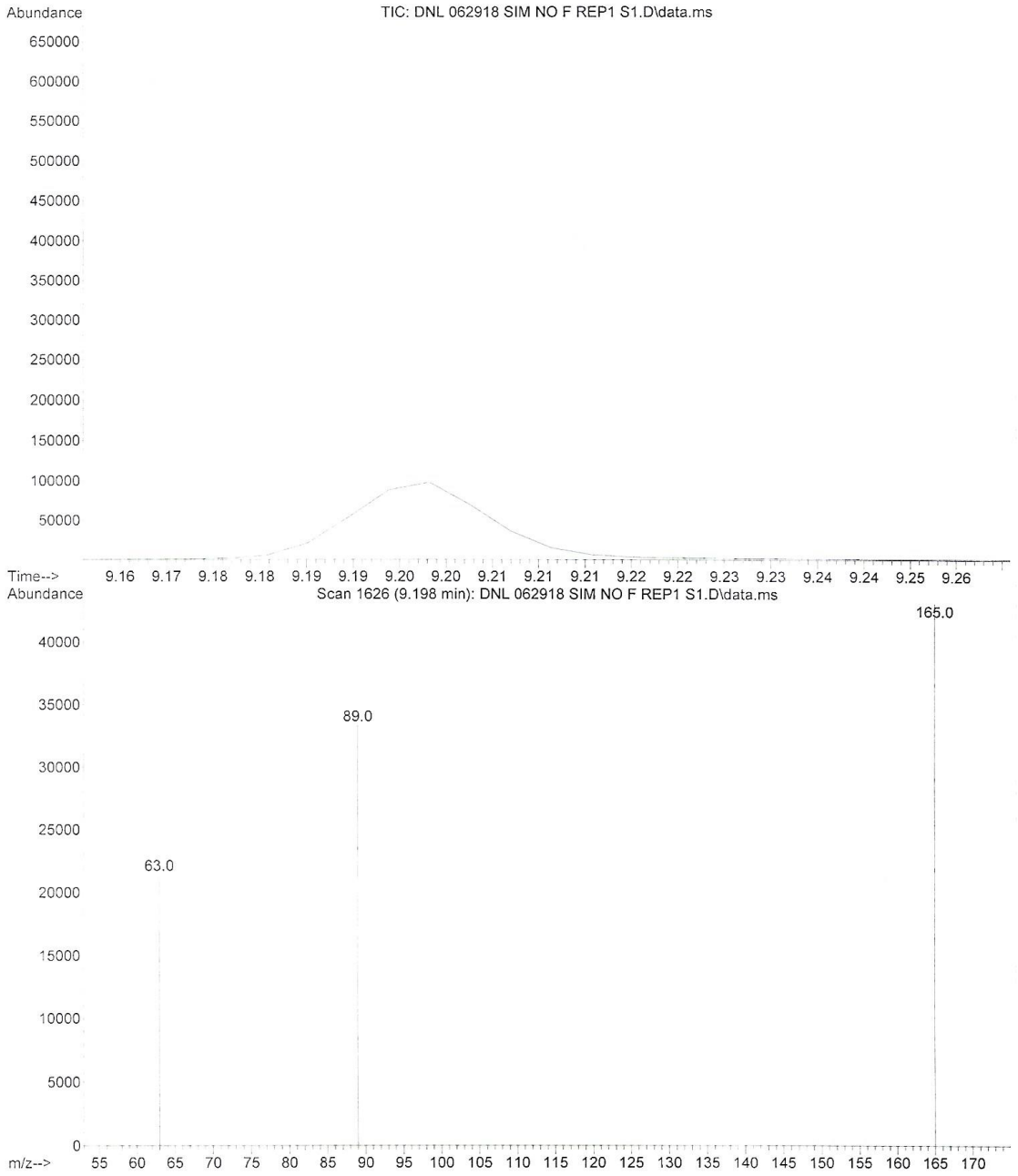

```
File       :C:\msdchem\1\data\TWW_Explosives\ALS Run 080818\2-4 DNL 3 ng
...          rep 1.D
Operator   :
Instrument :    5975 MSD
Acquired   :  8 Aug 2018  21:29     using AcqMethod TWW 2-4 DNL SIM DEFAULT.M
Sample Name: 2-4 DNL 3 ng
Misc Info  :
```

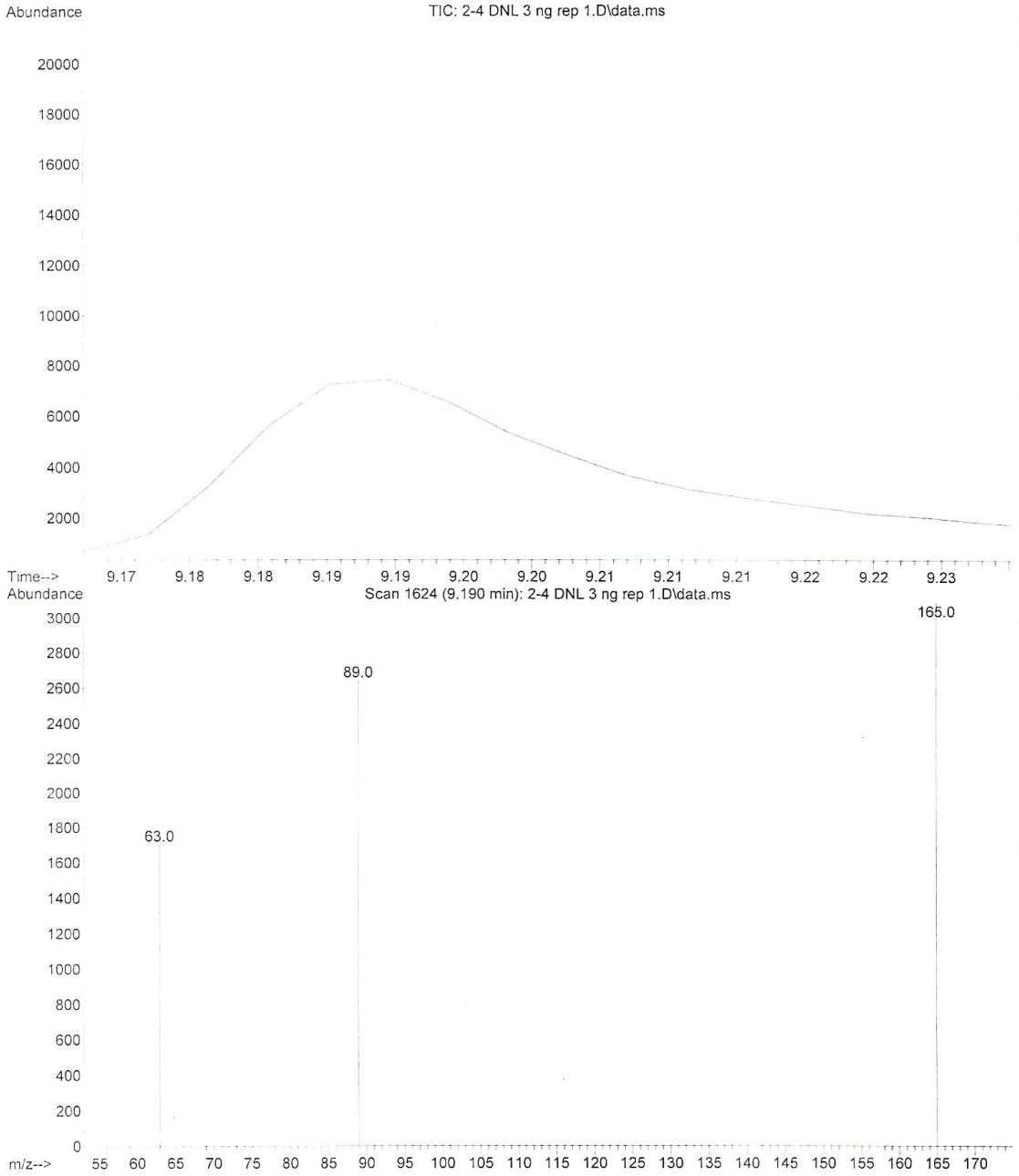

```
File       :C:\msdchem\1\data\TWW_Explosives\ALS Run 080818\2-4 DNL 2 ng
...          rep 1.D
Operator   :
Instrument :    5975 MSD
Acquired   :  8 Aug 2018  21:51     using AcqMethod TWW 2-4 DNL SIM DEFAULT.M
Sample Name: 2-4 DNL 2 ng
Misc Info  :
```

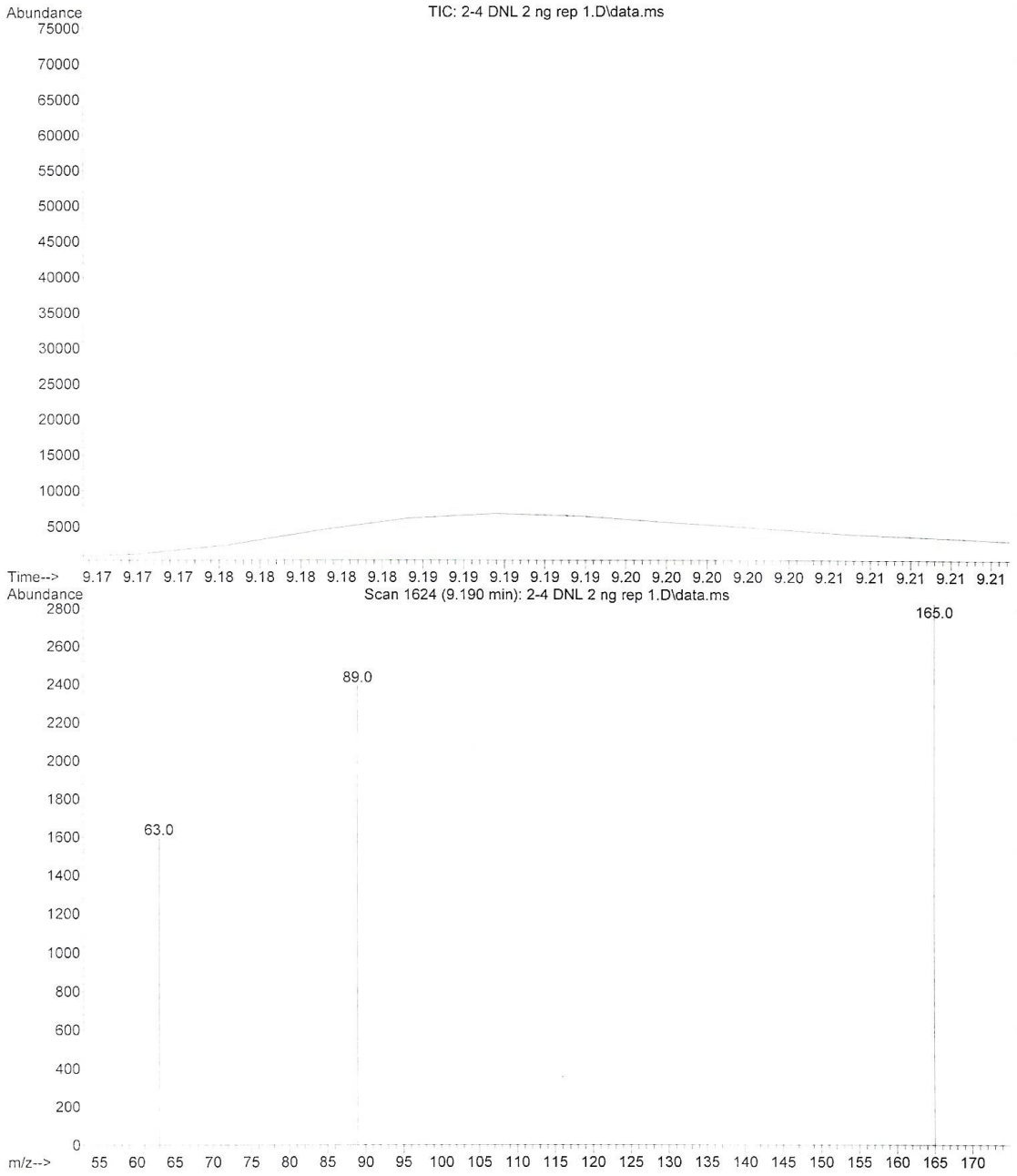

```
File       :C:\msdchem\1\data\TWW_Explosives\ALS Run 080818\204 DNL 1 ng
...          rep 1.D
Operator   :
Instrument :    5975 MSD
Acquired   :  8 Aug 2018  22:13     using AcqMethod TWW 2-4 DNL SIM DEFAULT.M
Sample Name: 2-4 DNL 1 ng
Misc Info  :
```

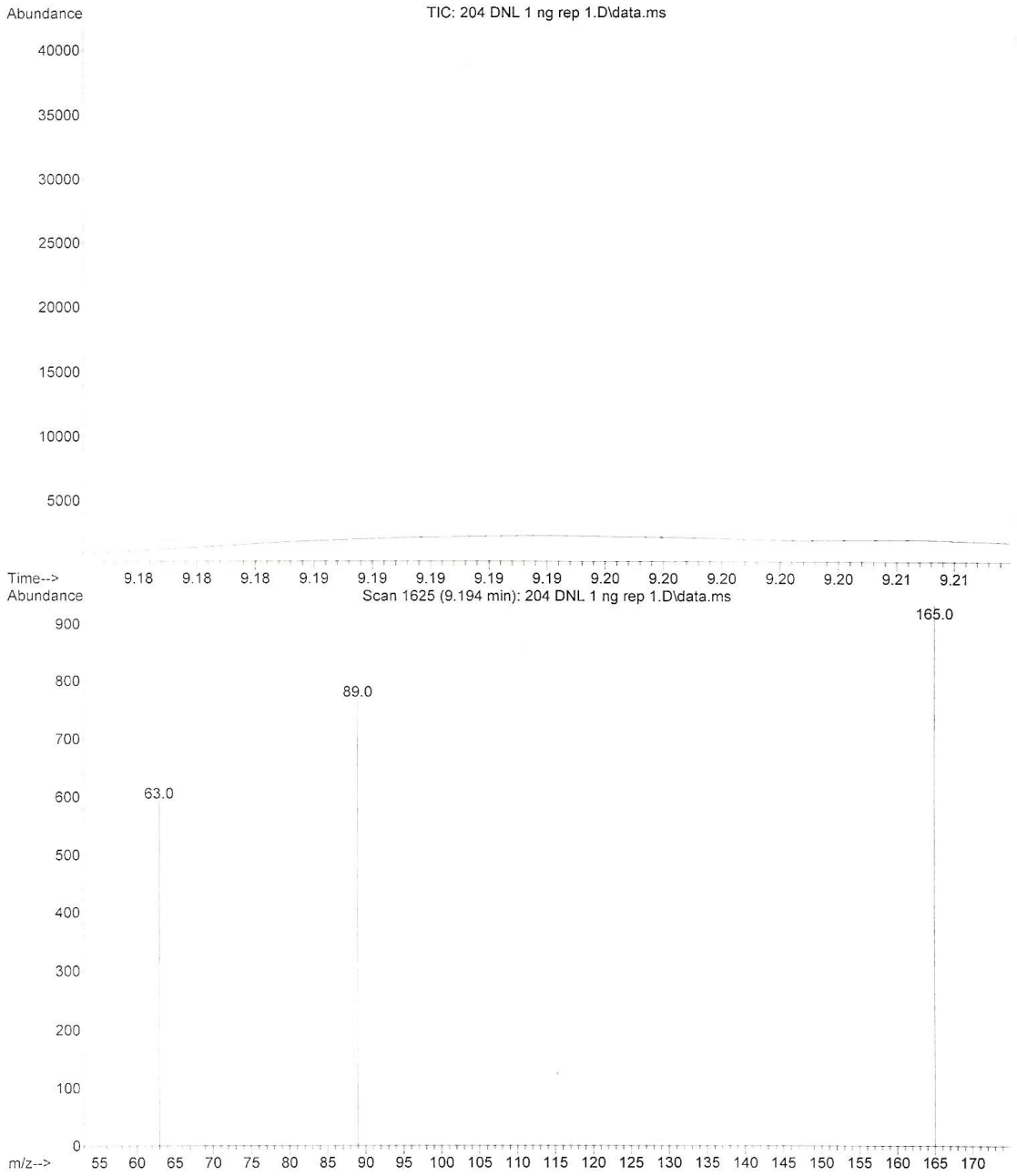

```
File       :C:\msdchem\1\data\TWW_Explosives\ALS Run 080818\2-4 DNL half
...          ng rep 1.D
Operator   :
Instrument :    5975 MSD
Acquired   :  8 Aug 2018  22:34     using AcqMethod TWW 2-4 DNL SIM DEFAULT.M
Sample Name: 2-4 DNL .5 ng
Misc Info  :
```

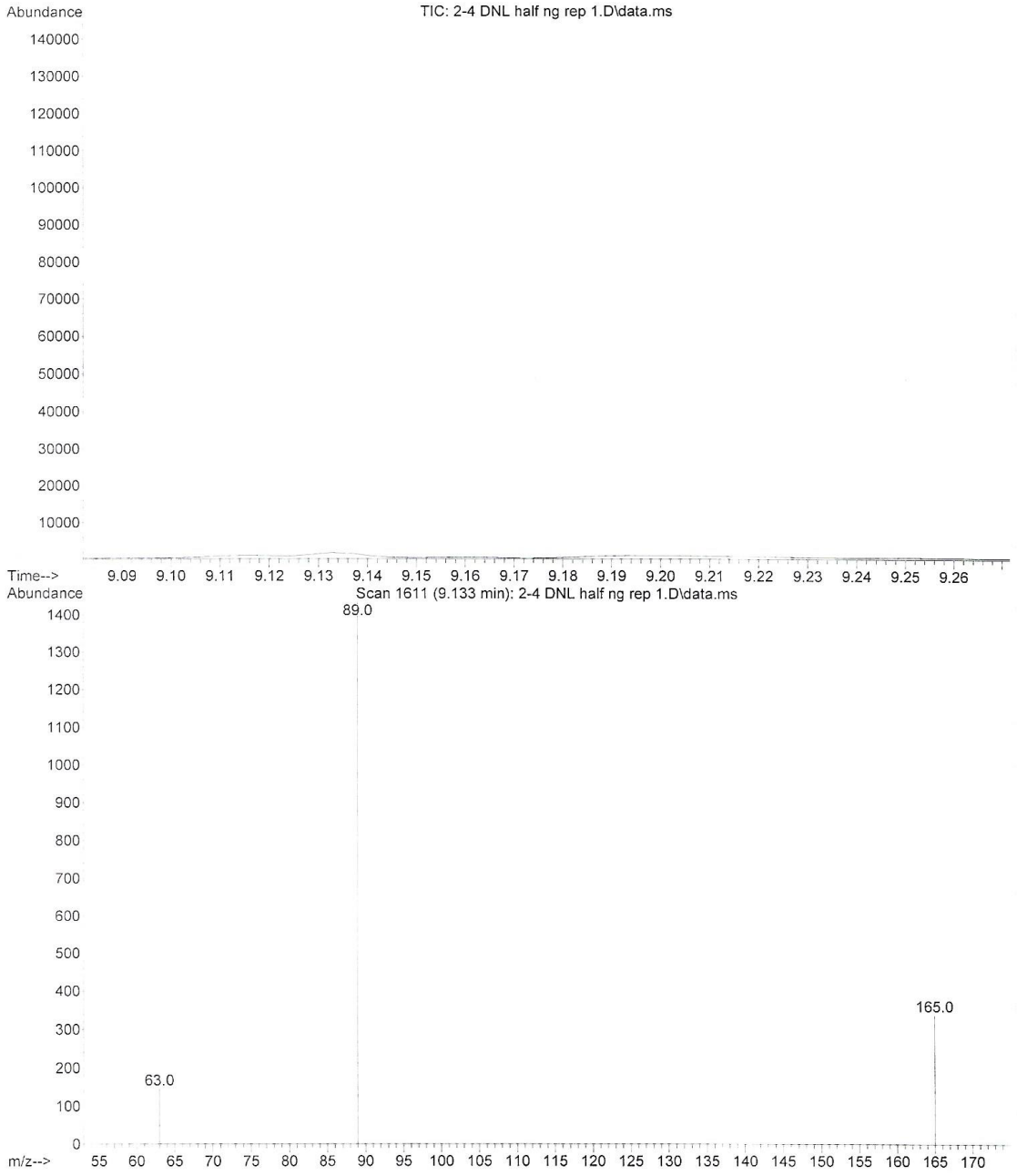

```
File        :C:\msdchem\1\data\TWW_Explosives\2-4 Dinotrotoluene\2-4 DNL
...          62018 SIM 80MSEC COTTON REP1 S1.D
Operator    :
Instrument  :     5975 MSD
Acquired    : 20 Jun 2018  13:37     using AcqMethod TWW_UNI1 SIM TEST 2-4 DNL 80
Sample Name: 10 ng/uL 2-4 DNL COTTON 80MSEC
Misc Info   :
```

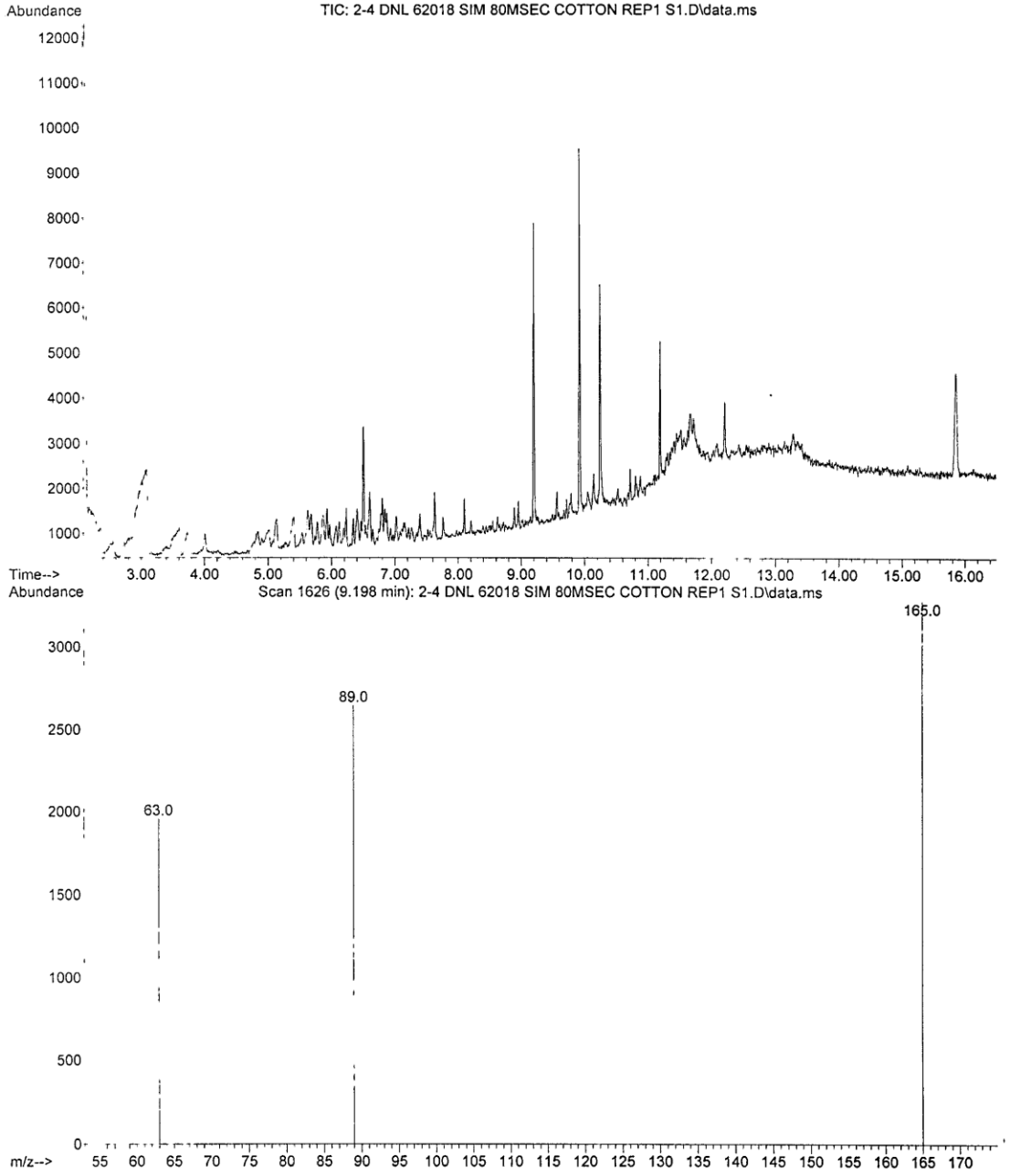

```
File       :C:\msdchem\1\data\TWW_Explosives\2-4 Dinotrotoluene\2-4DNL 0
...         71118 SIM COTN REP1 S1.D
Operator   :
Instrument :    5975 MSD
Acquired   : 11 Jul 2018  11:48     using AcqMethod TWW_UNI1 SIM TEST 2-4 DNL 80
Sample Name: 2-4DNL 5 ng/ul 100% COTTON REP1 S1
Misc Info  :
```

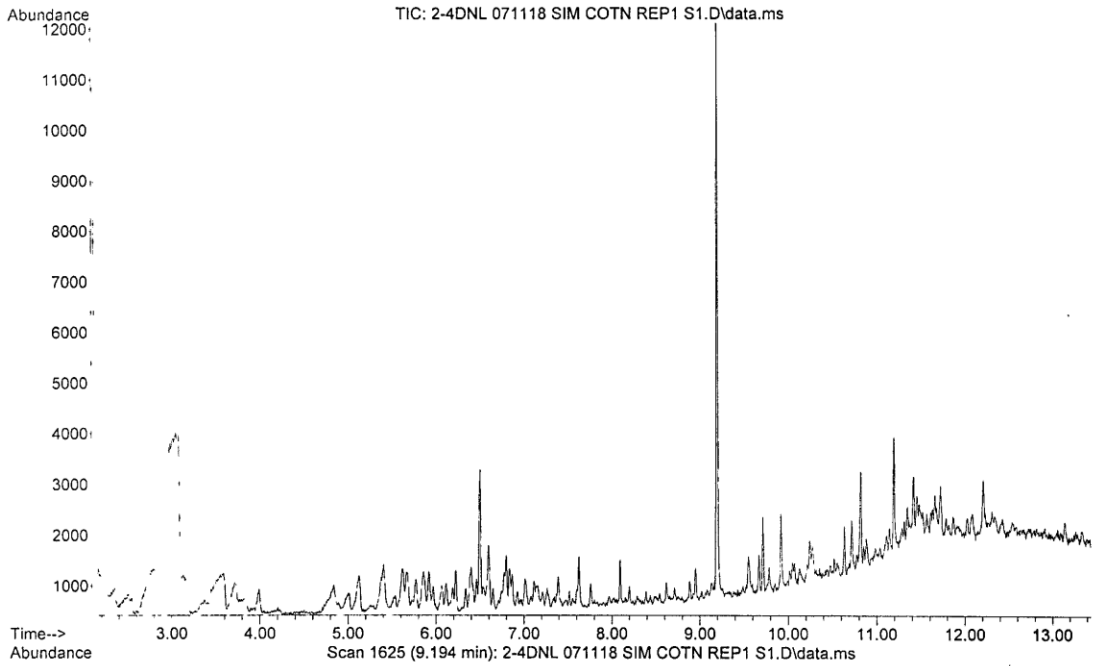

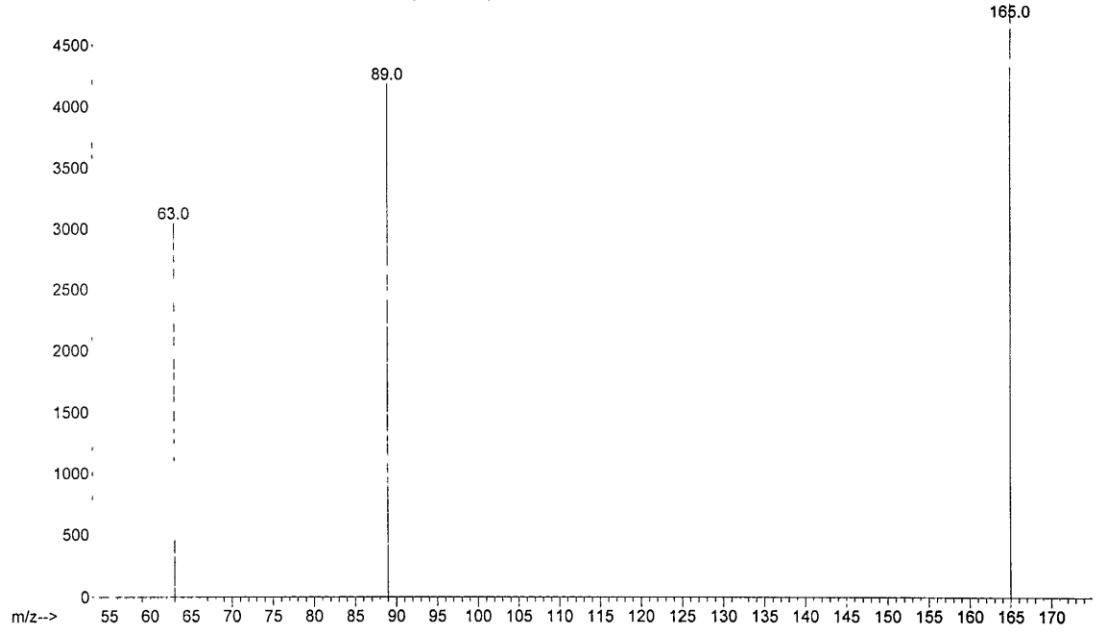

```
File       :C:\msdchem\1\data\TWW_Explosives\2-4 Dinotrotoluene\2-4 DNL
...         71318 10 NGUL BLOOD REP1 S1.D
Operator   :
Instrument :    5975 MSD
Acquired   : 13 Jul 2018  11:26     using AcqMethod TWW_UNI1 SIM TEST 2-4 DNL 80
Sample Name: 2-4 DNL 10ng/ul BLOOD REP1 S1
Misc Info  :
```

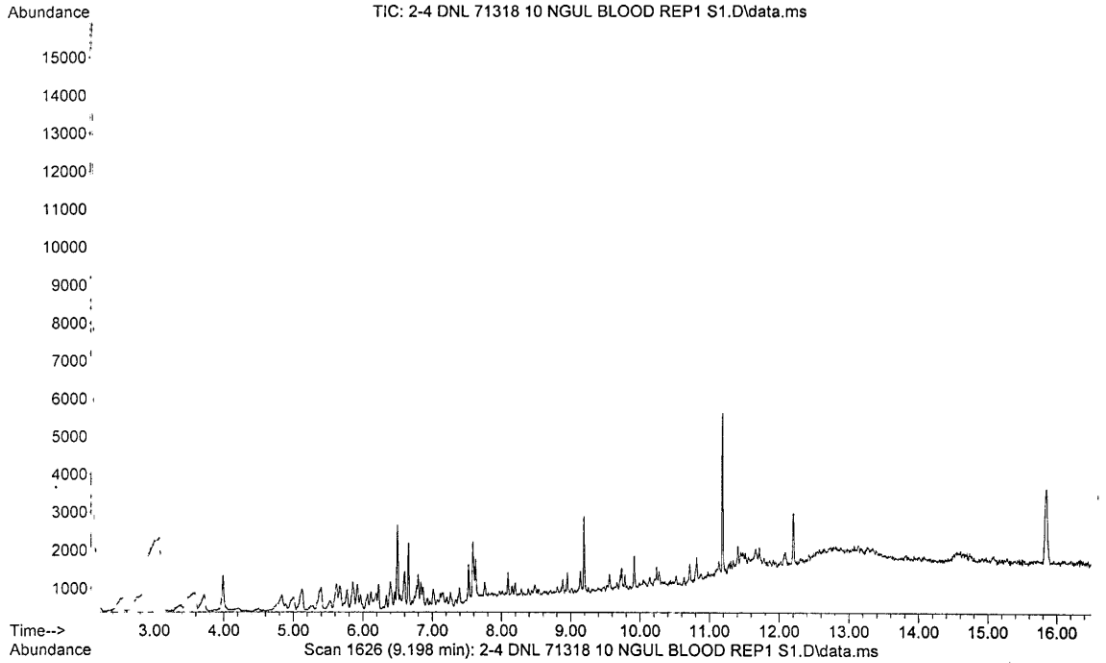

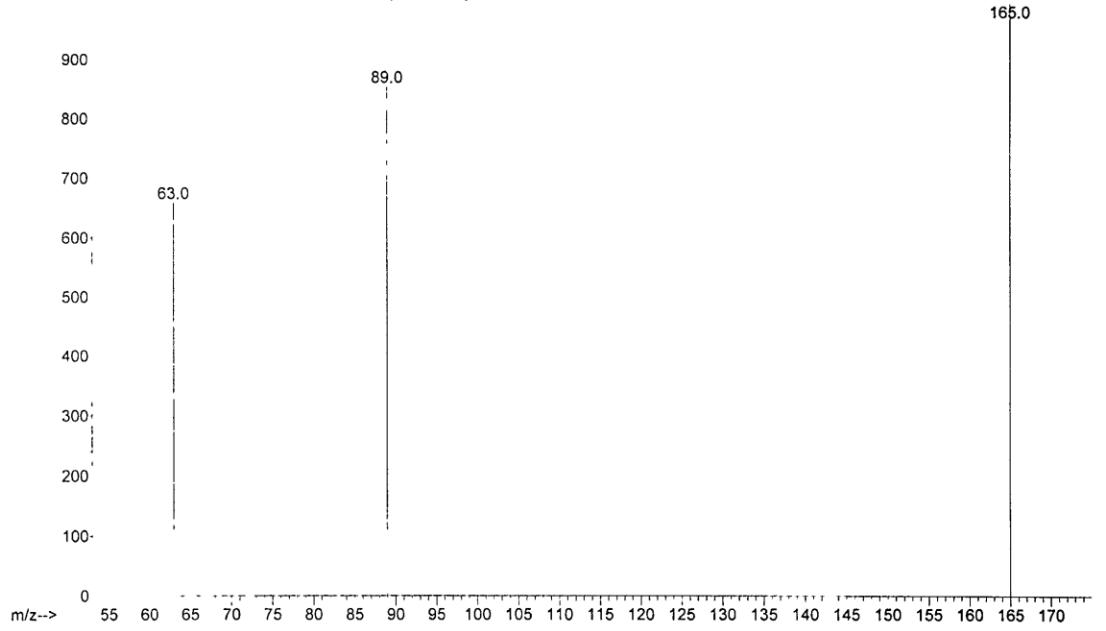

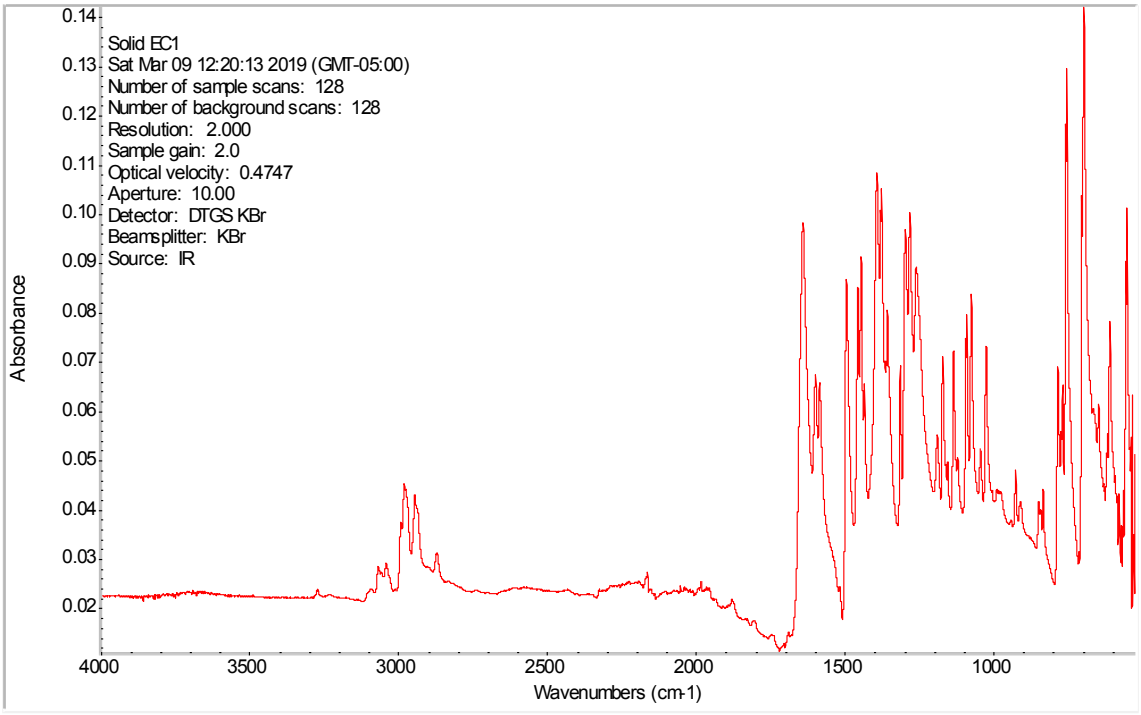
Solid EC1
Sat Mar 09 12:20:13 2019 (GMT-05:00)
Number of sample scans: 128
Number of background scans: 128
Resolution: 2.000
Sample gain: 2.0
Optical velocity: 0.4747
Aperture: 10.00
Detector: DTGS KBr
Beamsplitter: KBr
Source: IR
Absorbance
0.14
0.13
0.12
0.11
0.10
0.09
0.08
0.07
0.06
0.05
0.04
0.03
0.02
4000
3500
3000
2500
2000
1500
1000
Wavenumbers (cm-1)

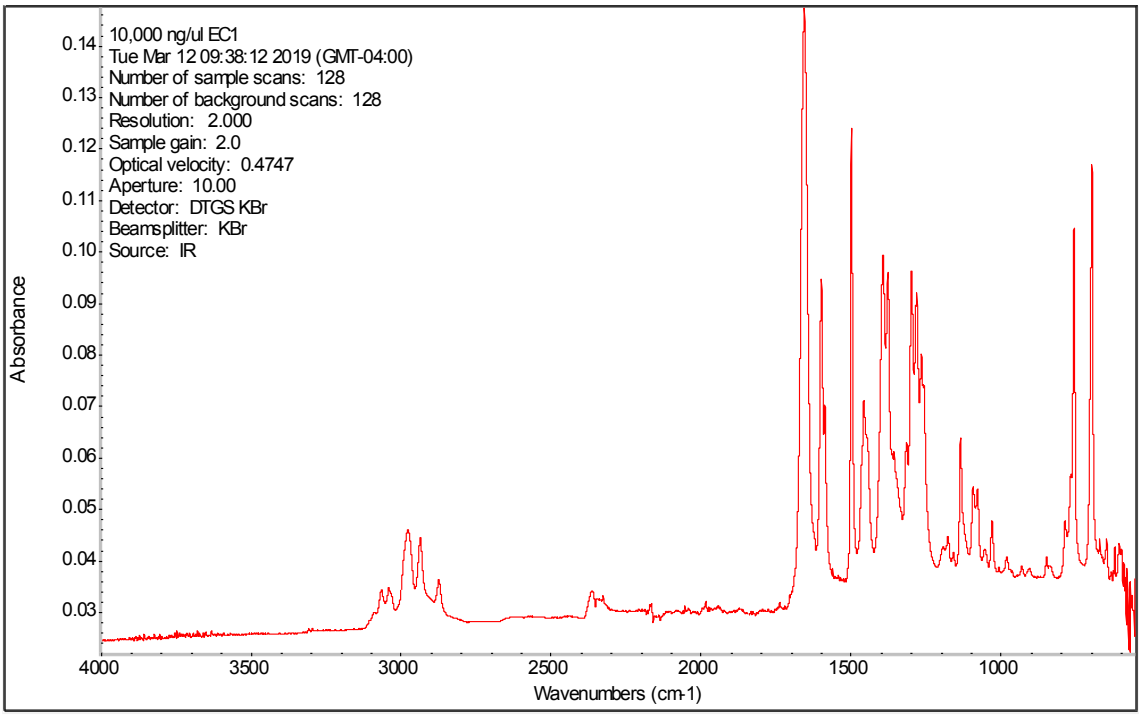
10,000 ng/ul EC1
Tue Mar 12 09:38:12 2019 (GMT-04:00)
Number of sample scans: 128
Number of background scans: 128
Resolution: 2.000
Sample gain: 2.0
Optical velocity: 0.4747
Aperture: 10.00
Detector: DTGS KBr
Beamsplitter: KBr
Source: IR
Absorbance
0.14
0.13
0.12
0.11
0.10
0.09
0.08
0.07
0.06
0.05
0.04
0.03
4000
3500
3000
2500
2000
1500
1000
Wavenumbers (cm-1)

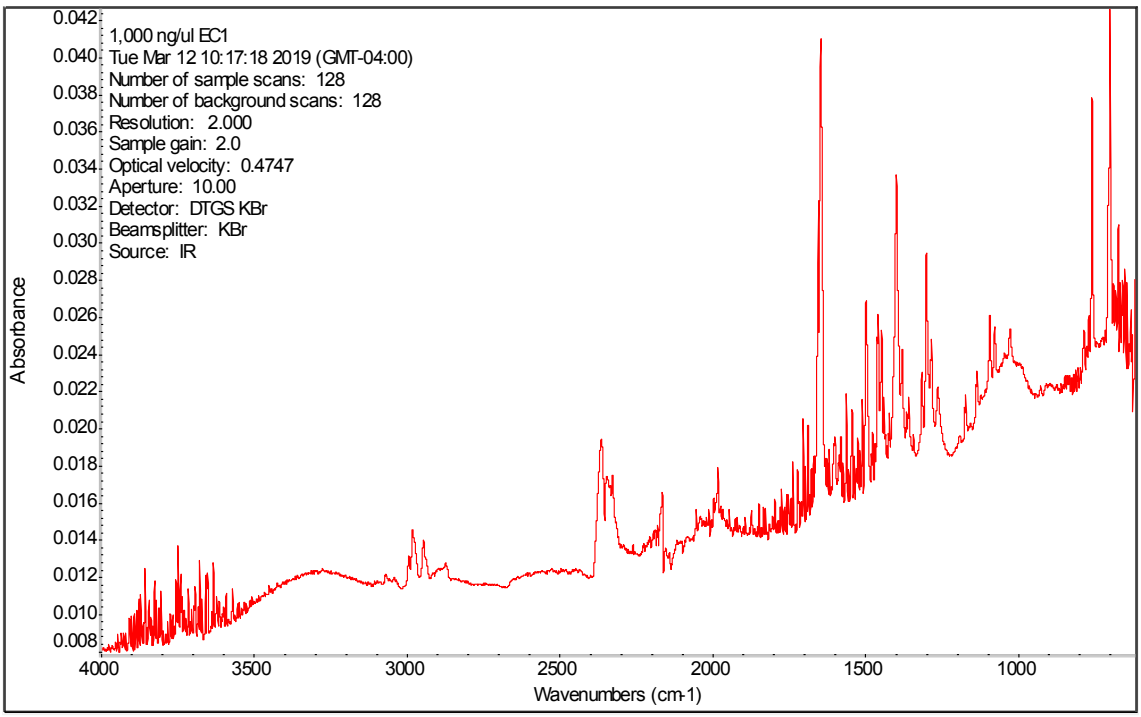
1,000 ng/ul EC1
Tue Mar 12 10:17:18 2019 (GMT-04:00)
Number of sample scans: 128
Number of background scans: 128
Resolution: 2.000
Sample gain: 2.0
Optical velocity: 0.4747
Aperture: 10.00
Detector: DTGS KBr
Beamsplitter: KBr
Source: IR
Absorbance
0.042
0.040
0.038
0.036
0.034
0.032
0.030
0.028
0.026
0.024
0.022
0.020
0.018
0.016
0.014
0.012
0.010
0.008
4000
3500
3000
2500
2000
1500
1000
Wavenumbers (cm-1)

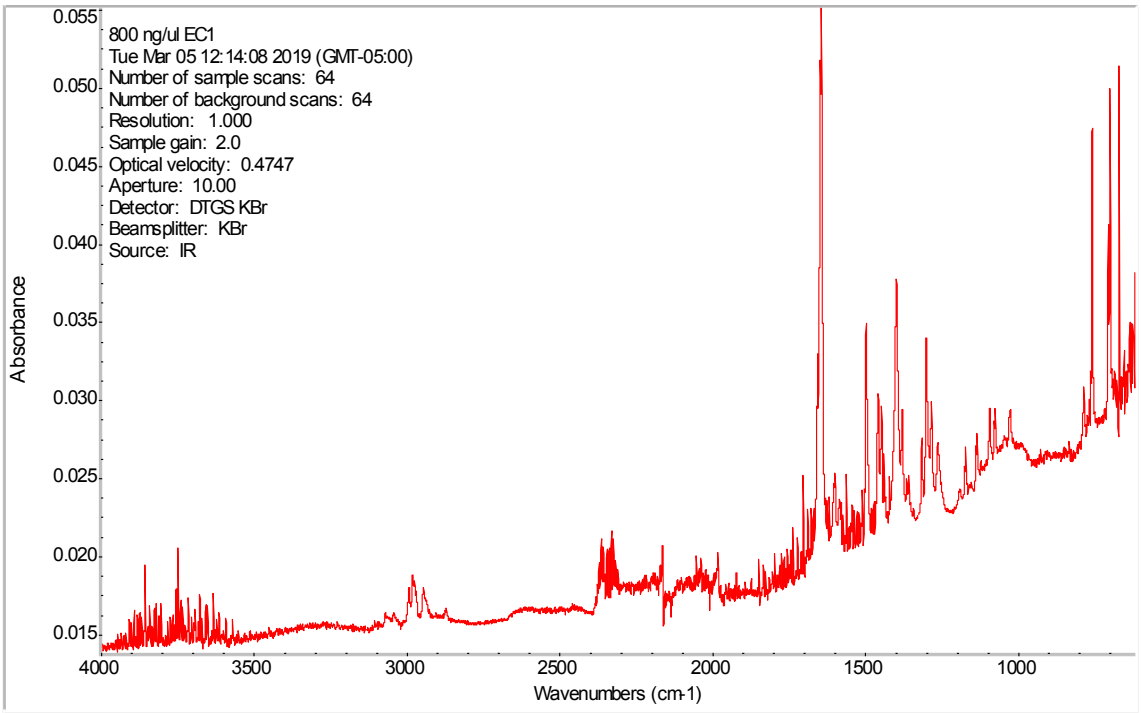
800 ng/ul EC1
Tue Mar 05 12:14:08 2019 (GMT-05:00)
Number of sample scans: 64
Number of background scans: 64
Resolution: 1.000
Sample gain: 2.0
Optical velocity: 0.4747
Aperture: 10.00
Detector: DTGS KBr
Beamsplitter: KBr
Source: IR
Absorbance
0.055
0.050
0.045
0.040
0.035
0.030
0.025
0.020
0.015
4000
3500
3000
2500
2000
1500
1000
Wavenumbers (cm-1)

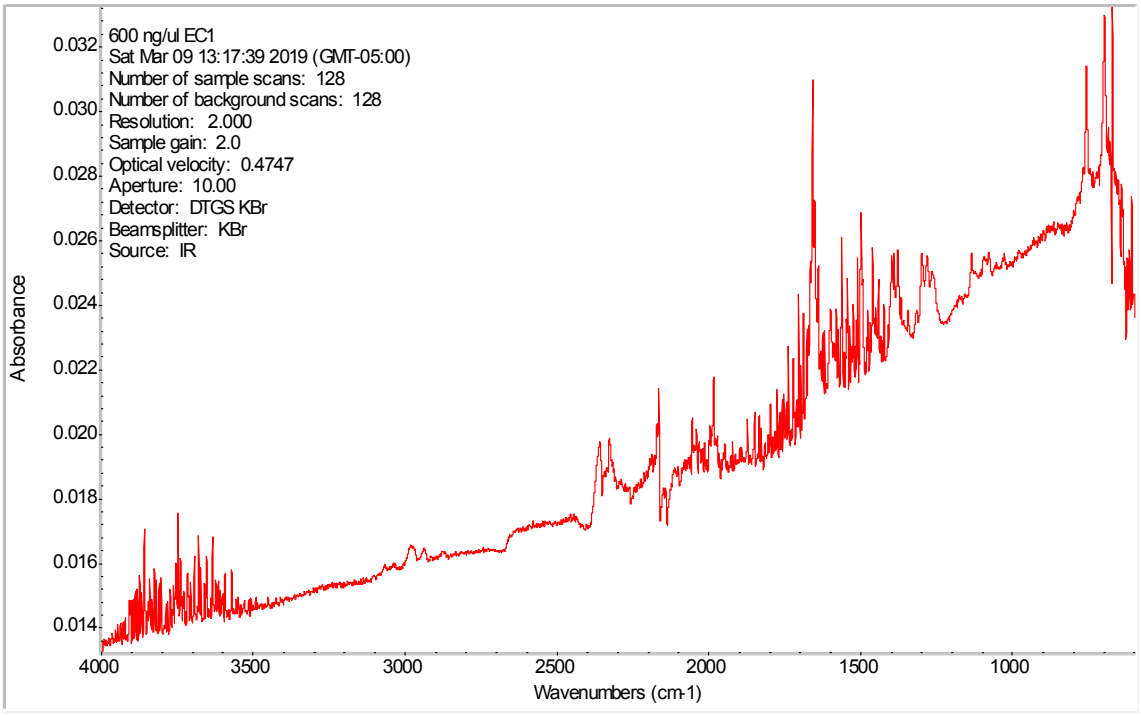
600 ng/ul EC1
Sat Mar 09 13:17:39 2019 (GMT-05:00)
Number of sample scans: 128
Number of background scans: 128
Resolution: 2.000
Sample gain: 2.0
Optical velocity: 0.4747
Aperture: 10.00
Detector: DTGS KBr
Beamsplitter: KBr
Source: IR
Absorbance
0.032
0.030
0.028
0.026
0.024
0.022
0.020
0.018
0.016
0.014
4000
3500
3000
2500
2000
1500
1000
Wavenumbers (cm-1)

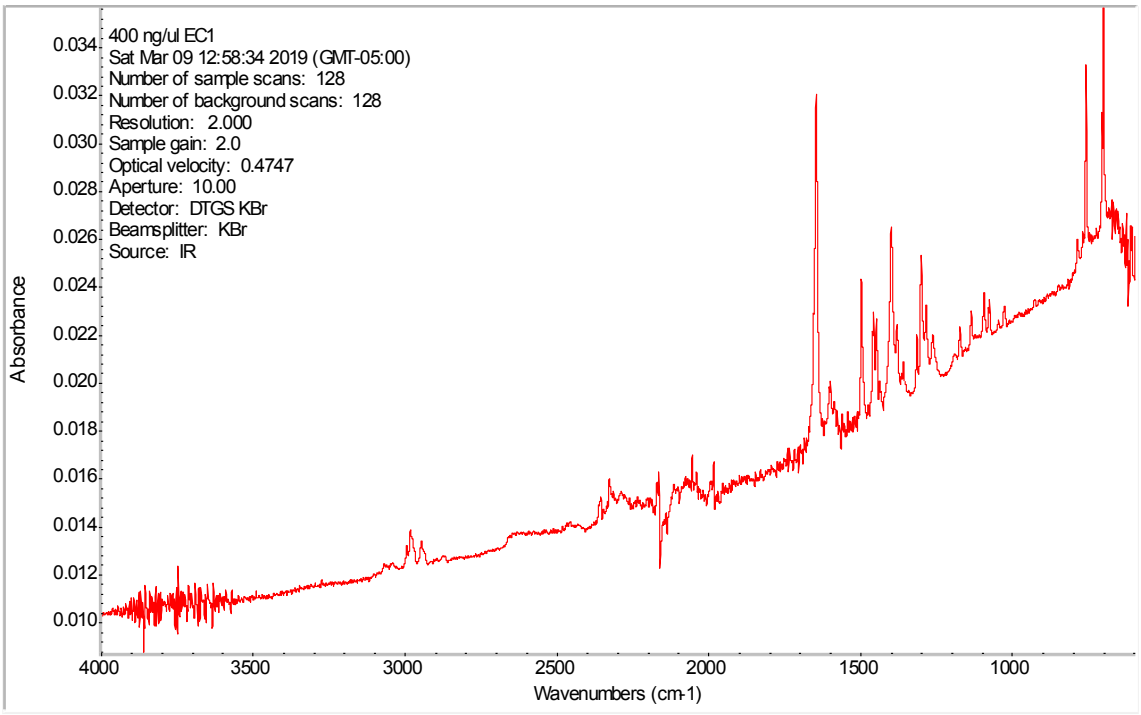
400 ng/ul EC1
Sat Mar 09 12:58:34 2019 (GMT-05:00)
Number of sample scans: 128
Number of background scans: 128
Resolution: 2.000
Sample gain: 2.0
Optical velocity: 0.4747
Aperture: 10.00
Detector: DTGS KBr
Beamsplitter: KBr
Source: IR
Absorbance
0.034
0.032
0.030
0.028
0.026
0.024
0.022
0.020
0.018
0.016
0.014
0.012
0.010
4000
3500
3000
2500
2000
1500
1000
Wavenumbers (cm-1)

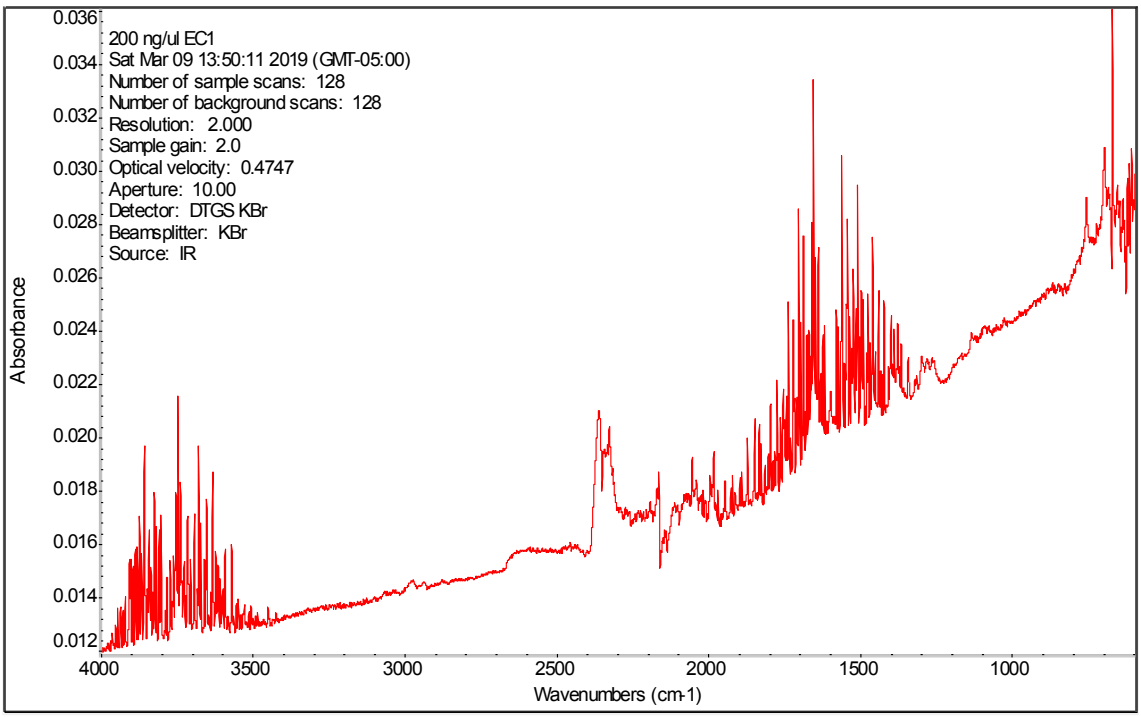
200 ng/ul EC1
Sat Mar 09 13:50:11 2019 (GMT-05:00)
Number of sample scans: 128
Number of background scans: 128
Resolution: 2.000
Sample gain: 2.0
Optical velocity: 0.4747
Aperture: 10.00
Detector: DTGS KBr
Beamsplitter: KBr
Source: IR
Absorbance
0.036
0.034
0.032
0.030
0.028
0.026
0.024
0.022
0.020
0.018
0.016
0.014
0.012
4000
3500
3000
2500
2000
1500
1000
Wavenumbers (cm-1)

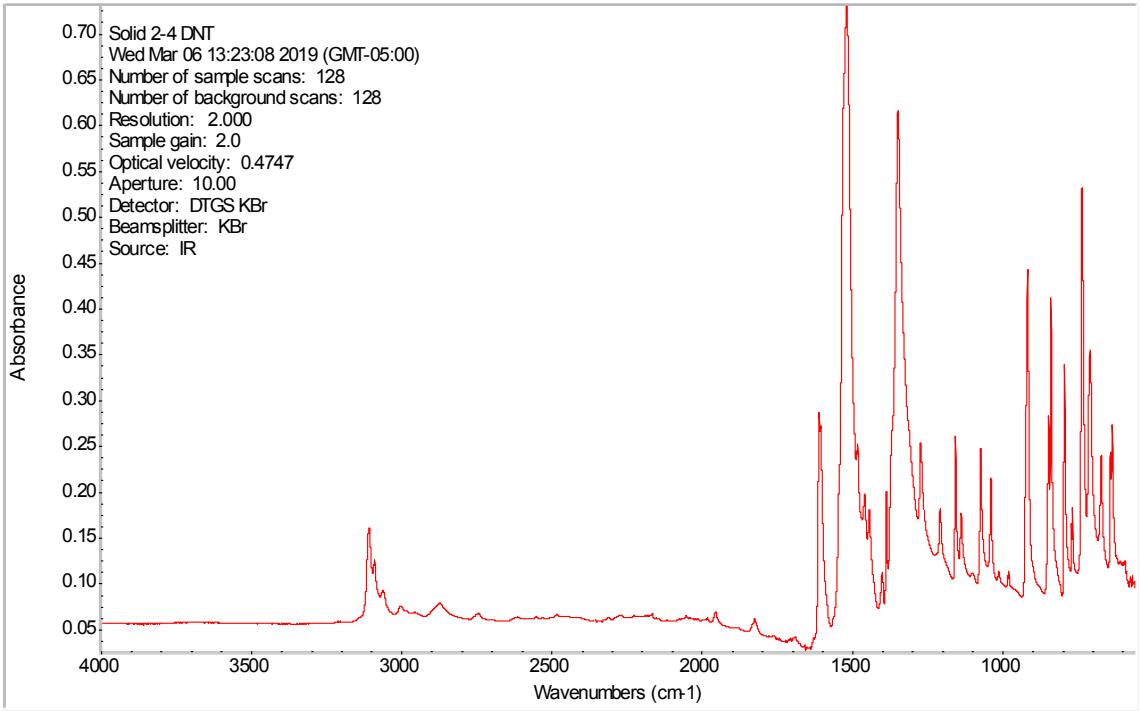
Solid 2-4 DNT
Wed Mar 06 13:23:08 2019 (GMT-05:00)
Number of sample scans: 128
Number of background scans: 128
Resolution: 2.000
Sample gain: 2.0
Optical velocity: 0.4747
Aperture: 10.00
Detector: DTGS KBr
Beamsplitter: KBr
Source: IR
Absorbance
0.70
0.65
0.60
0.55
0.50
0.45
0.40
0.35
0.30
0.25
0.20
0.15
0.10
0.05
4000
3500
3000
2500
2000
1500
1000
Wavenumbers (cm-1)

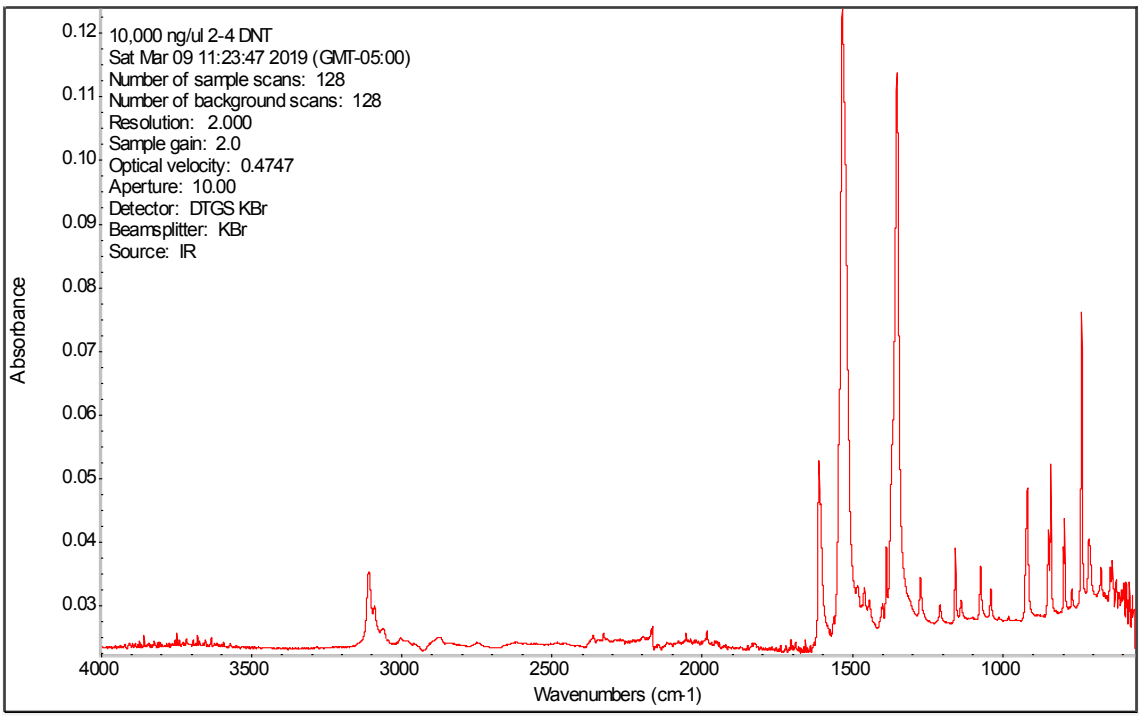
10,000 ng/ul 2-4 DNT
Sat Mar 09 11:23:47 2019 (GMT-05:00)
Number of sample scans: 128
Number of background scans: 128
Resolution: 2.000
Sample gain: 2.0
Optical velocity: 0.4747
Aperture: 10.00
Detector: DTGS KBr
Beamsplitter: KBr
Source: IR
Absorbance
0.12
0.11
0.10
0.09
0.08
0.07
0.06
0.05
0.04
0.03
4000
3500
3000
2500
2000
1500
1000
Wavenumbers (cm-1)

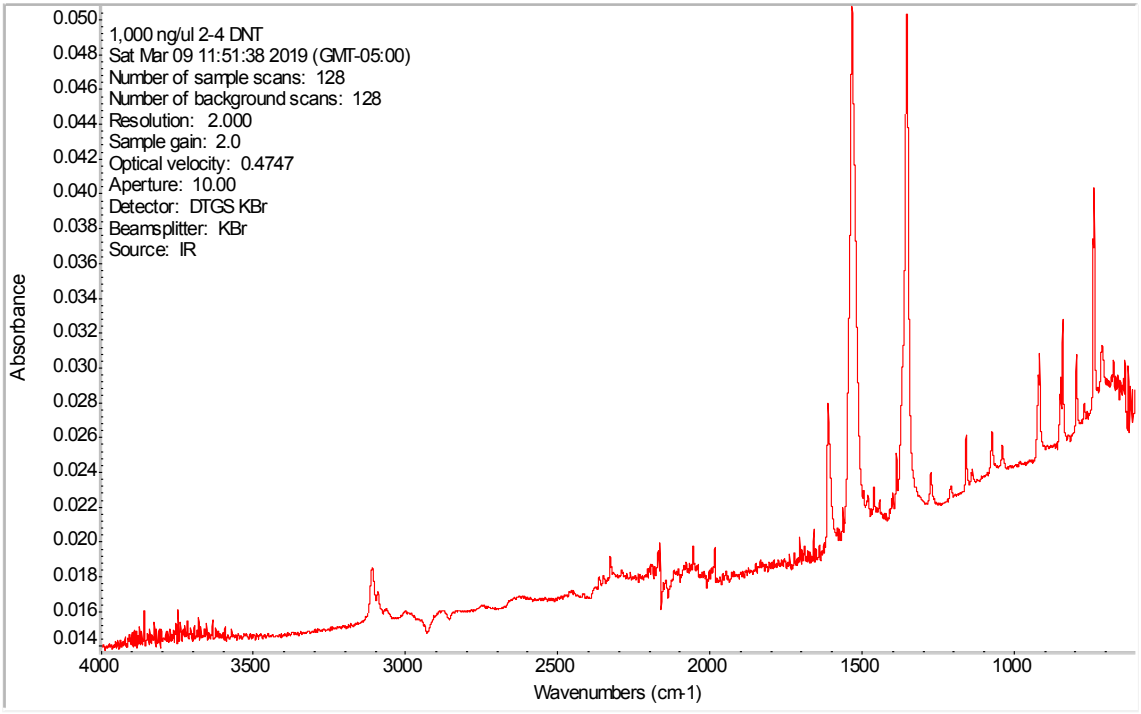
1,000 ng/ul 2-4 DNT
Sat Mar 09 11:51:38 2019 (GMT-05:00)
Number of sample scans: 128
Number of background scans: 128
Resolution: 2.000
Sample gain: 2.0
Optical velocity: 0.4747
Aperture: 10.00
Detector: DTGS KBr
Beamsplitter: KBr
Source: IR
Absorbance
0.050
0.048
0.046
0.044
0.042
0.040
0.038
0.036
0.034
0.032
0.030
0.028
0.026
0.024
0.022
0.020
0.018
0.016
0.014
4000
3500
3000
2500
2000
1500
1000
Wavenumbers (cm-1)

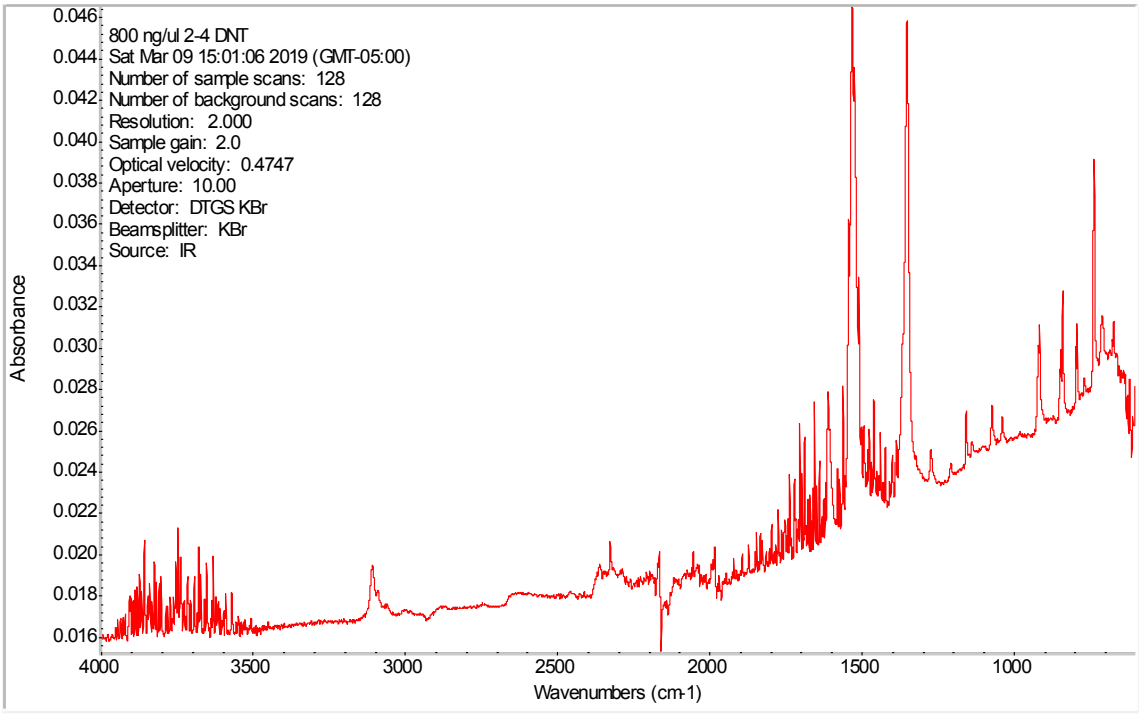
800 ng/ul 2-4 DNT
Sat Mar 09 15:01:06 2019 (GMT-05:00)
Number of sample scans: 128
Number of background scans: 128
Resolution: 2.000
Sample gain: 2.0
Optical velocity: 0.4747
Aperture: 10.00
Detector: DTGS KBr
Beamsplitter: KBr
Source: IR
Absorbance
0.046
0.044
0.042
0.040
0.038
0.036
0.034
0.032
0.030
0.028
0.026
0.024
0.022
0.020
0.018
0.016
4000
3500
3000
2500
2000
1500
1000
Wavenumbers (cm-1)

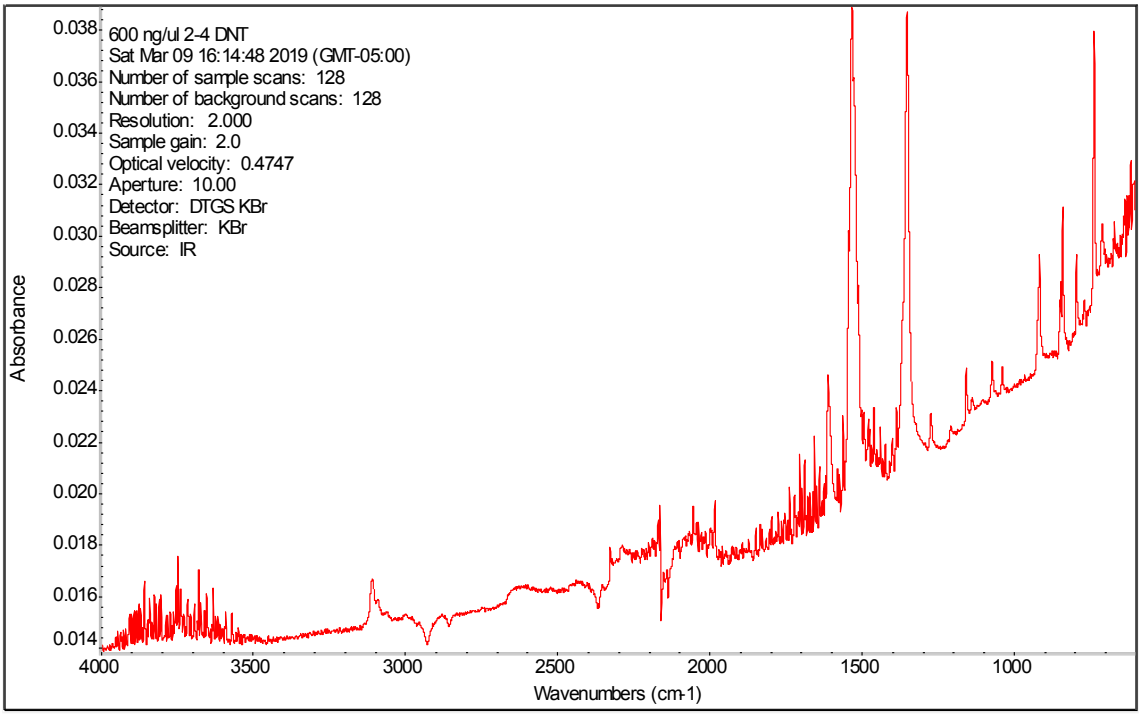
600 ng/ul 2-4 DNT
Sat Mar 09 16:14:48 2019 (GMT-05:00)
Number of sample scans: 128
Number of background scans: 128
Resolution: 2.000
Sample gain: 2.0
Optical velocity: 0.4747
Aperture: 10.00
Detector: DTGS KBr
Beamsplitter: KBr
Source: IR
Absorbance
0.038
0.036
0.034
0.032
0.030
0.028
0.026
0.024
0.022
0.020
0.018
0.016
0.014
4000
3500
3000
2500
2000
1500
1000
Wavenumbers (cm-1)

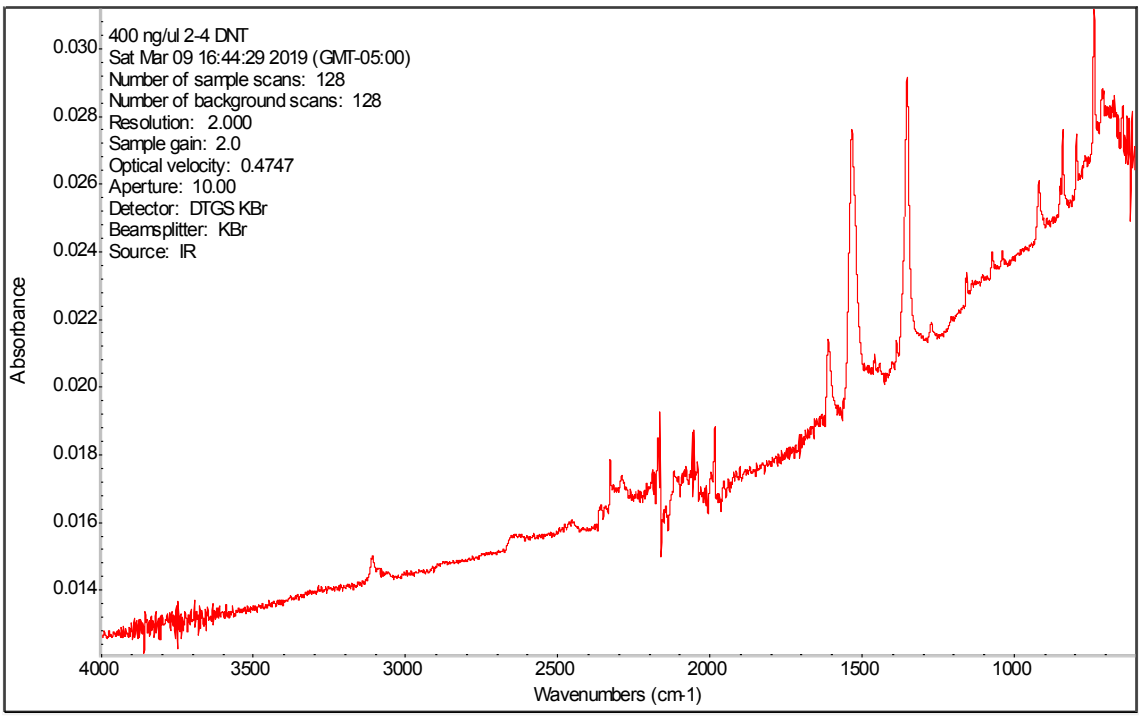
400 ng/ul 2-4 DNT
Sat Mar 09 16:44:29 2019 (GMT-05:00)
Number of sample scans: 128
Number of background scans: 128
Resolution: 2.000
Sample gain: 2.0
Optical velocity: 0.4747
Aperture: 10.00
Detector: DTGS KBr
Beamsplitter: KBr
Source: IR
Absorbance
0.030
0.028
0.026
0.024
0.022
0.020
0.018
0.016
0.014
4000
3500
3000
2500
2000
1500
1000
Wavenumbers (cm-1)

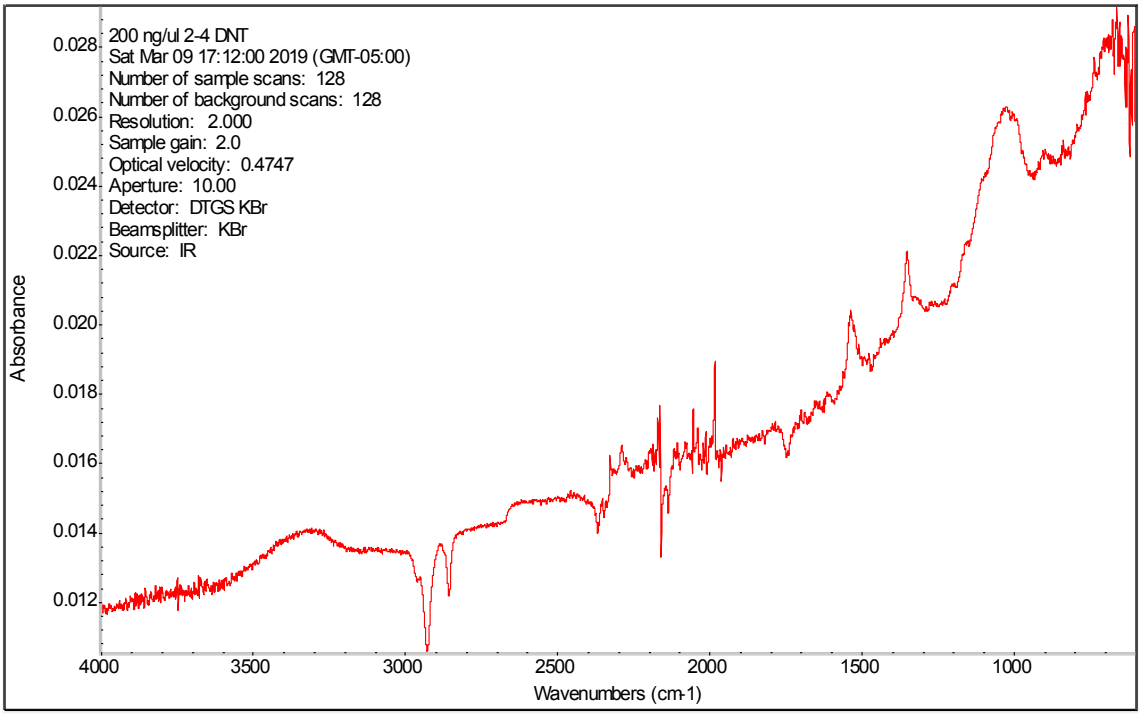
200 ng/ul 2-4 DNT
Sat Mar 09 17:12:00 2019 (GMT-05:00)
Number of sample scans: 128
Number of background scans: 128
Resolution: 2.000
Sample gain: 2.0
Optical velocity: 0.4747
Aperture: 10.00
Detector: DTGS KBr
Beamsplitter: KBr
Source: IR
Absorbance
0.028
0.026
0.024
0.022
0.020
0.018
0.016
0.014
0.012
4000
3500
3000
2500
2000
1500
1000
Wavenumbers (cm-1)

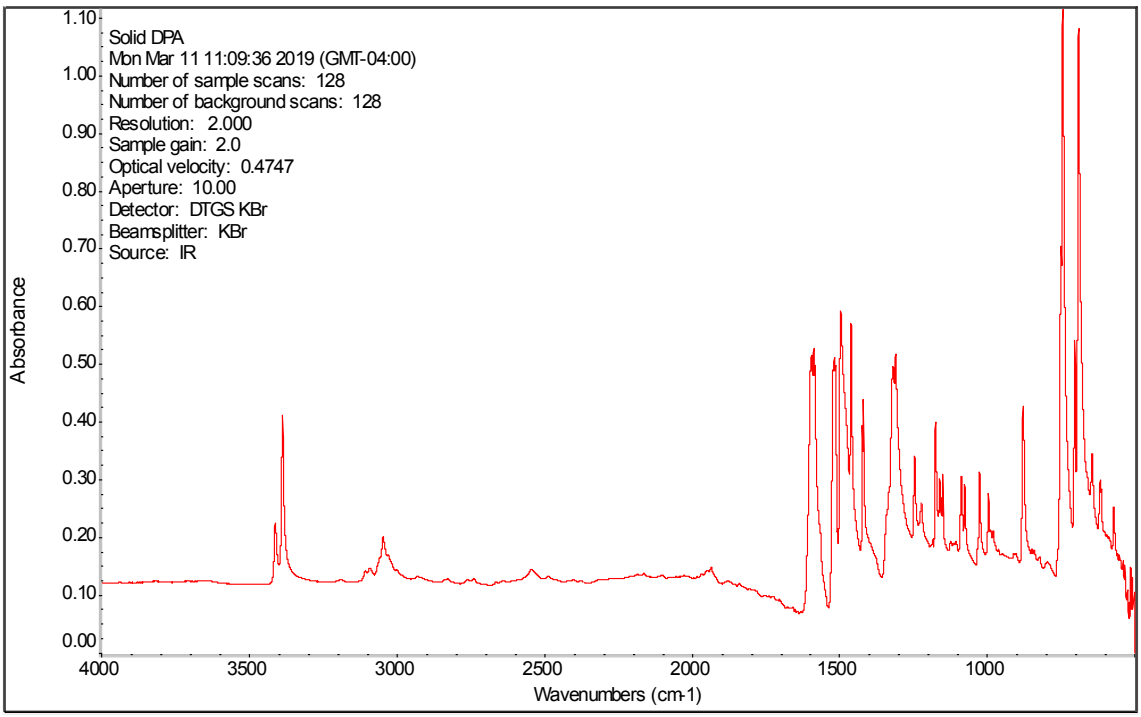
Solid DPA
Mon Mar 11 11:09:36 2019 (GMT-04:00)
Number of sample scans: 128
Number of background scans: 128
Resolution: 2.000
Sample gain: 2.0
Optical velocity: 0.4747
Aperture: 10.00
Detector: DTGS KBr
Beamsplitter: KBr
Source: IR
Absorbance
1.10
1.00
0.90
0.80
0.70
0.60
0.50
0.40
0.30
0.20
0.10
0.00
4000
3500
3000
2500
2000
1500
1000
Wavenumbers (cm-1)

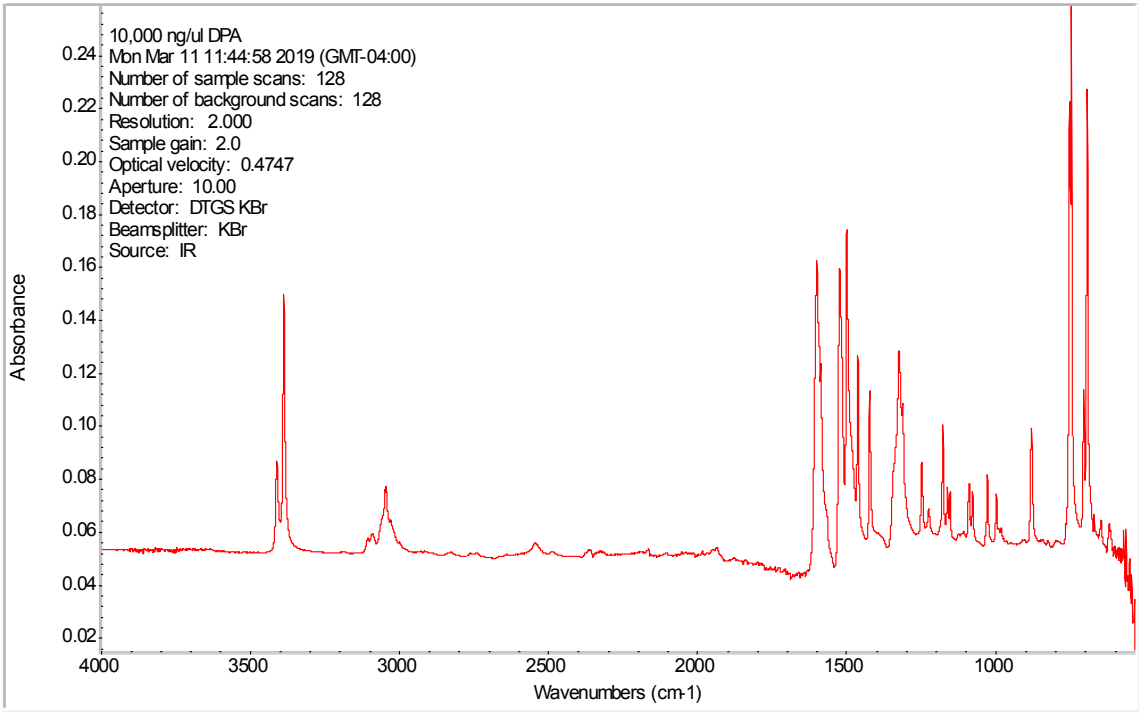
10,000 ng/ul DPA
Mon Mar 11 11:44:58 2019 (GMT-04:00)
Number of sample scans: 128
Number of background scans: 128
Resolution: 2.000
Sample gain: 2.0
Optical velocity: 0.4747
Aperture: 10.00
Detector: DTGS KBr
Beamsplitter: KBr
Source: IR
Absorbance
0.24
0.22
0.20
0.18
0.16
0.14
0.12
0.10
0.08
0.06
0.04
0.02
4000
3500
3000
2500
2000
1500
1000
Wavenumbers (cm-1)

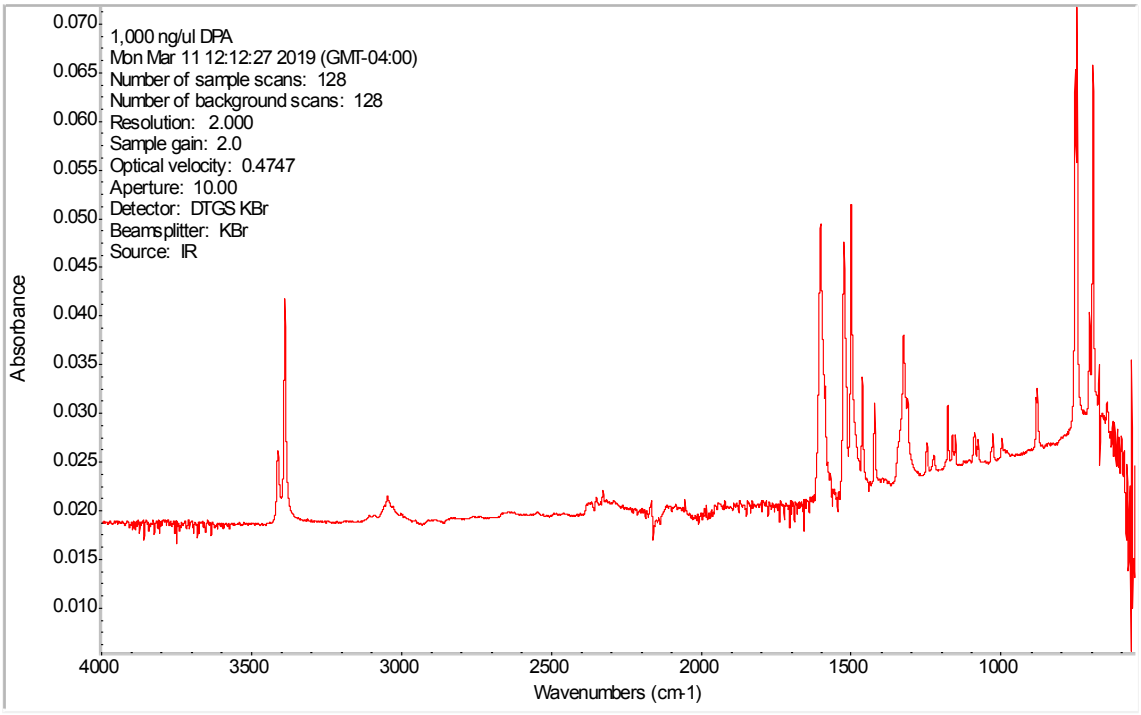
1,000 ng/ul DPA
Mon Mar 11 12:12:27 2019 (GMT-04:00)
Number of sample scans: 128
Number of background scans: 128
Resolution: 2.000
Sample gain: 2.0
Optical velocity: 0.4747
Aperture: 10.00
Detector: DTGS KBr
Beamsplitter: KBr
Source: IR
Absorbance
0.070
0.065
0.060
0.055
0.050
0.045
0.040
0.035
0.030
0.025
0.020
0.015
0.010
4000
3500
3000
2500
2000
1500
1000
Wavenumbers (cm-1)

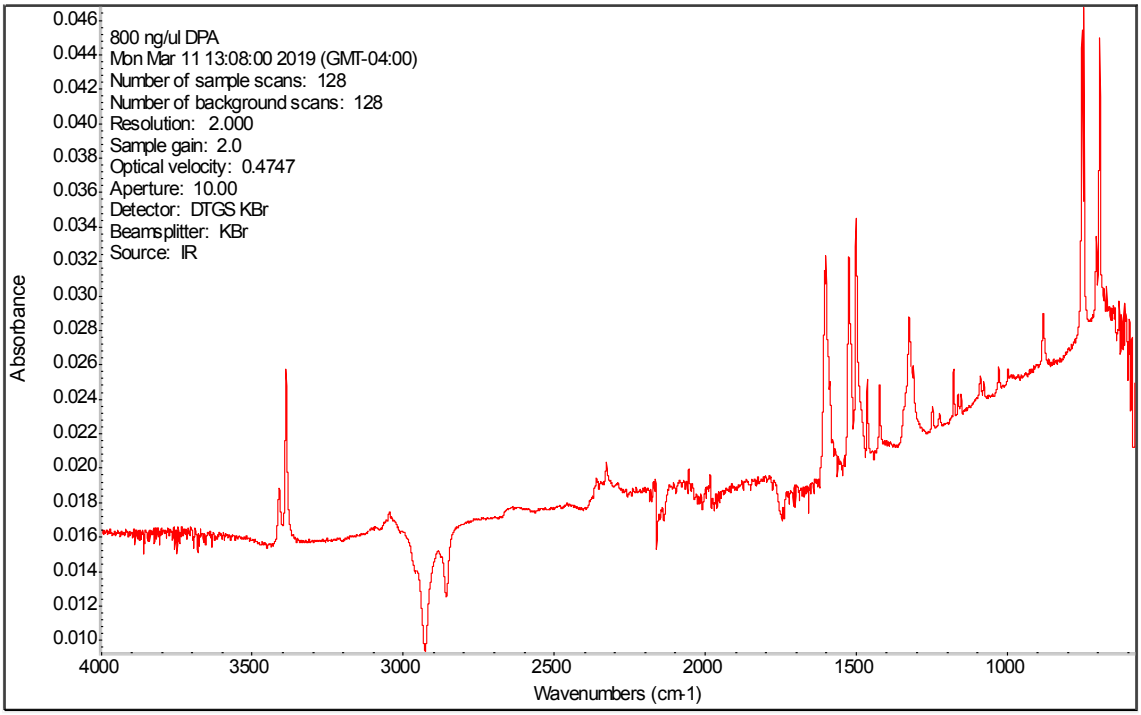
800 ng/ul DPA
Mon Mar 11 13:08:00 2019 (GMT-04:00)
Number of sample scans: 128
Number of background scans: 128
Resolution: 2.000
Sample gain: 2.0
Optical velocity: 0.4747
Aperture: 10.00
Detector: DTGS KBr
Beamsplitter: KBr
Source: IR
Absorbance
0.046
0.044
0.042
0.040
0.038
0.036
0.034
0.032
0.030
0.028
0.026
0.024
0.022
0.020
0.018
0.016
0.014
0.012
0.010
4000
3500
3000
2500
2000
1500
1000
Wavenumbers (cm-1)

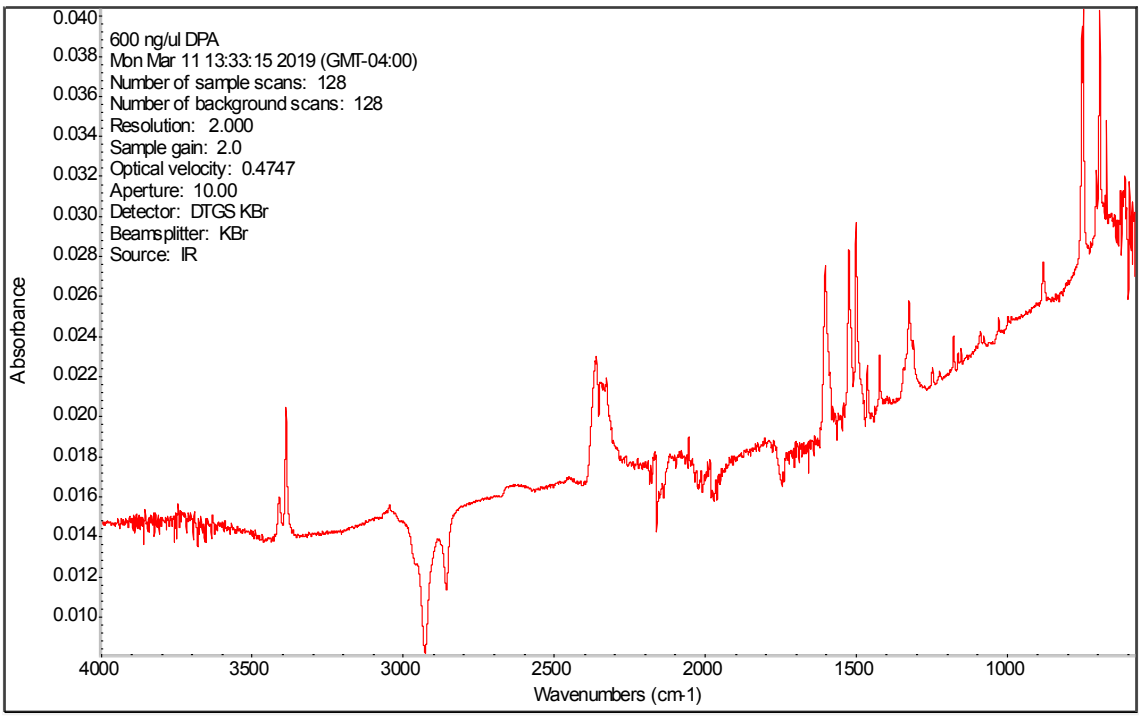
600 ng/ul DPA
Mon Mar 11 13:33:15 2019 (GMT-04:00)
Number of sample scans: 128
Number of background scans: 128
Resolution: 2.000
Sample gain: 2.0
Optical velocity: 0.4747
Aperture: 10.00
Detector: DTGS KBr
Beamsplitter: KBr
Source: IR
Absorbance
0.040
0.038
0.036
0.034
0.032
0.030
0.028
0.026
0.024
0.022
0.020
0.018
0.016
0.014
0.012
0.010
4000
3500
3000
2500
2000
1500
1000
Wavenumbers (cm-1)

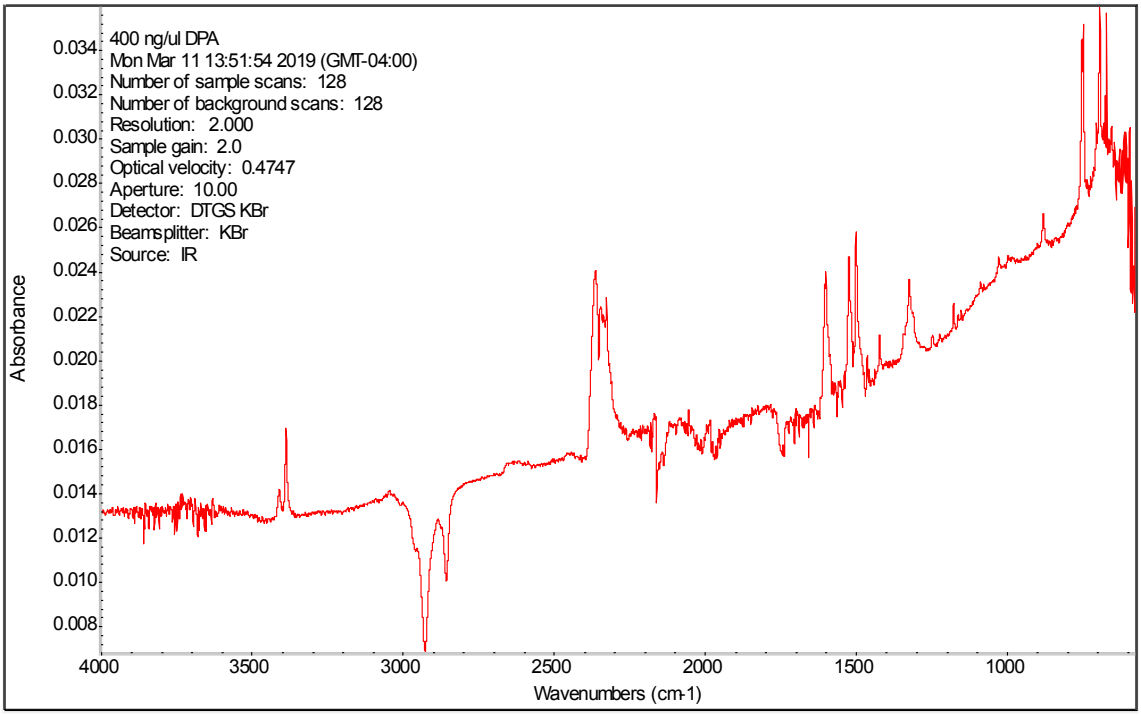
400 ng/ul DPA
Mon Mar 11 13:51:54 2019 (GMT-04:00)
Number of sample scans: 128
Number of background scans: 128
Resolution: 2.000
Sample gain: 2.0
Optical velocity: 0.4747
Aperture: 10.00
Detector: DTGS KBr
Beamsplitter: KBr
Source: IR
Absorbance
0.034
0.032
0.030
0.028
0.026
0.024
0.022
0.020
0.018
0.016
0.014
0.012
0.010
0.008
4000
3500
3000
2500
2000
1500
1000
Wavenumbers (cm-1)

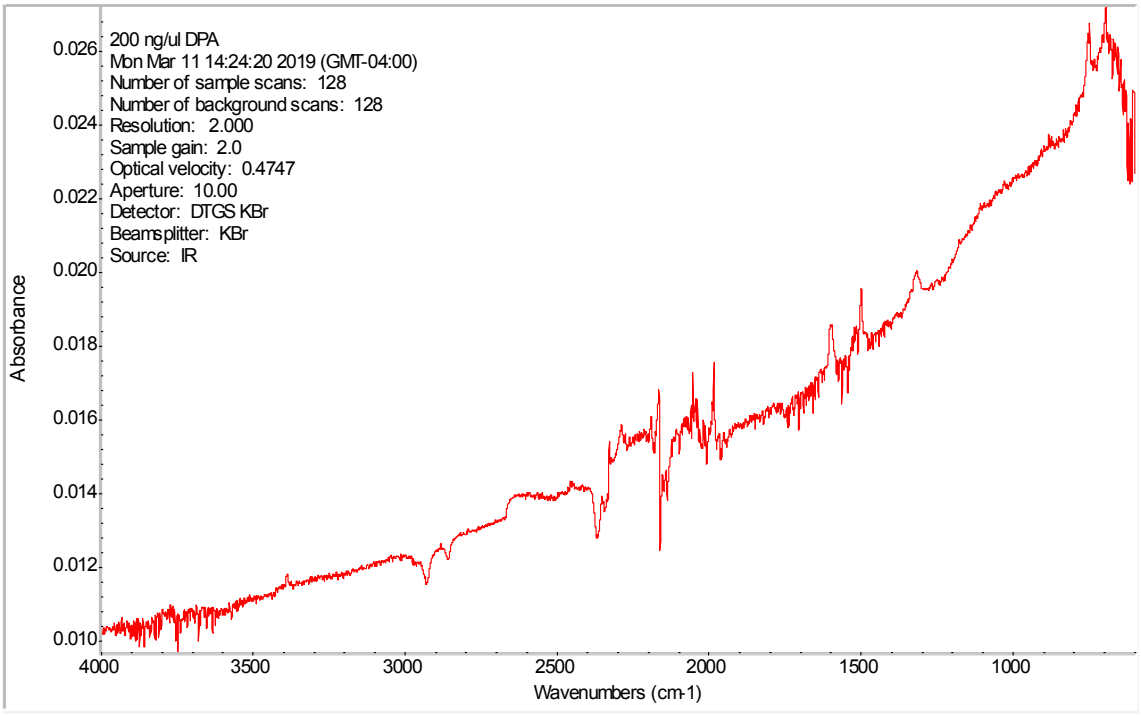
200 ng/ul DPA
Mon Mar 11 14:24:20 2019 (GMT-04:00)
Number of sample scans: 128
Number of background scans: 128
Resolution: 2.000
Sample gain: 2.0
Optical velocity: 0.4747
Aperture: 10.00
Detector: DTGS KBr
Beamsplitter: KBr
Source: IR
Absorbance
0.026
0.024
0.022
0.020
0.018
0.016
0.014
0.012
0.010
4000
3500
3000
2500
2000
1500
1000
Wavenumbers (cm-1)

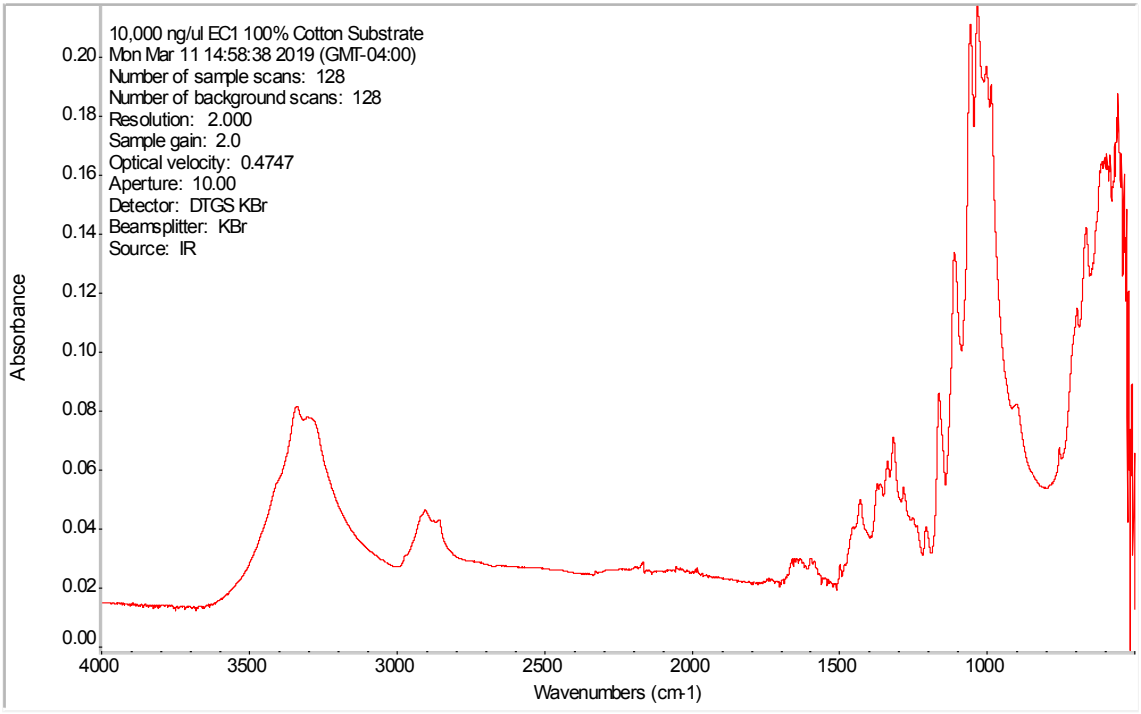
10,000 ng/ul EC1 100% Cotton Substrate
Mon Mar 11 14:58:38 2019 (GMT-04:00)
Number of sample scans: 128
Number of background scans: 128
Resolution: 2.000
Sample gain: 2.0
Optical velocity: 0.4747
Aperture: 10.00
Detector: DTGS KBr
Beamsplitter: KBr
Source: IR
Absorbance
0.20
0.18
0.16
0.14
0.12
0.10
0.08
0.06
0.04
0.02
0.00
4000
3500
3000
2500
2000
1500
1000
Wavenumbers (cm-1)

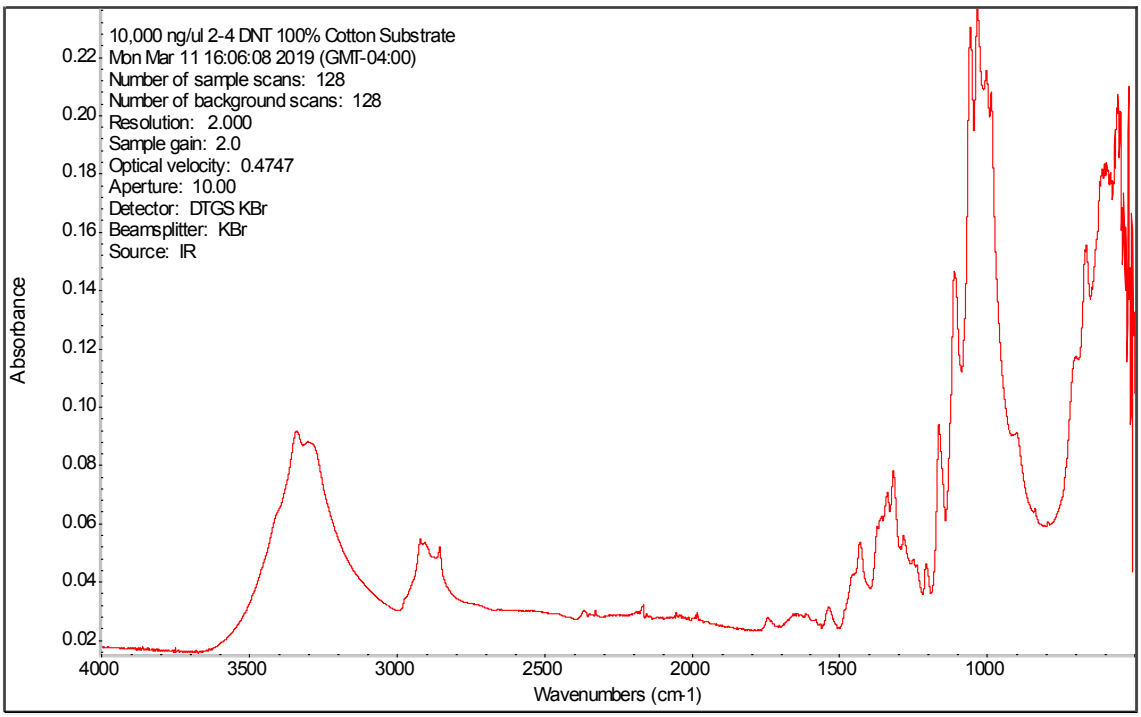
10,000 ng/ul 2-4 DNT 100% Cotton Substrate
Mon Mar 11 16:06:08 2019 (GMT-04:00)
Number of sample scans: 128
Number of background scans: 128
Resolution: 2.000
Sample gain: 2.0
Optical velocity: 0.4747
Aperture: 10.00
Detector: DTGS KBr
Beamsplitter: KBr
Source: IR
Absorbance
0.22
0.20
0.18
0.16
0.14
0.12
0.10
0.08
0.06
0.04
0.02
4000
3500
3000
2500
2000
1500
1000
Wavenumbers (cm-1)

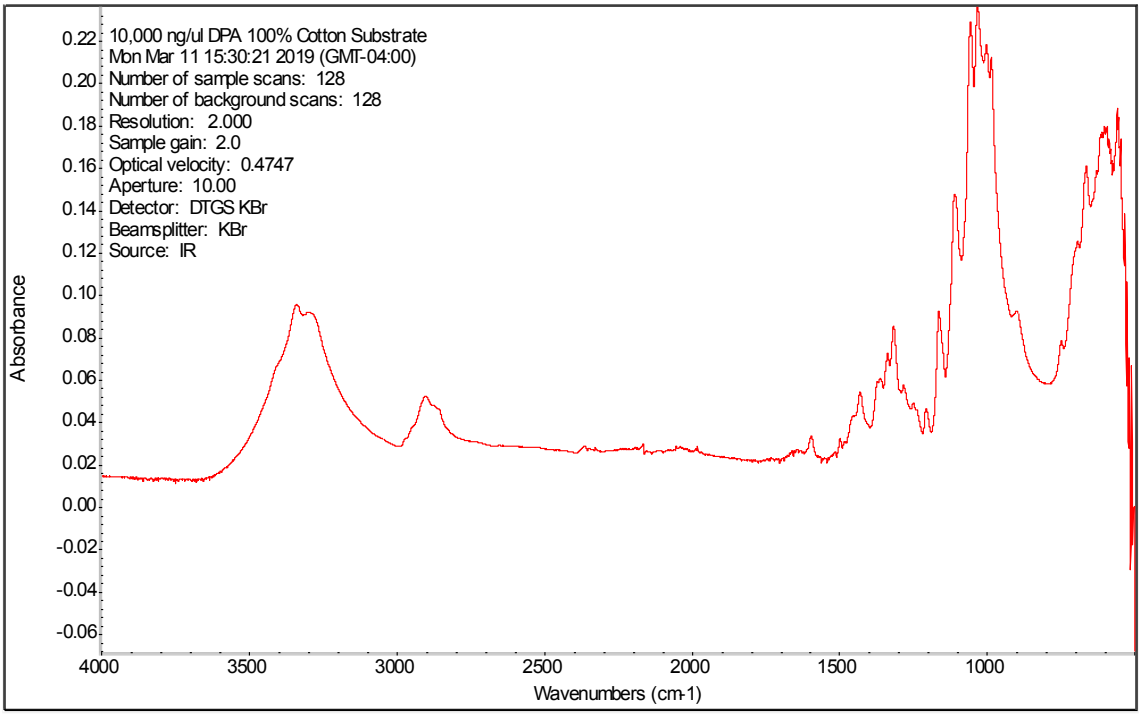
10,000 ng/ul DPA 100% Cotton Substrate
Mon Mar 11 15:30:21 2019 (GMT-04:00)
Number of sample scans: 128
Number of background scans: 128
Resolution: 2.000
Sample gain: 2.0
Optical velocity: 0.4747
Aperture: 10.00
Detector: DTGS KBr
Beamsplitter: KBr
Source: IR
Absorbance
0.22
0.20
0.18
0.16
0.14
0.12
0.10
0.08
0.06
0.04
0.02
0.00
-0.02
-0.04
-0.06
4000
3500
3000
2500
2000
1500
1000
Wavenumbers (cm-1)

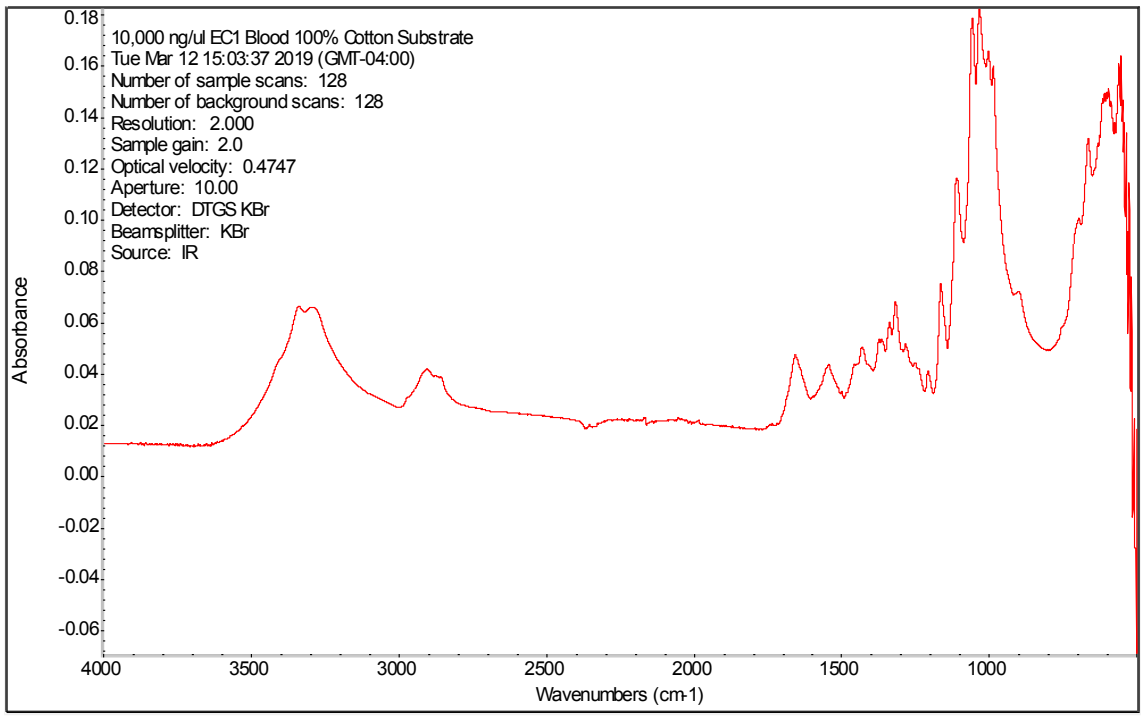
10,000 ng/ul EC1 Blood 100% Cotton Substrate
Tue Mar 12 15:03:37 2019 (GMT-04:00)
Number of sample scans: 128
Number of background scans: 128
Resolution: 2.000
Sample gain: 2.0
Optical velocity: 0.4747
Aperture: 10.00
Detector: DTGS KBr
Beamsplitter: KBr
Source: IR
Absorbance
0.18
0.16
0.14
0.12
0.10
0.08
0.06
0.04
0.02
0.00
-0.02
-0.04
-0.06
4000
3500
3000
2500
2000
1500
1000
Wavenumbers (cm-1)

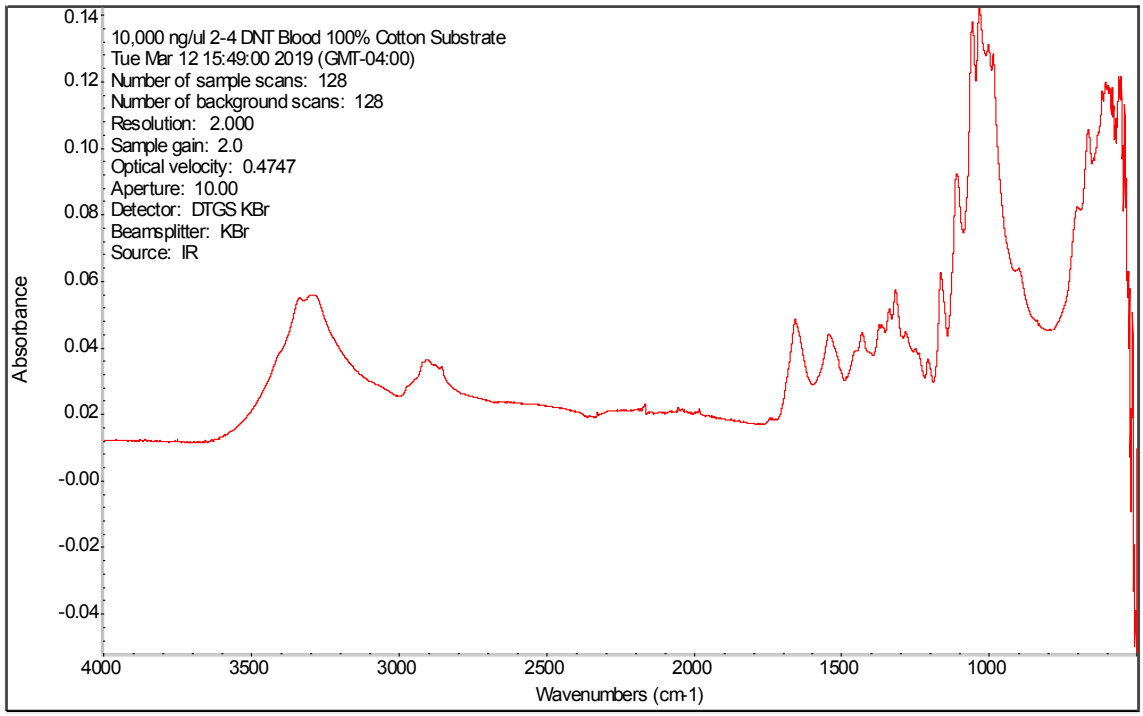
10,000 ng/ul 2-4 DNT Blood 100% Cotton Substrate
Tue Mar 12 15:49:00 2019 (GMT-04:00)
Number of sample scans: 128
Number of background scans: 128
Resolution: 2.000
Sample gain: 2.0
Optical velocity: 0.4747
Aperture: 10.00
Detector: DTGS KBr
Beamsplitter: KBr
Source: IR
Absorbance
0.14
0.12
0.10
0.08
0.06
0.04
0.02
-0.00
-0.02
-0.04
4000
3500
3000
2500
2000
1500
1000
Wavenumbers (cm-1)

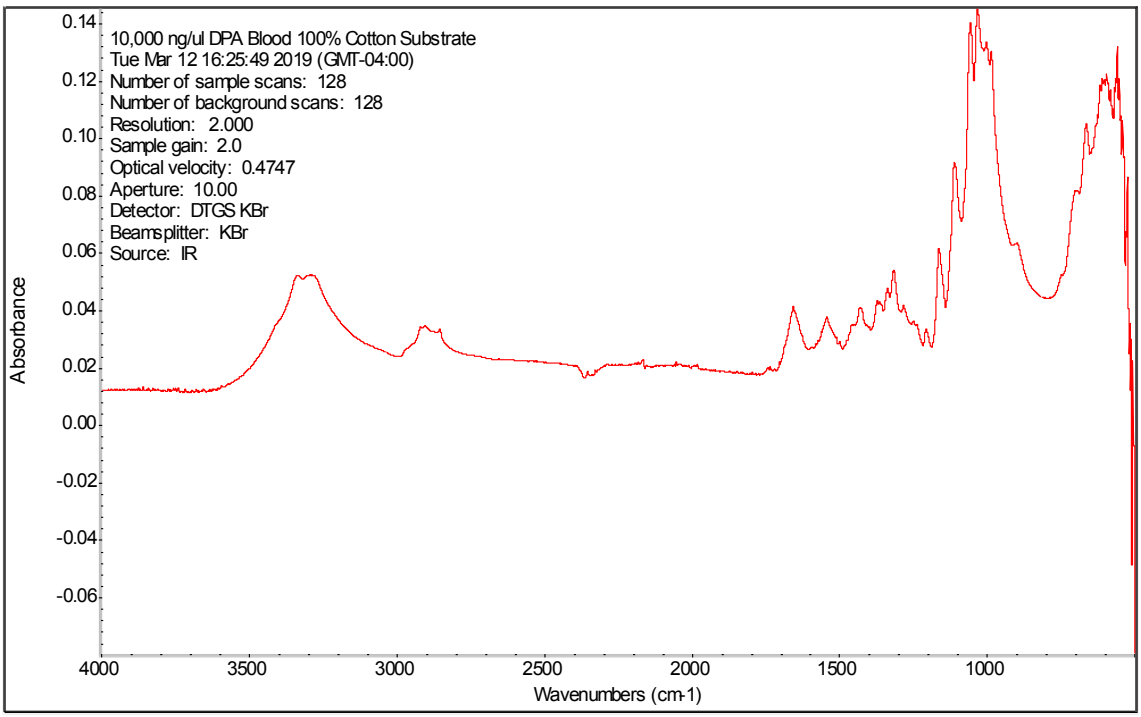
10,000 ng/ul DPA Blood 100% Cotton Substrate
Tue Mar 12 16:25:49 2019 (GMT-04:00)
Number of sample scans: 128
Number of background scans: 128
Resolution: 2.000
Sample gain: 2.0
Optical velocity: 0.4747
Aperture: 10.00
Detector: DTGS KBr
Beamsplitter: KBr
Source: IR
Absorbance
0.14
0.12
0.10
0.08
0.06
0.04
0.02
0.00
-0.02
-0.04
-0.06
4000
3500
3000
2500
2000
1500
1000
Wavenumbers (cm-1)

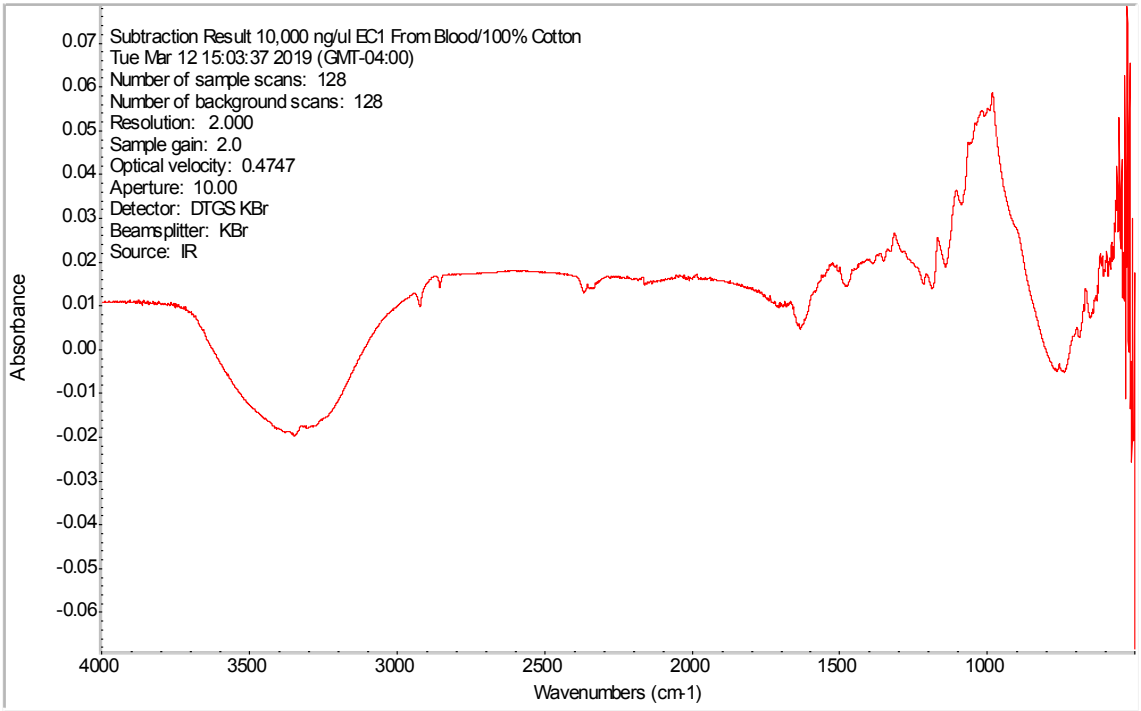
Subtraction Result 10,000 ng/ul EC1 From Blood/100% Cotton
Tue Mar 12 15:03:37 2019 (GMT-04:00)
Number of sample scans: 128
Number of background scans: 128
Resolution: 2.000
Sample gain: 2.0
Optical velocity: 0.4747
Aperture: 10.00
Detector: DTGS KBr
Beamsplitter: KBr
Source: IR
Absorbance
0.07
0.06
0.05
0.04
0.03
0.02
0.01
0.00
-0.01
-0.02
-0.03
-0.04
-0.05
-0.06
4000
3500
3000
2500
2000
1500
1000
Wavenumbers (cm-1)

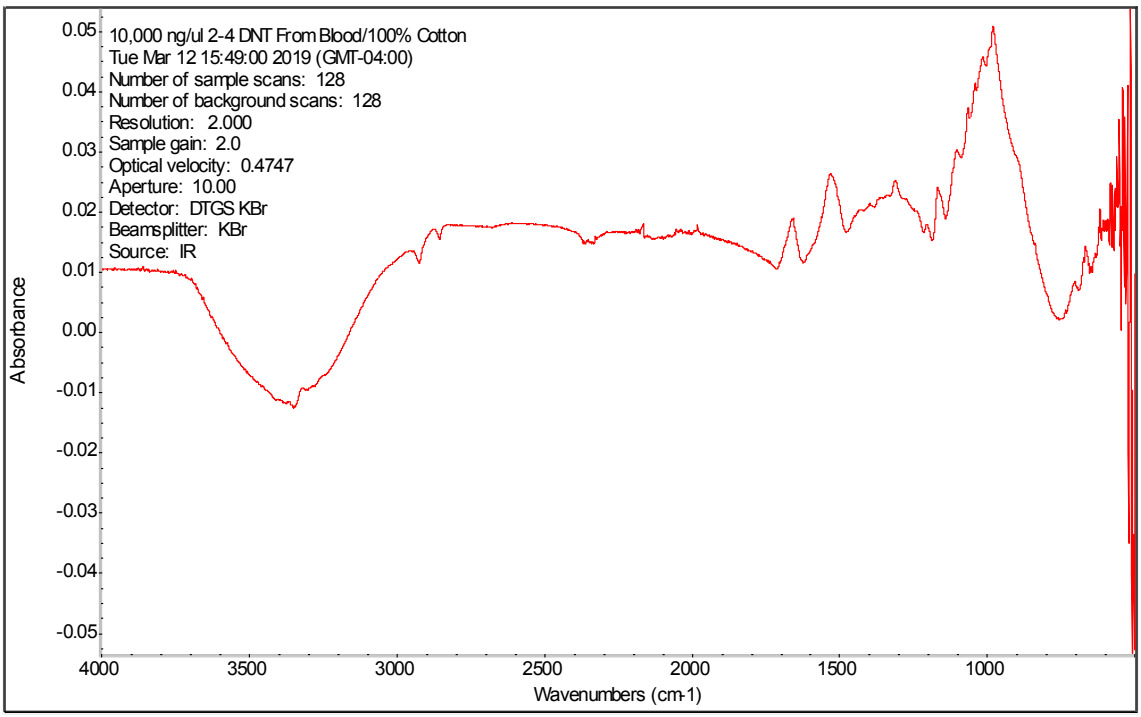
10,000 ng/ul 2-4 DNT From Blood/100% Cotton
Tue Mar 12 15:49:00 2019 (GMT-04:00)
Number of sample scans: 128
Number of background scans: 128
Resolution: 2.000
Sample gain: 2.0
Optical velocity: 0.4747
Aperture: 10.00
Detector: DTGS KBr
Beamsplitter: KBr
Source: IR
Absorbance
0.05
0.04
0.03
0.02
0.01
0.00
-0.01
-0.02
-0.03
-0.04
-0.05
4000
3500
3000
2500
2000
1500
1000
Wavenumbers (cm-1)

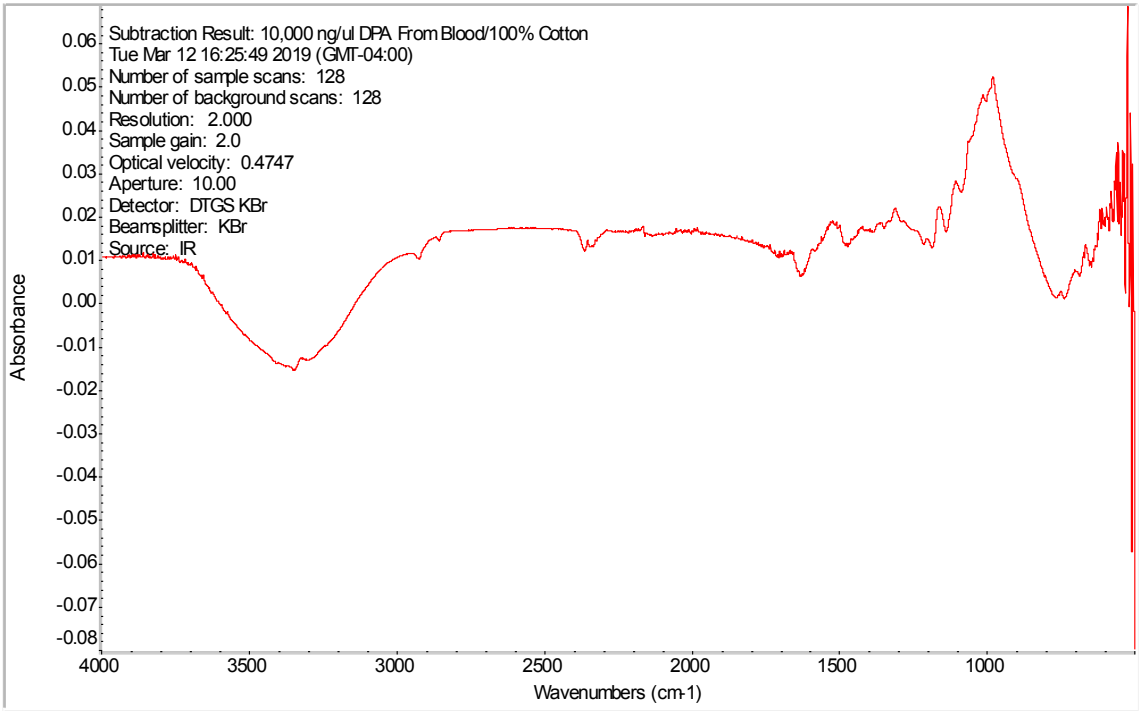
Subtraction Result: 10,000 ng/ul DPA From Blood/100% Cotton
Tue Mar 12 16:25:49 2019 (GMT-04:00)
Number of sample scans: 128
Number of background scans: 128
Resolution: 2.000
Sample gain: 2.0
Optical velocity: 0.4747
Aperture: 10.00
Detector: DTGS KBr
Beamsplitter: KBr
Source: IR
Absorbance
0.06
0.05
0.04
0.03
0.02
0.01
0.00
-0.01
-0.02
-0.03
-0.04
-0.05
-0.06
-0.07
-0.08
4000
3500
3000
2500
2000
1500
1000
Wavenumbers (cm-1)

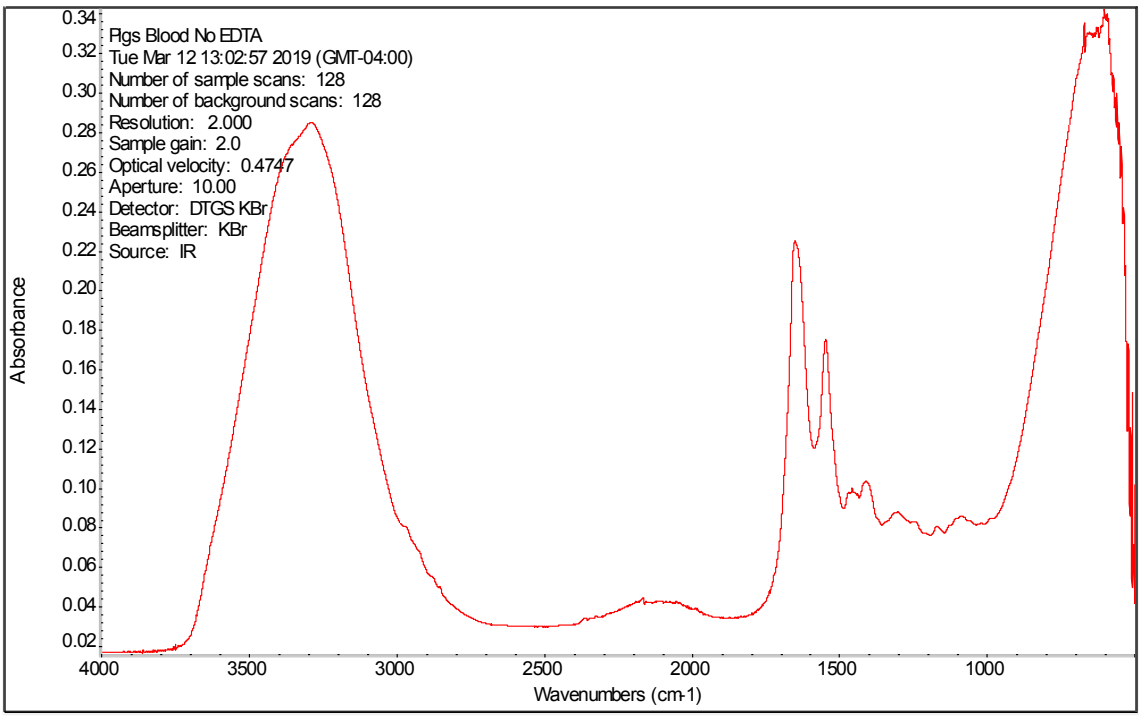
Pigs Blood No EDTA
Tue Mar 12 13:02:57 2019 (GMT-04:00)
Number of sample scans: 128
Number of background scans: 128
Resolution: 2.000
Sample gain: 2.0
Optical velocity: 0.4747
Aperture: 10.00
Detector: DTGS KBr
Beamsplitter: KBr
Source: IR
Absorbance
0.34
0.32
0.30
0.28
0.26
0.24
0.22
0.20
0.18
0.16
0.14
0.12
0.10
0.08
0.06
0.04
0.02
4000
3500
3000
2500
2000
1500
1000
Wavenumbers (cm-1)

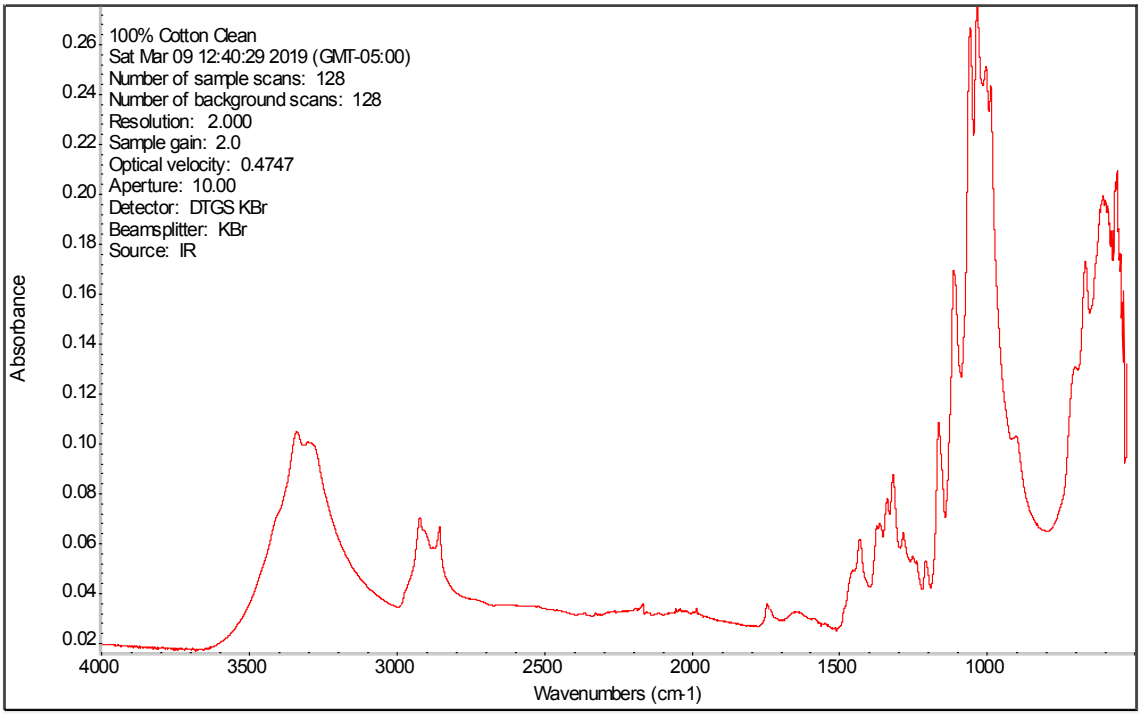
100% Cotton Clean
Sat Mar 09 12:40:29 2019 (GMT-05:00)
Number of sample scans: 128
Number of background scans: 128
Resolution: 2.000
Sample gain: 2.0
Optical velocity: 0.4747
Aperture: 10.00
Detector: DTGS KBr
Beamsplitter: KBr
Source: IR
Absorbance
0.26
0.24
0.22
0.20
0.18
0.16
0.14
0.12
0.10
0.08
0.06
0.04
0.02
4000
3500
3000
2500
2000
1500
1000
Wavenumbers (cm-1)

References

[1] Hofstetter, C., M. Maitre, A. Beavis, C. P. Roux, C. Weyermann, A. L. Gassner. A study of transfer and prevalence of organic gunshot residues. Forensic Science International. 277 (2017) 241-251.

[2] Taudte, Regina Verena, Alison Beavis, Lucas Blanes, Nerida Cole, Philip Doble, and Claude Roux. "Detection of Gunshot Residues Using Mass Spectrometry." BioMed Research International 2014 (2014): 1-16. Web.

[3] Chang, Kah Haw, Paul Thomas Jayaprakash, Chong Hooi Yew, and Ahmad Fahmi Lim Abdullah. "Gunshot Residue Analysis and Its Evidential Values: A Review." Australian Journal of Forensic Sciences 45.1 (2013): 3-23.

[4] Gassner, Anne-Laure, and Celine Weyermann. "LC-MS Method Development and Comparison of Sampling Materials for the Analysis of Organic Gunshot Residues."Forensic Science International 264 (2016): 47-55.

[5] Goudsmits, E., G.P. Sharples, J.W Birkett. Preliminary classification of characteristic organic gunshot residue compounds. Science and Justice. 56 (2016) 421-425.

[6] Grabmuller, M., P. Cachee, B. Madea, C. Courts. How far does it get? The effect of shooting distance and type of firearm on the simultaneous analysis of DNA and RNA from backspatter recovered from inside and outside surfaces of firearms. Forensic Science International. 258 (2016) 11-18.

[7] "Gun Violence." National Institute of Justice. Office of Justice Programs, n.d. Web. 25 Sept. 2017.

[8] Taudte, Regina Verena, Claude Roux, and Alison Beavis. "Stability of Smokeless Powder Compounds on Collection Devices." Forensic Science International 270 (2017): 55-60. Web.

[9] Schwoeble, A. J., and David L. Exline. Current Methods in Forensic Gunshot Residue Analysis. CRC Press, 2000.

[10] Clark, Jim. Mass Spectra - Fragmentation Patterns, Feb. 2014, www.chemguide.co.uk/analysis/masspec/fragment.html.

[11] Clark, Jim. The Mass Spectrometer - How It Works, Feb. 2015, www.chemguide.co.uk/analysis/masspec/howitworks.html#top.

[12] “NIST Chemistry WebBook, SRD 69.” Ethyl Centralite, National Institute of Standards and Technology, 2014, webbook.nist.gov/cgi/cbook.cgi?ID=C85983&Units=SI&Mask=200#Mass-Spec.

[13] “NIST Chemistry WebBook, SRD 69.” Methyl Centralite, National Institute of Standards and Technology, 2014, webbook.nist.gov/cgi/cbook.cgi?ID=C611927&Units=SI&Mask=200#Mass-Spec.

[14] “NIST Chemistry WebBook, SRD 69.” Nitroglycerin, National Institute of Standards and Technology, 2014, webbook.nist.gov/cgi/cbook.cgi?ID=C55630&Mask=200#Mass-Spec.

[15] “NIST Chemistry WebBook, SRD 69.” Nitroguanidine, National Institute of Standards and Technology, 2014, webbook.nist.gov/cgi/cbook.cgi?ID=C556887&Units=SI&Mask=200#Mass-Spec.

[16] Taudte, Regina Verena, Claude Roux, Lucas Blanes, Mark Horder, K. Paul Kirkbride, and Alison Beavis. "The Development and Comparison of Collection Techniques for Inorganic and Organic Gunshot Residues." Analytical and Bioanalytical Chemistry 408.10 (2016): 2567-2576.

[17] Joshi, Monica, Kia Rigsby, and Jose R. Almirall. "Analysis of the Headspace Composition of Smokeless Powders Using GC-MS, GC-uECD and Ion Mobility Spectrometry."*Forensic Science International* 208.1-3 (2011): 29-36. Web.

[18] Tarifa, Anamary, and Jose R. Almirall. "Fast Detection and Characterization of Organic and Inorganic Gunshot Residues on the Hands of Suspects by CMV-GC-MS and LIBS."*Science & Justice* 55.3 (2015): 168-75. Web.

[19] Jadhav, Shri R K. "Gun Propellant." *Defense Research and Development Organization*. N.p., n.d. Web.

[20] "Benzene, 1-methyl-2,4-dinitro." *Benzene, 1-methyl-2,4-dinitro-*. National Institute of Standards and Technology, 2018. Web. 19 Mar. 2019. <https://webbook.nist.gov/cgi/cbook.cgi?ID=C121142&Mask=200#Mass-Spec>.

[21] Diphenylamine." *Diphenylamine*. National Institute of Standards and Technology, 2018. Web. 19 Mar. 2019. <https://webbook.nist.gov/cgi/cbook.cgi?ID=C122394&Mask=200#Mass-Spec>.

[22] Goudsmits, Ellen, George P. Sharples, and Jason W. Birkett. "Recent Trends in Organic Gunshot Residue Analysis." *TrAC Trends in Analytical Chemistry* 74 (2015): 46-57. Web.

[23] López-López, María, Juan José Delgado, and Carmen García-Ruiz. "Ammunition Identification by Means of the Organic Analysis of Gunshot Residues Using Raman Spectroscopy." *Analytical Chemistry* 84.8 (2012): 3581-585. 2012. Web. 2019.

[24] Bueno, Justin, Vitali Sikirzhytski, and Igor K. Lednev. "Attenuated Total Reflectance-FT-IR Spectroscopy for Gunshot Residue Analysis: Potential for Ammunition Determination." *Analytical Chemistry* 85.15 (2013): 7287-294. 2013. Web. 2019.

[25] Zeng, Jianbo, Ji Qi, Fuquan Bai, Jorn Chi Chung Yu, and Wei-Chuan Shih. "Analysis of Ethyl and Methyl Centralite Vibrational Spectra for Mapping Organic Gunshot Residues." *The Analyst* 139.17 (2014): 4270-278. 2014. Web. 2018.

[26] Nordberg, Markus, Ema Ceco, Sara Wallin, and Henric Östmark. "Detection Limit of Imaging Raman Spectroscopy." *Detection and Sensing of Mines, Explosive Objects, and Obscured Targets XVII* (2012): n. pag. 2012. Web. 2018.

[27] Brown, Kristopher, Hyungie Doo, Honest Makamba, and Seong S. Seo. "Spectroscopic and Electrochemical Characterization of Iron(II) and 2,4-Dinitrotoluene." *Analytical Letters* 48.15 (2015): 2482-492. 2015. Web. 2018.

[28] Sett, P., A.k. De, S. Chattopadhyay, and P.k. Mallick. "Raman Excitation Profile of Diphenylamine." *Chemical Physics*276.2 (2002): 211-24. 2001. Web. 2018.

[29] Skoog, Douglas A. *Principles of Instrumental Analysis / Douglas A. Skoog*. Philadelphia ; Toronto: Saunders College Pub., 1985., 2007. Print.

[30] "FT-IR vs. Dispersive Infrared." *Thermo*. Thermo Electron, 2002. Web. 2019. <http://www.thermo.com.cn/Resources/200802/productPDF_21615.pdf>.

[31] Kumar, Dipesh, Bhaskar Singh, Kuldeep Bauddh, and John Korstad. "Bio-oil and Biodiesel as Biofuels Derived from Microalgal Oil and Their Characterization by Using Instrumental Techniques." *Algae and Environmental Sustainability* (2015): 87-95. 2015. Web. 2019.

[32] Ausili, Alessio & Sánchez, Marina & Gómez-Fernández, Juan. (2015). Attenuated total reflectance infrared spectroscopy: A powerful method for the simultaneous study of structure and spatial orientation of lipids and membrane proteins. Biomedical Spectroscopy and Imaging. 4. 159-70. 10.3233/BSI-150104.

[33] "Database of ATR-FT-IR Spectra of Various Materials." *Database of ATRFTIR Spectra of Various Materials*. N.p., 2015. Web. 22 Mar. 2019.

[34] Mistek, Ewelina, and Igor K. Lednev. "Identification of Species' Blood by Attenuated Total Reflection (ATR) Fourier Transform Infrared (FT-IR) Spectroscopy." *Analytical and Bioanalytical Chemistry* 407.24 (2015): 7435-442. 2015. Web. 2019.

[35] Dennis, Dana-Marie Karine. "Chemical Analysis, Databasing, and Statistical Analysis of Smokeless Powders for Forensic Application." Diss. U of Central Florida, 2015. 2015. Web. 2019.

[36] Lloyd, J. B. F. "Liquid Chromatography of Firearms Propellants Traces." *Journal of Energetic Materials* 4.1-4 (1986): 239-71. 2006. Web. 2019.

[37] Basu, Srismrita. "Surface Enhanced Raman Scattering (SERS) Substrates and Probes." Diss. Louisiana State U, 2017. *Surface Enhanced Raman Scattering (SERS) Substrates and Probes*. 2017. Web. 2019.

[38] Urry, Francis M., Mark Kushnir, Gordon Nelson, Mitzi Mcdowell, and Tom Jennison. "Improving Ion Mass Ratio Performance at Low Concentrations in Methamphetamine GC-MS Assay through Internal Standard Selection." *Journal of Analytical Toxicology* 20.7 (1996): 592-95. 1996. Web. 2019.

[39] Lu, Zhenyu, Stephanie A. Dejong, Brianna M. Cassidy, Raymond G. Belliveau, Michael L. Myrick, and Stephen L. Morgan. "Detection Limits for Blood on Fabrics Using Attenuated Total Reflection Fourier Transform Infrared (ATR FT-IR) Spectroscopy and Derivative Processing." *Applied Spectroscopy* 71.5 (2016): 839-46. 2016. Web. 2019.

[40] Ian J. Maybury, David Howell, Melissa Terras, and Heather Viles. “Comparing the Effectiveness of Hyperspectral Imaging and Raman Spectroscopy: A Case Study on Armenian Manuscripts.” *Heritage Science* 6:42 (2018). Web. 2019.